Applying nuclear forensic signatures in response to a nuclear security event from a South African nuclear facility

ND Mokhine

Orcid.org/0000-0001-6069-1294

Thesis accepted in fulfilment of the requirements for the degree Doctor of Philosophy in Science with Radiation Science at the North-West University

Supervisor: Prof M Mathuthu

Graduation: October 2022

Student number: 23161396

DECLARATION

I, **Naomi Dikeledi Mokhine**, declare that the dissertation, which I herewith submit to the North-West University as *partial completion* of the requirements set for the Doctor of Philosophy in Science with Radiation Science degree, is my work and has not been submitted to any other university.

Signed by student……  **…2 October 2022**

Naomi Dikeledi Mokhine **Date**

Singed by Supervisor …… **…2 October 2022**

Prof Manny Mathuthu **Date**

ACKNOWLEDGEMENT

- Firstly, I would like to thank the Almighty God for granting me strength, wisdom and providing me with his love and protection during this journey of studying.
- I would like to express my sincere gratitude to my Ph.D. supervisor and mentor Prof. Manny Mathuthu for his support, advice, patience, and guidance through my studies.
- I would also like to acknowledge North-West University Bursary, NRF, and HWSETA for their financial support, from the support it was possible to carry out my studies.
- I acknowledge with thanks to IAEA and NWU for allowing me to conduct this research under the IAEA CRPJ02013 project.
- I am also grateful for the support and assistance received from my colleagues at the NWU, Centre for Applied Radiation Science and Technology.
- Finally, I am very thankful to my mother who has been there during difficult times and for the support and love, she provided me with throughout my studies.

ABSTRACT

Uranium ore concentrates, also known as yellowcake, are a critical component of the nuclear fuel cycle and the result of uranium mining and processing. Uranium ore concentrate s refers to a group of uranium chemical compounds that include U_3O_8, UO_3, UO_2, and UO_4xH_2O (where x = 2 or 4). The distributions of trace elements in uranium ore concentrates may be linked to the geologic conditions under which the parent uranium ore developed, and so are unique to each deposit type. These chemical signatures might subsequently be employed as a crucial tool in nuclear forensic examination. In this study, several samples of uranium ore concentrate and uranium ore samples have been analyzed for their trace elements, rare earth elements, morphology, and isotopic ratios. This project aimed to apply nuclear forensic signatures in responding to nuclear security events from a nuclear facility in SA. Uranium ore concentrates and uranium ore samples were analyzed using gamma detector, SEM/EDS, and inductively coupled plasma mass spectrometry. It was found that the activity ratio of $^{235}U/^{238}U$ for uranium ore concentrates samples ranged between 0.0271 ± 0.0016 and 0.0393 ± 0.0082 respectively, while the activity ratio of $^{235}U/^{238}U$ for uranium ore samples ranged from 0.0326 ± 0.0021 and 0.0391 ± 0.00037. The sample images of uranium ore concentrates showed similar characteristics, as both have pores between their grains. They both have a grape-like shape stacked together. Uranium ore concentrates consisted of agglomerates particles. These results showed a difference in particle shape and texture. The aggregates of fine particles are reasonably common in all the uranium ore concentrates samples and may have been produced during vapor condensation, nucleation and coagulation of particulates in the mine furnace. SEM/EDS results in uranium ore concentrate samples contained 60 – 70 % of uranium. The uranium ore samples studied displayed a fine texture. SEM/EDS in uranium ore samples showed the oxygen (O), aluminum (Al), sulfur (S), potassium (K), iron (Fe) impurities and uranium was not detected. Uranium ore concentrate and uranium ore samples could be differentiated by elemental and rare earth elements concentrations. The results showed that the elemental concentrations of the uranium ore concentrates samples might be used to differentiate them from one another. Impurity elements, Ca, K, Mg and Na were the most dominant elements in both uranium ore samples. The mean concentrations in U ore1 were in the order K > Mg > Na > Ca respectively, while the mean concentrations in U ore2 were in the order K > Mg > Ca > Na respectively. Therefore, the differences displayed by impurity elements were not only different in the concentrations of these elements but the shapes of the spectrum formed were also significantly

different. The C1-chondrite rare earth elements patterns of UOC_{black} showed fractionation of light rare earth elements and flat enriched heavy rare earth elements and a significant negative Eu anomaly. UOC CUP-2 showed depleted light rare earth elements and flat heavy rare earth elements. ADU rare earth elements pattern showed fractionation for all the elements. The uranium ore concentrates analyzed showed large variability in rare earth element patterns as well as Eu anomalies. Rare earth element patterns for both uranium ore samples showed enriched light rare earth elements and depletion of heavy rare earth elements. During early ore processing of the uranium ore studied in this work, rare earth element abundances and U isotopes did not fractionate. The CN-REE patterns difference for all samples demonstrate that the rare earth element signatures remain effective forensic indications despite *in-situ* leaching processes. The (^{234}U)/ (^{238}U) isotope ratios of uranium ore concentrate samples ranged between 0.169 ± 0.00936 and 4.810 ± 4.540, where the (^{235}U)/ (^{238}U) is between 0.00615 ± 0.00005309 and 0.348 ± 0.326. The (^{234}U)/ (^{238}U) as isotope ratios of the U ore1 and U ore2 samples ranged between (21.90 ± 4.08) x $10^{-5}$and (5.65 ± 1.17) x 10^{-5}, where the (^{235}U)/ (^{238}U) is between 0.0289 ± 0.00496 and 0.00760 ± 0.00167 respectively. It was found that the results for the (^{235}U)/ (^{238}U) ratios showed large differences between the uranium ore concentrate and uranium ore samples. Similar to the (^{235}U)/ (^{238}U) ratios, there are a significant difference for the (^{234}U)/ (^{238}U) ratios of the uranium ore concentrate and uranium ore samples. The activity ratio of ^{234}U/^{238}U and ^{235}U/^{238}U of uranium ore concentrate and uranium ore samples was 10.144 and 0.047 respectively. Due to the natural abundance of ^{235}U being used to derive its isotopic concentration from the observed isotopic concentration of ^{238}U, the activity ratio for ^{235}U/^{238}U was equal to the continental average of 0.047 for all samples. The uranium ore concentrate and uranium ore samples showed that they could be differentiated from one another based on the study's findings. These results reported here demonstrate that they can be applied during nuclear forensic events.

Keywords: Nuclear security events, UOC, U ore, nuclear forensic signature, morphology, uranium isotopic ratios.

List of Abbreviations

ADU	Ammonium diuranate
AMS	Accelerator mass spectrometry
DU	Depleted uranium
EDS	Energy dispersive spectroscopy
EU	European Union
FSU	Former Soviet Union
HEU	High enriched uranium
HREE	Heavy rare earth element
IAEA	International Atomic Energy Agency
ITDB	Incident and trafficking database
ITU	Institute of Trans Uranium Elements
ITWG	International Technical Working Group
LIBS	Laser-Induced Breakdown Spectroscopy
LREE	Light rare earth element
MCA	Multichannel analyzer
MC-ICPMS	Multi-collector inductively coupled plasma mass spectrometry
NFC	Nuclear fuel cycle
NMAC	Nuclear material accounting and control
NWU-CARST	North-West University - Centre for Applied Radiation Science and Technology
REE	Rare earth elements
SEM	Scanning electron microscopy
SIMS	Secondary ion mass spectrometry
TIMS	Thermal ionization mass spectrometry
U	Uranium
UOC	Uranium ore concentrate
USA	United states of America
XRD	X-ray diffraction

LIST OF FIGURES

LIST OF TABLES

Table of Contents

CHAPTER 1: INTRODUCTION AND PROBLEM STATEMENT

1.1 Introduction

Illicit trafficking involves the illegal movement of nuclear material and other radioactive sources. The illicit trafficking of nuclear material began after the collapse of the Former Soviet Union (FSU). Many nuclear production and research facilities were shut down as the Soviet Union collapsed in 1991 (Kristo *et al.*, 2016). Since 1990, the independent states of FSU did not have adequate authority over their enormous nuclear materials supplies and material got lost (Wallenius *et al.*, 2007).

Establishing a birth date for nuclear forensics is difficult because many of the techniques and methods used in nuclear forensics have originated from the United States nuclear weapons program (Kristo, 2020). In the early 1990s, a kilogram of highly enriched uranium would cost thousands of pounds to produce inside a well-established enrichment program and therefore theft and sale of nuclear materials started (Moody *et al.*, 2014). In 1991, the breakdown of the Soviet Union brought about Russia, Belarus, Ukraine, and Kazakhstan acquiring atomic weapons stores (Moody *et al.*, 2014). With the breaking down of the Soviet Union in the early 1990s, a new phenomenon called nuclear smuggling was observed. This new phenomenon was being observed in Switzerland and Italy where the first case of nuclear smuggling was reported (Mayer *et al.*, 2007). However, the IAEA's illicit trafficking database showed around 11 incidents of smuggled highly enriched uranium or plutonium in Russia and Europe in 1992. As a result, concerns about the nuclear or radioactive material's origin, trafficking route and intended purpose have arisen. Finally, nuclear forensics was established as a research branch to address these outstanding concerns in collaboration with law enforcement and intelligence.

The use of nuclear and other radioactive materials is strictly controlled. Nuclear material, such as uranium and plutonium, are stored under strict physical protections, is accurately accounted for, and an international monitoring regime established to ensure that nuclear material does not bypass the civil nuclear fuel cycle (Mayer *et al.*, 2015). Nonetheless, there have been instances of criminal accidents involving such products. President Barack Obama summarized the international community's consensus *that 'nuclear terrorism is one of the most challenging dangers to international security'*, in his remarks at the Nuclear Security Summit in Washington D.C. (Kristo & Tumey, 2013b).

1.2 Nuclear forensic science

Nuclear material have become a part of forensic investigations, results in the formation of nuclear forensic science. Nuclear science offers techniques that are being utilized to enhance productivity while conserving valuable resources required for day-to-day life. Nuclear forensic science is a novel discipline that blends nuclear analytical technologies with conventional forensic science, as well as traditional safeguards (Pajo, 2001). This branch was developed to study the planned usage of the seized nuclear or radioactive material, their origin and possible paths used during trafficking as well as to recognize and characterize interdicted illicit nuclear and radioactive material.

To identify the confiscated radioactive materials, it is necessary to conduct systematic investigations utilizing established nuclear analytical procedures. In recent years, the worldwide community has increasingly acknowledged nuclear forensic science as an important component of a comprehensive investigation. In the communique and work plans of the previous three nuclear security summits (2010, 2012, 2014), nuclear forensic science was expressly recognized as a key research priority topic (Kristo *et al.*, 2016).

The investigation of nuclear or other radioactive material tries to recognize what the materials are, how, when, and where the materials were made, and what were their proposed uses (IAEA, 2015). To prove nuclear attribution, intercepted nuclear or radioactive material, as well as any connected material, must be analyzed (IAEA, 2006). Nuclear forensic provide answers to questions like what is the material and what was its intended use. Who was the last rightful owner? How was it made? Answers to these questions help investigators in determining the origin of the material, that is, the production place or the facility where the material got out of regulatory control (Evans & Hanusa, 2019)**.** Even if the origin of the nuclear or other radioactive material cannot be in every case uniquely determined, the exclusion of several facilities from considerations as the last legal owner of the material is often equally important.

Many physical and chemical techniques are used to investigate isotopic concentrations of noteworthy nuclides, trace element content, microstructure and the lapsed time since the material was finally purified. The outcomes of these studies determine a special significance for a material that can aid in revealing its provenance, origin, date of fabrication or purification and the route used to transport material from its origin to the point of interception (Mayer *et al.*, 2012).

Developing nuclear forensic signatures and deciding the kinds of facts that are essential to search for, can assist in distinguishing one radiological or nuclear material from another and can additionally be used to perceive the procedure and processes that were used to manufacture these types of materials (Wallenius *et al.*, 2014). In various physical forms, purity, enrichment, and even amount, prohibited nuclear materials can be identified. These materials are generated through the various phases of the nuclear fuel cycle. The fuel cycle is therefore defined here with a focus on the topic of concern, i.e. uranium ore concentrate (UOCs) manufacturing, popularly known as yellow cakes. Processes leading to the manufacturing of UOCs (front end of the fuel cycle) are more prominent than the back end cycle owing to easier access to materials from the front end of the fuel cycle.

1.3 Incident and trafficking database (ITDB)

A nuclear and other radioactive material security issue has existed since the early 1990s after reports went to the IAEA about material thefts and losses, including plutonium, highly-enriched uranium, and other radioactive sources (Bull & Smith, 2015). Ongoing reports of unregulated nuclear and other radioactive materials exist. In 1995, the incident trafficking database (ITDB) system was developed to record illegal trade in nuclear and other radioactive material incidents. The ITDB was developed by the IAEA to document and examine nuclear and other radioactive materials out of regulatory control (IAEA, 2019). The ITDB's scope includes all types of nuclear material such as uranium, plutonium, and thorium as defined by the Agency's Statute, as well as naturally occurring and intentionally created radioisotopes and radioactively contaminated items, such as scrap metal (IAEA, 2020). Identifying the origin and proprietor from radiological signatures of these materials should aid in identifying who is responsible for remediation of a region, which has been affected. Since 2016, the ITDB has divided incidents into three categories (IAEA, 2020):

- Group I: incidents that are likely to be related to human trafficking or malicious use;
- Group II: incidents with unknown intent; and
- Group III: incidents that are not or are unlikely to be related to human trafficking or malicious use.

According to the IAEA's ITDB, the year 1994 set a new record, with 45 reported cases of nuclear material trafficking (Wallenius *et al.*, 2007). Since then, the number of cases has declined and is

now about 10 cases in a year. In addition, the majority of recent seizures have been made of natural or depleted uranium, with nuclear-grade content appearing in just a few cases. As a result, natural uranium in early fuel cycle products like ores and ore concentrate is often intercepted. Consequently, there is a global need to better understand and record the forensic signatures of various types of ores so that the origin of seized material as well as its country can be identified (IAEA, 2015).

The database is comprised of three main categories (Reading, 2016):

a) Unauthorized ownership and associated illegal activities, such as the transfer of nuclear materials with the intent to export them,

b) Theft or loss of nuclear materials from facilities or during transportation, and

c) Illegal activities and events such as illegal shipment of nuclear or radioactive materials, illegal disposals of materials, or the detection or discovery of uncontrolled sources.

It is vital to recognize that regardless of the great efforts of border controls and the IAEA ITDB, there are good-sized quantity of trafficking and smuggling that go undetected and unreported. For example, stolen nuclear materials from within the European Union (EU) Schengen area would probably go undetected in transit due to open borders between the EU countries (Reading, 2016). Additionally, detecting low amounts of nuclear material at border controls is tough due to technological constraints and because nuclear materials can be protected from radiation detectors and concealed inside larger inconspicuous consignments.

The number of incidents being reported to the IAEA is a serious subject, and consequently, nuclear laboratories must improve their procedures for investigating and reporting accurate, rapid, and positive results for identifying the origins of nuclear substances out of regulatory control. Laboratories like the Lawrence Livermore National Laboratory in the United States of America (USA), the Institute for Trans uranium Elements in Germany, and the Atomic Weapons Establishment in the United Kingdom as well as the Center for Applied Radiation Science and Technology (CARST) at the North-West University in South Africa, have expressed interest in conducting forensic investigations to ascertain the illegal nuclear materials' intended use, origin, and possible trafficking path (Reading, 2016). Today, countries from all across the world take part

in the Nuclear Forensics International Technical Working Group (ITWG) which was set up in 1996 with the aid of the G-8 (Kristo, 2011; L'Annunziata, 2012) and is made up of 28 countries and organizations (Smith & Niemeyer, 2004).

In 2019, 36 states reported 189 incidents to the ITDB, suggesting that illegal activities and events involving nuclear and other radioactive materials, including incidents of trafficking and malicious use, continue to occur (Figure 1.1) (IAEA, 2020). The ITDB had 3686 confirmed cases registered by participating States since 1993 to 31 December 2019. There were 290 cases involving a reported or probable act of trafficking or malicious use among the 3686 confirmed incidents (IAEA, 2020).

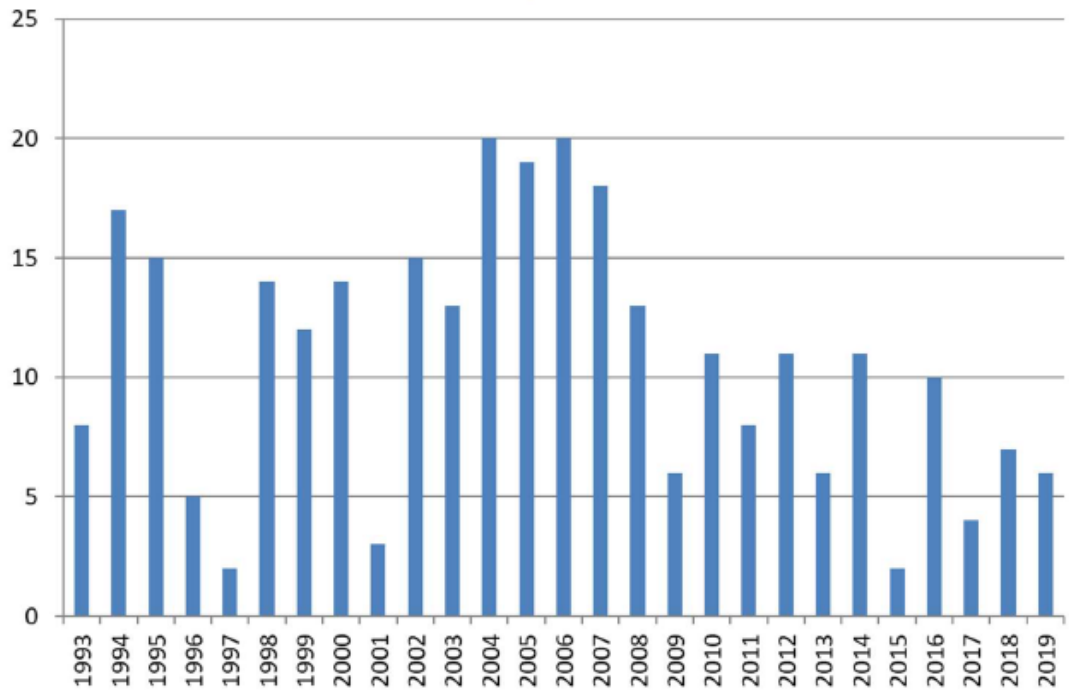

Figure 1. 1: Confirmed incidents involving nuclear or radioactive materials were reported to the ITDB from 1993 to 2019 (IAEA, 2020).

At the Nuclear Security Summits in Washington (2010), Seoul (2012), and The Hague (2014), nuclear material out of regulatory command became a subject of discussion. The hazard from regulatory management linked to nuclear substances is due to its radiological hazard and the risk of proliferation (Mayer *et al.*, 2015). Its practical use in malicious acts, even in acts of nuclear terrorism, requires appropriate steps to prevent such acts and to investigate and prosecute the illegal ownership, transfer, or use of nuclear material. Whenever nuclear material is intercepted, the intended use of the material from illegal trafficking issues arises. Nuclear forensics is relatively

a fresh self-discipline in science that aims to respond exactly to these issues. Essentially, nuclear forensic science shares the basis of all forensic investigations, recognized as the principle of Lockard: "every contact leaves a trace" (Mayer *et al.*, 2015).

According to the ITDB, natural (e.g. uranium ore concentrates) and depleted uranium was involved in approximately 68 percent of the accidents. Based on the ITDB, it can be concluded that 90% of the nuclear material involved originates from the front end of the fuel cycle (Krajko, 2016), while only 10% comes from the fuel cycle back-end processes. Thus, much of the production of nuclear forensic signatures currently focuses on natural uranium materials. A brief introduction to the front end of the fuel cycle will be provided in the next chapter to better understand the term "natural uranium."

1.4 Problem statement

At present, smuggling of nuclear materials is a serious concern and a problem that needs to be addressed on a global scale. The International Atomic Energy Agency (IAEA) has verified that the smuggling of nuclear materials has increased dramatically over the past few years (Jones *et al.*, 2014). Examples of presently perceived hazards to contemporary culture are the dispersion of such products over metropolitan regions, their introduction into the food chain, or the drinking water system (Schenkel *et al.*, 2003). Trafficking of radiological and nuclear materials has become a danger over the past 20 years because the aim of stealing nuclear material may be unknown. It is anticipated that member states of the IAEA will plan and execute methods to address this danger and prevent the spread of illicit nuclear material (IAEA, 2013) to ensure the safety of humans and also to prevent terrorists activities. In South Africa, there have been three reported cases of illicit trafficking of nuclear materials. About 11.52 kg of U-235 was reported in 2011, 1.2 kg, 0.5 kg, and 0.8 kg of uranium content in 2012, and depleted uranium of radiation dose of 0.58 Sv was reported in 2013 (Mogafe *et al.*, 2015). As these materials emit radiation, they present a danger to human health and safety and there needs to be adequately controlled. More importantly and in the context of this study, nuclear materials are also fissionable and could be used for proliferation purposes (Mayer *et al.*, 2015). Unlawful ownership of such materials may provide basis of malicious intentions.

Nuclear forensics is a strong analytical methodology that can help solve nuclear safety incidents and determine the origin and planned use of these materials when intercepted (Mayer *et al.*, 2011). Critically developing signatures for a specific nuclear or radioactive material can achieve this. Nuclear forensics aims to promote nuclear safety and the peaceful use of nuclear energy, and as well as encourage the fight against nuclear trafficking (Fedchenko, 2014).

All states have acknowledged as a matter of concern the danger of nuclear terrorism. States also acknowledge that nuclear safety in one state may rely on the efficacy of other states ' nuclear safety regime. Appropriate global cooperation is increasingly needed to improve nuclear safety globally (IAEA, 2013). Each nation must have its nuclear library to enable it to share or exchange data in the case of illicit trafficking of nuclear material to achieve non-proliferative goals. In addition, nuclear material accounting and control (NMAC) is a significant activity required by the IAEA for each nation to decrease or deter the proliferation of materials. Therefore, South Africa is required to identify signatures and set up its nuclear library instantly after the end of the NMAC practice.

Several features of the materials of concerned are used in nuclear safeguards and forensics either to confirm the stated origin or to identify the source of unknown nuclear material. These features include, for instance, levels of significant traces, the isotopic composition of impurities of Pb, Sr, or U, material morphology, or molecular structure (Varga *et al.*, 2017). The origin of a sample in question can be verified with greater confidence using the complicated set of parameters. However, as there are several types of technologies used for ore leaching, uranium extraction and purification with different types of feed materials, the interpretation of such characteristics is very difficult in most cases because they can be dominated by the feed material or altered by the process and the regents used. As a result, their elevated variability, certain measurable features do not serve as a helpful signature (Varga *et al.*, 2017). Most of the time, uranium ore concentrate (UOC), a product of the nuclear fuel cycle, is traded internationally. Uranium ores are leached and extracted to produce UOCs. As a result, their physical characteristics, chemical compositions, and impurity levels are highly dependent on the nature of the raw uranium ore as well as the milling processes used, and they have geographical and geological signatures to some extent (Lina *et al.*, 2014). In South Africa, the nuclear forensic branch is still in its early stages, and the isotopic composition of radioactive material contributes to the development of a nuclear fingerprint as a characteristic that can be used to make conclusions based on the likely origin of the material.

At present, one of the most important concerns of the public is the use of nuclear energy and the possible diversion of nuclear material for malicious purposes. The main aim of the IAEA safeguards of nuclear materials is to ensure timely detection and the diversion of such materials. A known nuclear material is required to identify the origin of the unknown intercepted material to develop nuclear signatures for nuclear materials, hence the need for database. This project's focus therefore seeks to apply uranium signatures from a nuclear plant to determine the possible geographical origin of the source of the nuclear material and help prevent, theft, sabotage, unauthorized access, illegal transfer, or other malicious acts involving nuclear material.

1.5. Aim and objectives

1.5.1. Aim:

This project aimed to determine the nuclear forensic signatures applied in responding to nuclear security and safeguards events from in a nuclear facility in South Africa.

1.5.2. Objectives:

The main objectives of this project were to:

- investigate the radioactivity ratio of $^{235}U/^{238}U$ in UOC/U_3O_8, also called yellow cake and uranium ore samples using a gamma spectrometer;
- determine the elemental concentration and morphology of the UOC and uranium ore samples using Scanning electron microscope and ICP-MS;
- establish the geochemical REE signatures retained in the processing of UOC/ U_3O_8;
- determine the origin of the uranium ore and its concentration for nuclear forensic signatures;
- apply isotopic ratio, elemental and mineralogical data from uranium ores to resolve the nuclear forensic signatures of the Facility nuclear material (Ore).

CHAPTER 2: LITERATURE REVIEW

2.1 Introduction

Nuclear forensics is a relatively young and dynamically advancing branch of science, which involves nuclear material characterization and data interpretation (Krajkó *et al.*, 2014). Nuclear forensics is defined by the IAEA as an assessment of intercepted nuclear or radioactive material and any related material to provide proof of atomic attribution (IAEA, 2006). In reacting to suspected trafficking activities, deterring nuclear terrorism and ensuring that international treaties are being maintained in this critical branch of analytical chemistry, identical methodologies are often used to respond to or monitor unintentional environmental releases of nuclear materials. One of the best mechanisms for deterring the potential use of nuclear weapons is the ability to quickly detect and respond to a nuclear incident (Schwerdt *et al.*, 2018). Critical information of interdicted nuclear materials and debris from the explosion of a nuclear weapon is provided by Nuclear Forensics to help distinguish signatures indicative of the past and origin of material processing. On the other hand, the purpose of nuclear safeguards is to avoid the proliferation of materials and technologies for nuclear weapons through policy and treaty verification (Schwerdt *et al.*, 2018). A variety of nuclear forensic techniques is needed to acquire key response information if a nuclear incident occurs, such as system type, material origin, travel path, and likely/ unlikely responsible parties. Ultimately, such details may lead to legal, civil, or even retaliatory acts and must be extremely defensible. To determine the sources of unattributed material, the nuclear forensic analysis uses principles from physics, radiochemistry and nuclear safeguards. Nuclear forensics is a procedure that uncovers knowledge using nuclear material. That material's elemental and isotopic composition, as well as its microscopic and macroscopic appearance, reveal the essence of this manufacturing approach. (Mayer *et al.*, 2005b).

2.2 The role of nuclear forensics in nuclear security

Nuclear forensics, or the examination of interdicted nuclear material to offer information to law enforcement and national intelligence, is still a hot topic among scientists and policymakers (Kristo, 2020). From a technical viewpoint, nuclear forensics needs the knowledge of nuclear materials analysis and the properties given on those materials by production procedures in the civilian and military nuclear fuel cycles. Nuclear and other radioactive materials are widely

employed in various sectors, including in research, medical and biological investigations, and other technological and scientific applications, as well as in the nuclear fuel cycle (IAEA, 2015). South Africa should put in place a nuclear security infrastructure to safeguard its nuclear material which goes back to the nuclear weapons program of the Apartheid era (Pabian, 2015). The nation should also have measures to prevent, detect, and respond to nuclear security incidents.

The most prominent application of the nuclear forensic method is undoubtedly the nuclear security field. It aims to prevent the unauthorized removal, identification, and response to nuclear security incidents of nuclear or other radioactive materials, as well as to combat illicit trafficking. Nuclear forensic analysis is a vital technique that uses signatures contained in nuclear or other radioactive materials to provide information about their sources, development, and history (Fedchenko, 2014). This branch of analytical chemistry is crucial in responding to alleged drug trafficking, deterring nuclear terrorism, and ensuring that international treaties (e.g., the Non-Proliferation Treaty) are being complied with; similar methodologies are often used in responding to or monitoring intentional/unintentional nuclear material releases into the environment (Stanley, 2012). Nuclear forensics plays an essential role in identifying the origin of any discovered material and contributes to reinforcing the safeguards of such material to be put to real-world application.

Notwithstanding the existence of national nuclear security systems, instances of material out of regulatory control continue to occur inadvertently, either intentionally, through theft, or due to a criminal demonstration (Wong *et al.*, 2015). With this background, South Africa needs to develop its capabilities to help prevent, detect, and respond to any nuclear or other radioactive material-related occurrences with nuclear security consequences.

The following definitions can be used to encapsulate all conceivable uses of the techniques in question (Fedchenko, 2014):

Nuclear forensics analysis is the analysis of a sample of nuclear or radioactive material and any accompanying information to offer evidence for identifying the history of the sample's material. Nuclear forensics comprises categorization, characterization, nuclear forensic interpretation, and reconstruction.

Categorization entails swiftly identifying the content of interest as belonging to a pre-defined group and selecting how it will be handled.

Characterization is the process of determining the characteristics of a sample. It usually entails the chemical and elemental examination of the sample, as well as isotopic analysis of nuclear material like U and Pu, as well as minor elements like Pb. At this stage, forensic nuclear laboratories measure and describe the material to the best of their ability and for the goals of the investigation.

Nuclear forensic interpretation is the process of matching the features of a sample to information about known material manufacturing, processing, and usage procedures. The nuclear forensic laboratories' end product is the information produced as a result of this approach.

Reconstruction is the process of combining nuclear forensic interpretation information with all other available information (e.g., from forensic analysis of non-nuclear evidence associated with the sample or from intelligence sources) to determine the most complete history of the nuclear or radioactive material or event possible.

2.2.1 Nuclear forensic model action plan

The nuclear forensics model action plan (Figure 2.1) is a procedure that aids in the investigation of a nuclear security incident to provides generic direction on how to conduct a nuclear forensic examination and related operations in the context of a nuclear security event investigation (IAEA, 2015). The plan encompasses operations carried out by authorities who seek nuclear forensic studies, as well as laboratories that may be called upon to conduct analysis and interpretation. Nuclear forensic examination and interpretation could reveal information about the material involved in a nuclear security incident. Conclusions concerning the relationships between the material and humans, locations, events, and manufacturing processes can be reached when paired with other components of the inquiry, such as typical forensic results (IAEA, 2015). While a nuclear forensic capability is unlikely to be used on a regular basis, it may be critical in the investigation of a nuclear security event. Because nuclear forensics can play an important part in the investigation of a nuclear security event, the nuclear forensics model action plan (Figure 2.1) should be incorporated into South Africa's national response plan.

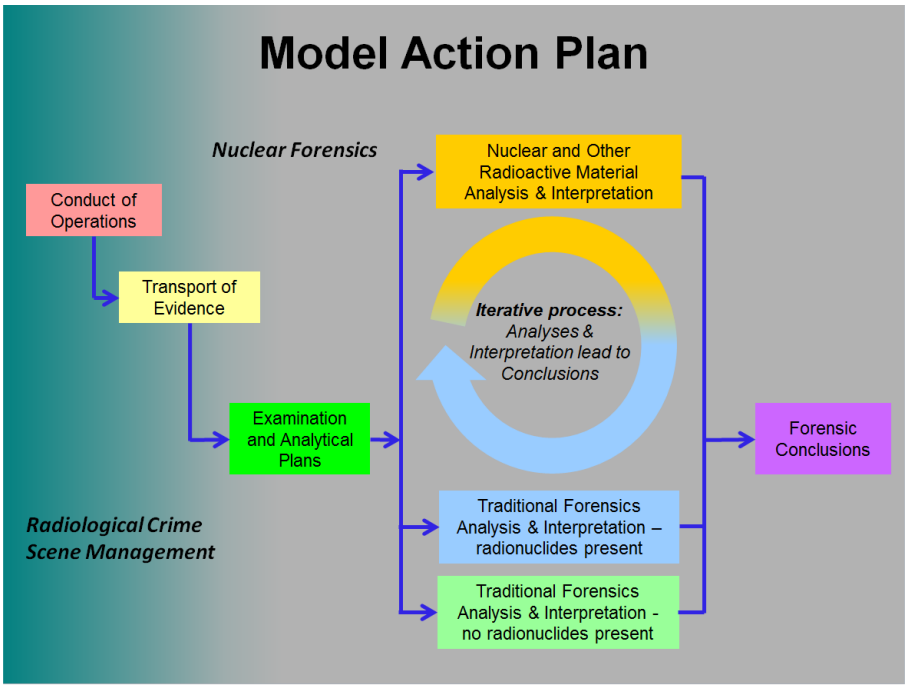

Figure 2. 1: A model action plan for nuclear forensics (IAEA, 2015).

2.3 Nuclear fuel cycle of uranium ore and UOC

The nuclear fuel cycle is an industrial method that encompasses all of the activities involved from uranium mining through to nuclear power reactors to electricity production. The processing of uranium ore concentrate (UOC) is one of the first steps in the nuclear fuel cycle. It all starts with the extraction of uranium from different ores in the deposit area. Uraninite (UO_2) or pitchblende (U_2O_5, UO_3, better known as U_3O_8) is the dominant ore mineral, with special deposits present in a variety of other uranium minerals (Krajko, 2016). The front end of the fuel cycle involves the process of mining and milling, as well as conversion, enrichment, and fuel processing. UOCs are a commonly traded commodity on the global market due to their high uranium content (>60%) and relative ease of transport (Kristo & Tumey, 2013a). As a result, UOCs are attractive materials for diverting for potential military production away from civilian influence. Modern UOCs are made up of various chemical compounds, such as ammonium diuranate, sodium diuranate, uranyl hydroxide, uranium peroxide, uranium diuranate, or uranium oxide, which contain 60-80 percent uranium (U_3O_8) (Kristo *et al.*, 2016). Complex trace elements and organic impurities are linked to UOCs. Figure 2.2 illustrates the descriptions of the different phases of the nuclear fuel cycle. On the other hand, uranium ores and ore concentrates (UOC) are examined in terms of their nuclear forensic properties, which are discussed in this chapter. Compared to materials produced later in

the fuel cycle, such as highly enriched uranium or plutonium, UOC is particularly attractive to nuclear forensic researchers because of its high impurity content (Kristo *et al.*, 2016). This research project is mainly focusing on the front end of the fuel cycle.

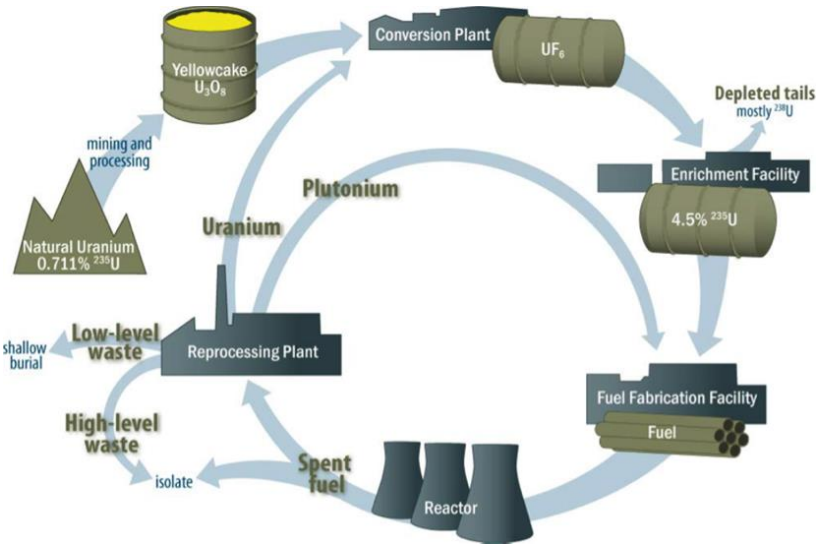

Figure 2. 2: Simple flow sheet of the nuclear fuel cycle (Nikitin *et al.*, 2010).

Uranium mining and milling

The uranium concentration in the ore can be as high as 20%. The traditional methods for extracting uranium ore from the mine are open pit and underground mining. The production of large volumes of solid and liquid residue is associated with uranium ore extraction, milling and chemical treatment of uranium ore concentrate, (U_3O_8) (Závodská *et al.*, 2008). The dry powder known as yellow cake is created during the uranium ore leaching process and after mining and milling, the end product, uranium ore concentration (UOC) is sent to a conversion facility where it is turned into uranium hexafluoride (Scheele, 2011). The most common minerals used to extract uranium are pitchblende and uraninite shown in Figure 2.3 (de Souza *et al.*, 2013). These minerals have low solubility in water and are found in hydrothermal veins of deposits in igneous and metamorphic rocks.

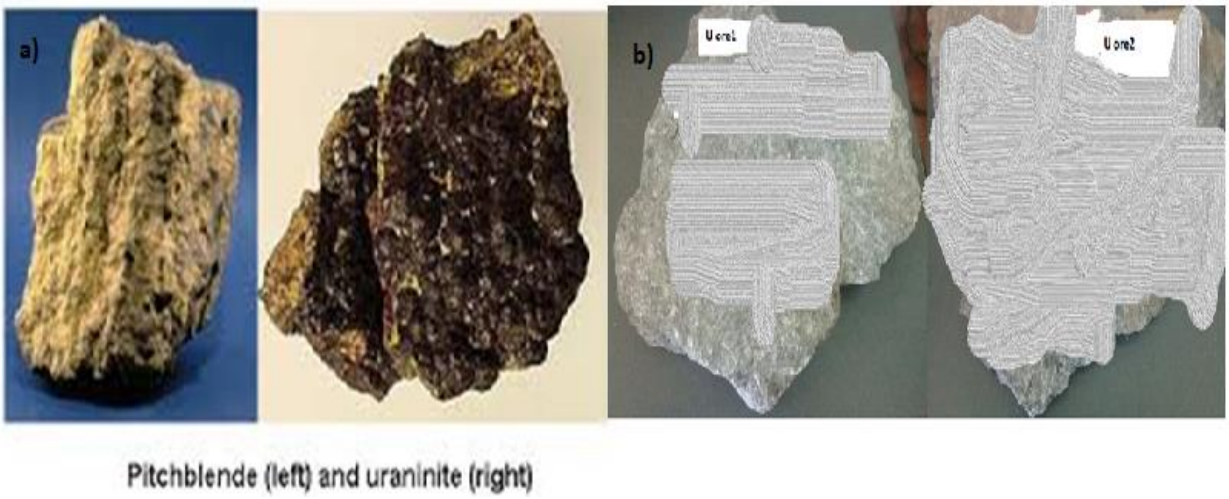

Figure 2. 3: (a) Unprocessed pitchblende and uraninite minerals (Kweto *et al.*, 2014), (b) uranium minerals used in this study.

Alternative approaches such as *in-situ* leaching (ISL) and heap leaching are gaining traction because of recent improvements in mining technologies (IAEA, 2001). Chemical solutions are pumped into subterranean deposits to dissolve uranium from the ore body via wells and bores (Nikitin *et al.*, 2010). The dissolved uranium is subsequently purified by bringing it to the surface. ISL, also known as solution mining, is leaving the ore in place and extracting the minerals by liquefying it and pumping the pregnant solution to the surface (Figure 2.4), where the minerals are extracted (WNA, 2020a). The leaching solution dissolves the uranium before being pumped to the surface treatment plant where the uranium is recovered as a precipitate. During the process of uranium recovery in ISL, in the areas with saline water tables, chloride is introduced (Quinn *et al.*, 2013) to allow the uranium to flow freely to the ground above where it can be processed. In this process, the number of procedures in the facilities including purification of leach solution and recovery of yellowcake by different precipitation methods is reduced (Lunt *et al.*, 2007).

Heap leaching is a hybrid of these two technologies in which uranium ore is first mined using traditional methods, then ground ore is heaped on an impermeable plastic and/or clay-lined leach pad and irrigated with a leach solution to dissolve uranium on-site. Only oxide ore resources are normally commercially viable for heap leaching. Weathering is a geological process that causes sulfide deposits to oxidize. As a result, oxide ore deposits are frequently found near the surface.

This strategy is beneficial in terms of downsizing and lowering capital and operating costs (Lunt *et al.*, 2007).

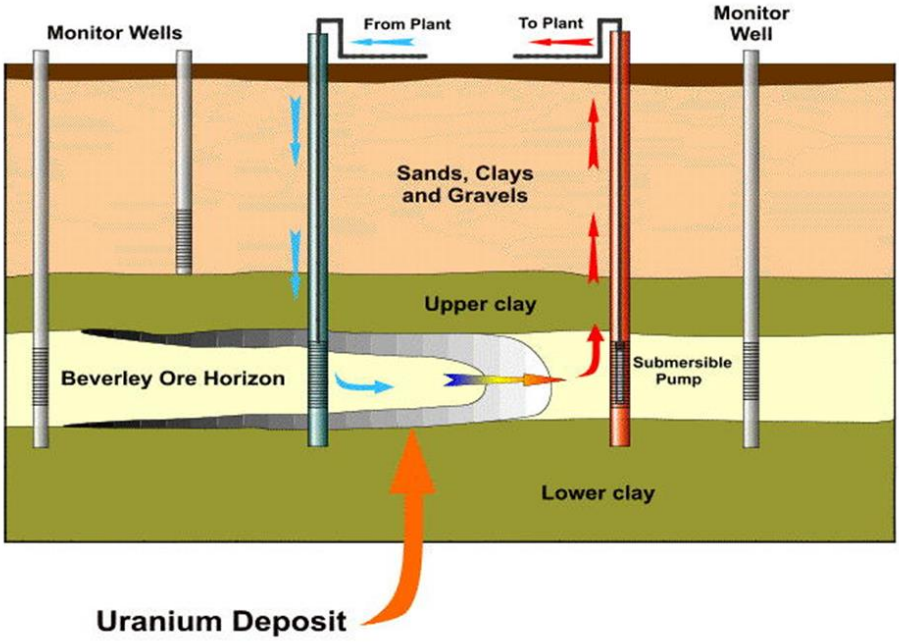

Figure 2. 4: *In-situ* leaching (ISL) (WNA, 2020a).

Conversion and enrichment

In the conversion plant, the yellowcake is refined, and then chemically treated with hydrofluoric acid in several procedures to produce uranium hexafluoride (UF6) gas, which is subsequently placed into cylinders and condensed to a solid. Uranium hexafluoride is made up of two isotopes of uranium: the heavier ^{238}U and the lighter, fissionable ^{235}U, which together account for around 0.7 percent of uranium by weight (Nikitin *et al.*, 2010). The concentration of fissile isotope ^{235}U needs to be enriched to at least 3-5%. For uranium to be enriched, it should be changed into a gaseous form. During the enrichment process, gaseous uranium hexafluoride is separated into two streams, first, one is being enriched to the required level known as low-enriched uranium, and secondly is depleted uranium in ^{235}U. The product that comes out of this stage of nuclear fuel cycles is enriched uranium hexafluoride which is reconverted to produce U_3O_8 that is stable, non-corrosive that can be safely stored and be used (WNA, 2021). Several studies aimed at identifying impurity signatures have led to the high concentration of elemental impurities in UOCs, with the hope that these signatures could be used to trace a UOC to the mine or mill of origin.

2.4 Uranium deposits in the world

Together with the propagation conditions and geological environment, the shift in uranium mobility means that deposits will usually contain up to a few percent of the uranium in percentage weight and, in some rare cases, up to 20 percent of uranium, such as Canada's McArthur river deposits. The world's uranium deposits can generally be classified into 14 groups based on the geological setting in which uranium mineralization occurred (Švedkauskaitė-LeGore *et al.*, 2008). Both uraninite and pitchblende the primary minerals, are present in almost all deposits of uranium, and typically contain elements of Th, Pb, and rare earth elements (REE). Uraninite is the UO^{2+}_{x} macrocrystalline type, is typically euhedral, and forms metamorphic rock, igneous rock, and vein deposits at high pressure and temperature. Pitchblende is a micro- or crypto-crystalline variety of low-grade metamorphic rock, metasediments, and sandstone with a botryoidal habit and shapes. Despite this, hexavalent, secondary minerals such as carnotite (uranium potassium vanadate), autinite (calcium uranyl phosphate), torbernite (copper uranyl phosphate), uranophane (uranium silicate), and brannerite (uranium titanium iron oxide) are the vast majority of uranium in rock (Dill, 2011). Most U minerals are also correlated with other metals and REE and may be unique to a specific deposit or area from time to time. There are four types of uranium deposits in Africa that produce the majority of the uranium (Winde *et al.*, 2017): archaen quartz conglomerate hosted gold uranium in South Africa; neopreterozoic end-ontogeny sheeted leucogranites and small stocks in Niger and Malawi; channel-hosted calcrete in Malawi and Namibia, and alluvial deposits in Namibia.

2.5 Uranium

Natural uranium is regarded as one of the most significant radioactive elements in the environment since it is the primary source of natural radiation to which all living things are exposed (Saleh & Abdel-Halim, 2016), and is primarily used for nuclear power generation, and in research reactors. Any of it may be traded illegally or come from illegal mining operations, and therefore there is an interest in whatever techniques could help to track the source of given uranium ore. On the other hand, uranium is unique in economic geology because it has been enriched by a wide range of processes in the Earth's crust to the level of ore deposits. This gives rise to not only a wide variety

of genetic forms of U-ore deposits, but also a wide selection of ore grades that are greater than for any other mineral product (Frimmel *et al.*, 2014).

Uranium has three main naturally occurring isotopes: ^{238}U (99.28%), ^{235}U (0.720%), and ^{234}U (0.0055%), and three anthropogenic isotopes (Saleh & Abdel-Halim, 2016). Natural uranium has two natural states of valence: U^{6+}, which under oxidizing conditions is soluble and mobile, and U^{4+}, which under reduction conditions is insoluble and immobile. Intrinsically, these two valences are related to the accumulation of U and the grade of global deposits.

2.5.1 Radioactive decay

The spontaneous shift within an unstable nucleus of an atom due to the nuclei having excess energy is radioactive decay (Martin, 2012). The release of energy also follows this process. This results in particles or electromagnetic radiation being expelled and, thus, the energy state of the nucleus is changed (Reading, 2016). Decay modes are usually alpha, beta, and gamma emissions, where certain unusual processes may occur, such as spontaneous fission. With one or more of these modes, each unstable isotope (radionuclide) will decay and will have a characteristic half-life of decay. The half-life depends on the amount of excess energy that the individual isotope has, along with the mode of decay and nucleus structure.

2.5.1.1 Alpha decay

The preferred mode of decay for heavy nuclei (Z > 83) is alpha (α) decay and it is characterized by the emission of a single alpha particle (Martin, 2012). The alpha particle is a nucleus of ^{4}He ($^{4}_{2}\mathrm{He}^{2+}$) with two protons and two neutrons, resulting in a physical transition to the parent isotope where Z-2 and A-4 are located. Alpha emissions have a short-range compared to other forms of radioactive emissions and can easily be stopped by paper. Alpha particles are tossed out with well-defined particles energies characteristic of the emitting nuclei thus permit spectroscopic measurement (Lilley, 2013). Equation 1 displays a typical decay of alpha nuclide. An example of Alpha decay is that of ^{238}U to ^{234}Th:

$$^{238}_{92}U = {}^{234}_{90}Th + {}^{4}_{2}He \qquad (1)$$

2.5.1.2 Beta decay

Beta (β) decay is identical to alpha decay, where a physical transition occurs in the parent nucleus and thereby becomes a separate isotope. An energetic electron (β^- decay) or positron (β^+decay) and a corresponding antineutrino or neutrino are released by the unstable nucleus. The beta decay process allows an unstable atom to achieve a more stable proton and neutron ratio (Lilley, 2013; Reading, 2016). In neutron-rich nuclei, β^- decay normally happens, and in proton-rich nuclei, β^+ decay occurs. β^- decay is a consequence of the conversion in the emitting nucleus of a neutron (n) into a proton (p) and results in no change in the number of atomic masses as shown in equation 2 (Martin, 2012). An example of β^- is that of thorium (${}^{234}_{90}Th$):

$$ {}^{234}_{90}Th = {}^{234}_{91}Pa + {}^{0}_{-1}e + \bar{\upsilon} \qquad (2) $$

2.5.1.3 Gamma decay

Gamma decay is characterized by photon emission and is commonly detected after decay methods that leave daughter nuclides in excited states. The latter is related to the energy levels of atomic and molecular spectroscopy. The product nuclide can also be left in an excited energy state by alpha and beta decay and is referred to as a nuclear isomer. Through the dissipation of energy as gamma (γ) photons in a process called isomeric transition, the isomer will collapse directly or in steps into the ground state (Simonetti *et al.*, 2013). The energy associated with each emission of photons is the difference between the parent and daughter states of the emitting nucleus with almost zero energy loss. Gamma radiation loses energy due to interactions with atomic electrons (Martin, 2012). It also travels great distances in dense material and is difficult to fully absorb.

2.5.1.4 Decay rates

To achieve stability, radioactive elements undergo radioactive decay. As a result, radioactive decay may be defined as the spontaneous conversion of an unstable parent nucleus into a more stable daughter nucleus. A group of comparable radionuclides will decay over time (t) according to an exponential function ($e^{-\lambda t}$) with a decay constant of λ. The half-life ($T_{1/2}$) is the time needed for half of the initial population of radionuclides to decay. The $T_{1/2}$ to λ relationship is given as $T_{1/2} = 0.639/\lambda$. The number of radioactive isotopes present after the time (Nt) can be demonstrated from an initial population of N_0 as follows:

$$ Nt = N_0 e^{-\lambda t}. \qquad (3) $$

When measuring the population of a daughter radionuclide, it is important to calculate the decay constants of both parent and daughter as the daughter population increases according to the parent's decay rate, but also decays according to its decay constant. The two radionuclides will finally be in a state of secular equilibrium when the parent's decay rate and half-life substantially exceed that of the daughter, as the number of daughter radionuclides created will equal the rate at which the same radionuclide decays. When researching the uranium decay sequence, secular equilibrium is of great significance because the long-lived chain head, ^{238}U, has a half-life of 4.47 billion years and far exceeds that of its daughter radionuclides. Therefore, all radionuclides up to ^{222}Rn will be present wherever ^{238}U is present in a closed system. In nature, four decay chains are observed: the uranium series, the actinium series, the thorium series, and the neptunium series, each generally known simply as the nuclide at the head of the decay chain (^{238}U, ^{235}U, ^{232}Th, and ^{237}Np, respectively). Figure 2.5 shows the uranium and thorium series.

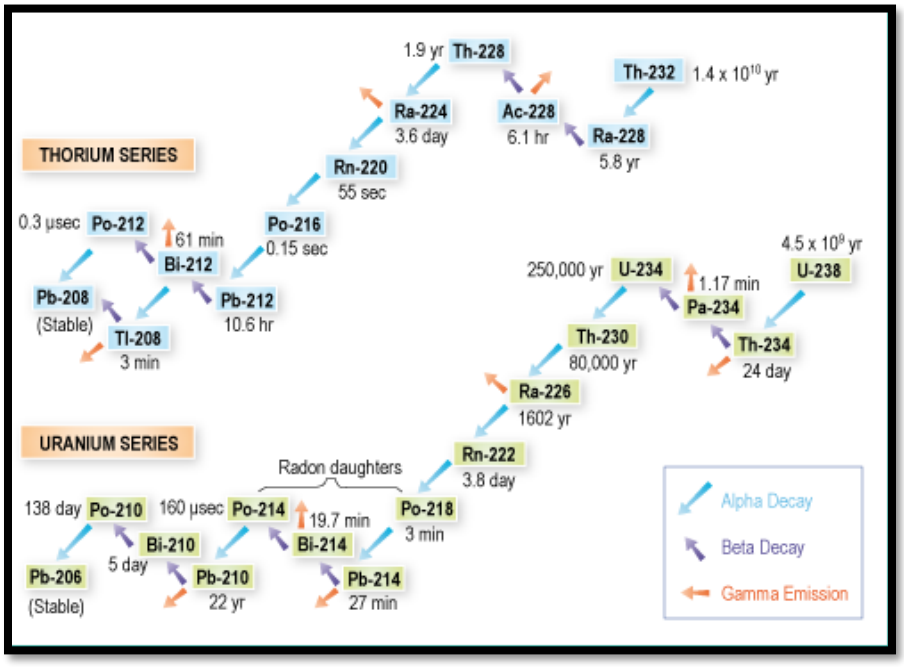

Figure 2. 5: Decay series of uranium and thorium (WNA, 2020b).

2.6 Investigations of nuclear forensic

Nuclear forensics has progressed over the past two decades by re-purposing and modifying approaches that have already been used for nuclear safeguards, material science, and geochemistry.

In the nuclear fuel cycle, as the range of chemical and physical forms of nuclear material is broad, different types of such materials have become part of nuclear forensic investigations. The case studies are summarized in the following section, and, more significantly, signatures are listed and used for interpretation. Such data can be classified as endogenous or exogenous, with the former referring to self-explanatory data (predictive approach) and the latter requiring comparative reference data (comparative approach) (Kristo & Tumey, 2013b; Mayer *et al.*, 2005b).

UOCs are intermediary materials containing natural uranium, as seen in the uranium fuel cycle. Although the emphasis is primarily on UOCs, this study will also discuss signatures that are relevant to other types of nuclear material. In addition to the production of signatures for forbidden industrial UOCs, it should be noted that, in the sense of nuclear fuel manufacturing, there are studies examining different aspects of the characteristics of particular UOCs. Although these subjects may not be specifically related to nuclear forensics, the relevant information is available which may be useful for further study. Methodologies have been developed and used in forensic investigations in recent years to determine the origin of confiscated nuclear material. Methods used to analyze many types of nuclear or radiological materials for forensic signatures are non-destructive analytical (alpha/ gamma spectroscopy, scanning electron microscopy, X-ray fluorescence) and destructive analytical (mass spectrometry and analytical separations) methods (Wallenius *et al.*, 2014).

2.6.1 Uranium pellet trafficking

Uranium pellets are known as an unusual substance that is banned. The first seizure, which led to nuclear forensic investigations in the Institute for Trans Uranium Elements (ITU), involved 72 uranium pellets (1.1 kg) intercepted in Augsburg, Germany in March 1992 (Mayer *et al.*, 2007). The physical dimensions and isotopic composition of the pellets were sufficient to suggest the planned use for the Russian graphite-moderated reactor of this low enriched uranium pellet. In a separate case that also occurred in Germany, 202 uranium pellets were recovered from a bank safe. The form of the pellets as fuel for light water reactors helped identify them. The 4.38 percent enrichment of ^{235}U suggested that the pellets were intended for reloading. Two nuclear manufacturing plants were identified as potential sources, and the roughness of the surface of the fuel eventually helped locate the plant (Koch, 2003). It may be easier to solve cases that involve pellets than powder. This is because the physical characteristics of fuel pellets for commercial use

(such as dimensions) are well known and databases are available and can be relied upon (Mayer *et al.*, 2007). Powders, on the other hand, are intermediate items and no such extensive databases are available that compile characteristic parameters. In addition to the measurement of the normal 8 parameters of uranium content and its isotopic composition, age and impurities, the microstructure of the sample gave a substantial indication of its processing history, while origin remained unknown (Wallenius *et al.*, 2006).

2.6.2 UOC trafficking

It has been stated that nuclear forensics has been used to examine actual cases involving UOCs and three of these cases have been disclosed. In Australia, one of the earliest cases occurred in which five barrels of yellowcake were stolen (Budinger *et al.*, 1980). In the Institute of Trans uranium elements (ITU) another sample, involving UOC was analyzed. The incident took place in December 2003, when a shipment of scrap metal at Rotterdam Harbor, the Netherlands, found 3 kg of radioactive material. The shipment had arrived from Jordan and through nuclear forensic inquiries; the discovered UOC was eventually tracked back to a facility in Iraq (Varga *et al.*, 2011b). More recently, the Australian Nuclear Science and Technology Organization (ANSTO) in which extensive nuclear forensic analysis was carried out published another unknown UOC case (NSR-F-130509) (Keegan *et al.*, 2008a).

2.7 Signatures used in nuclear forensics

Nuclear forensics is an important part of the process of attribution involving the study of nuclear material to identify forensic signatures resulting from established connections between material character and process background (Kristo *et al.*, 2016). Although nuclear forensics is a new discipline, a diverse range of work has been and is being carried out on the topic, concentrating primarily on methodologies that can be used, appropriate measuring techniques, and the identification of parameters that can be used to determine the origin of a substance.

As a result, nuclear forensic science must first identify those measurable parameters in or any combination of nuclear material that may be related to material history (Mayer *et al.*, 2007). These parameters are called "signatures". These parameters refer to any physical, chemical impurities, isotopic properties of uranium, morphology, and isotopic signatures of selected elements (Mayer *et al.*, 2012). Such signatures may be due to chemical activities such as

dissolution, extraction, ion exchange, or precipitation, or may be linked to physical operations such as neutron irradiation or radioactive decay (Mayer *et al.*, 2015). No single "signature" obtained for a sample can identify the origin of a sample with success. Instead, a variant of the above is implemented in order not to simply define an exact origin, but rather to minimize the origin ambiguities. It is therefore imperative that new signatures be developed and pre-existing techniques for the discipline be produced, as well as that data acquisition times for pre-existing techniques be improved. In nuclear forensic investigations, several parameters or a mixture of parameters have been used over the previous two centuries based on the nature of the seizures. Thus, nuclear forensics can help in the identification of the products, how, when, and where the materials were produced, and how they were designed to be used legally (Mayer *et al.*, 2015). Nuclear forensic science exploits data intrinsic to the nuclear material, converting the material into forensic evidence and revealing precious data to this "silent (radioactive) witness." Natural uranium signatures are correlated with one or both of the two types of the geological origin or related processes, similar to other materials applicable to nuclear forensics, e.g. plutonium or HEU.

During the nuclear fuel cycle (NFC), these signatures can be produced and lost, meaning that not all recognized nuclear forensic techniques could be applied to all the stages of the NFC. However, for example, in the conversion of U-ore to UOC, where additional process signatures are added, signatures can be carried through many stages of the NFC. Signatures collected from repeated measurements of known samples can be incorporated into a nuclear forensic database in which possible samples tested can be compared and the history and origin of the suspicious sample can be inferred. Isotopic composition, impurities, geometrical dimensions, age, and microstructure are the criteria used for such detection. These patterns are not appropriate for source attribution individually, but collectively minimize ambiguities and thus provide a clearer view of the potential sources (Kristo *et al.*, 2016). Figure 2.6 depicts a Venn diagram of legitimate nuclear forensic signatures that can be used to link material to its source. This section describes fundamental signatures, which are critical for the classification of uranium ore concentrate-based nuclear forensic investigations.

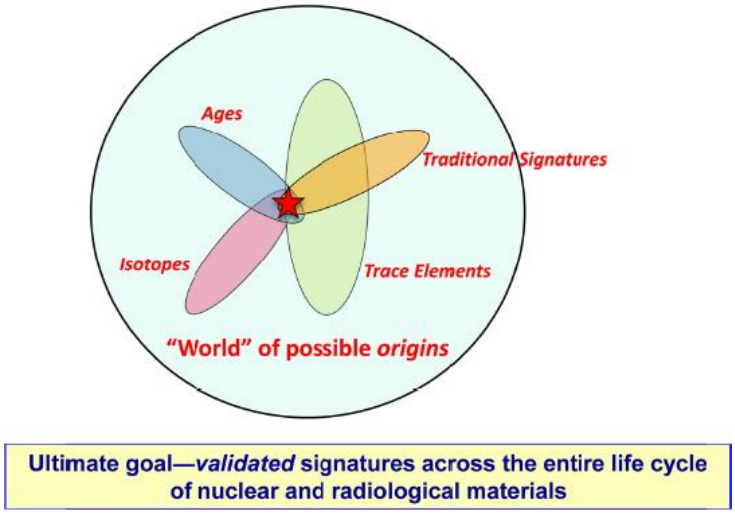

Figure 2. 6: Example of legitimate forensic nuclear signatures and the domain of potential material corresponding to such material signatures (Guenther *et al.*, 2013).

2.7.1 UOC Impurities and trace elements

2.7.1.1 Rare earth elements (REEs)

Lanthanide or rare earth elements (REE) are found in varying quantities in radioactive materials (uranium and plutonium). Certain lanthanides can be applied to nuclear materials on purpose. Burnable toxins like erbium and gadolinium, for example, are applied to nuclear fuel to control the reactivity of the fuel in nuclear reactors (Varga *et al.*, 2010b). Nuclear fission also results in the creation of REE in the reactor. Lanthanides can also be contained in small quantities in nuclear materials, either as contaminants from the raw material or as contamination from the manufacturing process.

Rare earth elements (REE) consist of 15 lanthanides plus yttrium and scandium. For nuclear forensic investigations, the REE concentration pattern in U-ore and UOC is an important signature (Varga *et al.*, 2010a) as the REE pattern is characteristic of the process of mineralization and the geological deposit (Mercadier *et al.*, 2011). Even after the milling process, the REE patterns remain largely unchanged and thus provide clear evidence of the origin of the interdicted UOC samples (Varga *et al.*, 2011b). These patterns are therefore an extremely significant signature, to provide details on the type of ore used for the production of the UOC.

In addition, due to REEs having the same oxidation state (3^+), except for Ce (IV) and Eu (II), there is no fractionation during the uranium milling process in the manufacture of UOC (Varga *et al.*, 2010b). Since the study's goal was to apply signatures, it is essential that each mine's fingerprint be unique in order to accurately identify its particular deposit type. This is achieved by employing a standard reference chondritic material with a known composition to normalize the REE data. To remove the impact of nuclear stability, the REE pattern is usually normalized to the C1-Chondrite values. The Oddo-Harkins rule stipulates that even atomic number elements are more common than elements with an odd atomic number. Odd-numbered elements tend to have lower energies for nuclear binding and are thus usually less stable than the elements themselves. After chemical separation with TRU resin, the REE concentrations were determined by HR-ICP-MS (Varga *et al.*, 2010b)**,** and more recently by laser ablating doped cation exchange resin with decreased isobaric interference from oxides and hydroxides and by electron probe microanalysis (EPM) (Keatley *et al.*, 2015)**.**

2.7.1.2 Anionic and organic compounds

In the milling process, several organic compounds are used, especially in the solvent extraction stage. Only one study has recorded observations of dioctylamine, triisoctylamine, and alamine ® 336 in uranium ore concentrates (UOCs) using the Twister ® stir bar sorptive extraction technique and gas chromatography-mass spectrometry detection (Kennedy *et al.*, 2013). One research was conducted to determine the variability and abundance of different organic constituents by extracting the organic components from the UOC and measuring through GC-MS between two separate UOC production lines (Kennedy *et al.*, 2013). There were very different organic fingerprints on the two production lines, and the author believes that this may be used as an identification technique for nuclear forensics.

Ion chromatography was used to investigate anion impurities in yellow cakes. By this process, several anions can be identified, such as Cl^-, F^-, Br^-, NO^{3-}, SO_4^{2-}, and PO_4^{3-} (Keegan *et al.*, 2012). The use of the ratio was found to be a more robust measure (based on the concentration of two anions such as SO_4^{2-}/Cl^-) than the individual anion concentration (Badaut *et al.*, 2009). The presence of phosphates, if any, may mean that rocks or materials based on phosphates were used to make the yellow cake. In addition, the existence of fluorides, which are not a reagent used in

the process of mining or milling, would mean that the substance may have come from mineral-containing fluoride such as apatite (Keegan *et al.*, 2014).

As possible signatures, anions such as sulfate, chloride, nitrate, and fluoride were examined in UOCs and were found to be either source-related (F^-/Cl^-) or process-related (SO_4^{2-}/Cl^-). UOCs produced from phosphate ores that usually contain apatite minerals ($Ca(PO_4)3FF$) have been found to contain elevated fluorine. Differences between uranium deposits used for UOC production were shown by other anionic impurities, such as nitrate/chloride and phosphate/chloride (Badaut *et al.*, 2009; Keegan *et al.*, 2012). The ratio of sulfate/chloride has been used to suggest milling facilities that use sulphuric acid for uranium leaching. In UOC, residual organic compounds from the milling process are present and provide details on the process and solvents used (mostly for purification of solvent extraction).

2.7.1.3 Major elements and trace elements

During the manufacture of uranium fuel, impurities are usually released from the crushing of the uranium ore, leaching uranium from the ore, purifying, precipitating, and calcination processes (Švedkauskaitė-LeGore *et al.*, 2008). The impurities indicate the production process as well as the geolocation (Wallenius *et al.*, 2006).

Impurities are added both purposely, to improve the end product, and unintentionally, as contaminats from feed or processing (Mayer *et al.*, 2012**).** As a result, the composition of nuclear material gives crucial information on the substance's characteristics. X-ray fluorescence (XRF) (energy and wave dispersion) has been used to classify bulk materials and UOC elemental compositions where the concentration of the main element was > 100 μg / g (Keegan *et al.*, 2008b). Keagan *et al* stated that the XRF data is comparable (within 20 percent uncertainty) to Inductively coupled plasma mass spectrometry (ICP-MS) data, but the XRF data was not shown. Laser-induced breakdown spectroscopy (LIBS) ionizes a sample's surface and produces a spectrum of photon emissions where a specific element is characteristic of each observed wavelength peak. With the assistance of principal components analysis (PCA), LIBS has been successfully used in the identification of UOC (Sirven *et al.*, 2009). Keegan *et al* researched elemental fingerprints in which they analyzed trace elements composition of UOC using XRF, ICP-MS, and PCA and discovered it to be a unique criterion for distinguishing three uranium mines in Australia (Keegan

et al., 2016). When dealing with bigger sample sets, the impurity pattern was shown to be beneficial in matching UOC samples to their deposit types and geo-source (Mayer *et al.*, 2012).

2.7.2 Patterns of isotopic composition in uranium deposits

Only minor differences in the isotopic composition are demonstrated by naturally occurring chemical elements. These elements are subjected to nuclear reactions, induced fission (n, f), and neutron capture (n, y) until irradiated in a nuclear reactor, altering the isotopic composition of the sample to the composition determined by the conditions of the reactor (neutron energy range, irradiation time, cooling time) (Nicolaou, 2006). The isotopic composition of chemical elements is often altered by manufacturing treatments such as chemical separation, thereby producing new patterns that can act as a distinguishing fingerprint. It is defined as natural uranium consisting of isotopes ^{234}U, ^{235}U, and ^{238}U. The ^{235}U isotope abundance is believed to be constant at about 0.71 percent, but highly accurate inductively coupled plasma mass measurements indicate that the $^{235}U/^{238}U$ ratio is variable and can be due to natural isotope fractionation (Hiess *et al.*, 2012).

Uranium has three naturally occurring isotopes: ^{238}U (half-live of 4.5×10^9 a), ^{235}U (half-live of 7.0×10^8 a), and the shorter-lived ^{234}U (half-live of 2.5×10^5 a). While the $^{235}U/^{238}U$ ratio has been determined to be stable across the Earth, the fluctuation of $^{234}U/^{238}U$ is widely known, except for Gabon, West Africa (Chen *et al.*, 1986). Weakly bound ^{234}U is more susceptible to extraction from minerals than lattice bound ^{234}U due to the combined effects of alpha-recoil from mineral grains during ^{238}U decay and subsequent damage to the crystal structure (Keegan *et al.*, 2008a). Uranium has a broad range of isotope compositions. Depleted uranium has a ^{235}U abundance of less than 0.72 %, natural uranium has a ^{235}U abundance of 0.72 %, low enriched uranium has a ^{235}U abundance of more than 0.72 % but less than 20 %, and highly enriched uranium has a ^{235}U abundance higher than 20 % (Mayer *et al.*, 2013).

Study have shown that the ratios of uranium isotopes vary from one geological material to another. Isotopic variations in the $^{234}U/^{238}U$, $^{235}U/^{238}U$, and $^{236}U/^{238}U$ ratios of natural uranium ores from different mines have been found in several studies (Keatley *et al.*, 2015). While the $^{235}U/^{238}U$ ratio of terrestrial materials has long been believed to be invariant, recent work has shown that the $^{235}U/^{238}U$ terrestrial ratio differs across a spectrum of 1.3 in various geological materials (Weyer *et al.*, 2008). In 2010, the $^{235}U/^{238}U$ ratio of UOC samples was also studied by (Brennecka *et al.*, 2010) to link the variations observed with the ore U mineralization.

An indication of neutron irradiation and uranium reprocessing (Simonetti *et al.*, 2013) is the presence of ^{236}U abundances in higher amounts than those determined in natural uranium samples. In 2011, an investigation of using ^{236}U abundances as a global nuclear forensics signature within uranium ores, and identified significant variations in the $^{236}U/^{238}U$ ratio for Australia, Brazil, and Canada samples (Srncik, 2011). From these observations, it was proposed that viable forensic signatures in ore samples were possible for uranium isotopic ratios. Although isotope ratios of uranium are significant parameters, ambiguities still exist. The same signatures were investigated in the UOC, but some ratios overlapped this time (Keatley *et al.*, 2015). To reduce ambiguity, it is, therefore, necessary to have several other signatures.

2.7.2.1 UOC Isotope composition

It is also possible to carry out the original evaluation of unknown nuclear content by studying the isotopic composition of unique elements. Two chemically identical compounds can have distinct stable isotope compositions if they come from separate sources. Some of the elements that have been successfully validated as signatures for source allocation are lead, strontium, sulphur, neodymium, and oxygen (Aggarwal, 2016).

- ***Uranium isotopes***

Uranium isotopic composition is a critical signature to be obtained from U-bearing compounds and can vary greatly, for example, whether a sample is enriched or depleted in ^{235}U, depending on the sample provenance in the NFC. The isotope ratio of $^{238}U/^{235}U$ has been widely accepted for many years as 137.88 and has been invariant until recently. However, more recent studies have shown that this is not the case as variability per mill level has been measured in near-surface environments that allowed the average terrestrial composition to have a higher precision value of 137.797 (Weyer *et al.*, 2008). The $^{234}U/^{238}U$ and $^{235}U/^{238}U$ can be rapidly calculated through gamma and alpha spectrometry, but mass spectrometry techniques (e.g. multi-collector inductively coupled plasma mass spectrometry (MC-ICPMS), thermal ionization mass spectrometry (TIMS), accelerator mass spectrometry (AMS), or secondary ion mass spectrometry (SIMS)) are needed for greater accuracy and precision. These ratios calculated in UOC and the ratio of $^{234}U/^{238}U$ showed the greatest difference between samples and geological deposits due to alpha recoil and subsequent leaching of U from the weakened mineral lattice, which means that it is possible to

determine the provenance of samples based on U isotopes (Brennecka *et al.*, 2010; Keegan *et al.*, 2008a). The analysis by Brennecka and his group (2010) showed that the ratios of $^{238}U/^{235}U$ is 137.792. Intra-mine variability is not measured by these studies and the conclusions are based on small sample sets. The authors suggest that the origin of an unknown UOC would take several isotope compounds (such as Pb and Sr) to be found.

- ***Lead and strontium***

Lead (Pb) has four known stable isotopes (^{204}Pb, ^{206}Pb, ^{207}Pb, and ^{208}Pb), of which only ^{204}Pb is non-radiogenic and the other three derived from the decay of radionuclides of uranium and thorium. The normal lead isotopic composition is $1.4 \pm 0.1\%$ ^{204}Pb, $24.1 \pm 0.1\%$ ^{206}Pb, $22.1 \pm 0.1\%$ ^{207}Pb and $52.4 \pm 0.1\%$ ^{208}Pb (Rosman & Taylor, 1998). The enormous difference between mines is observed, as U content, Th content and age of a deposit can differ, which can be a useful signature in determining the origin of UOCs (Fahey *et al.*, 2010; Keegan *et al.*, 2008b; Švedkauskaitė-LeGore *et al.*, 2008). It was also found that the existence of high ^{208}Pb levels produced by ^{232}Th decay was indicative of certain deposit forms, such as quartz-pebble conglomerate, known to contain high concentrations of thorium. In addition, given the low natural lead contribution (< 60 percent), the deposit age can be extracted from the $^{207}Pb/^{206}Pb$ ratio, thereby adding another attribution signature (Varga & Surányi, 2009). However, the considerable variety of lead isotopic composition within mines must be considered. In addition, Pb isotopes were used to differentiate between natural U samples resulting from production activities, and those resulting from anthropogenic activities (Fahey *et al.*, 2010). Švedkauskait-Le Gore (2008) showed that samples from the same geolocation tend to have largely identical Pb isotopes. However, Varga *et al* (2009) stated that there is substantial Pb variability in UOC due to heterogeneous Pb distribution in the ore body and due to the processing effects of chemical separation and dilution with natural Pb from the same mine site (Varga *et al.*, 2009).

^{87}Sr is not constant and is attributed to the long half-life of the ^{87}Rb parent nuclide, the cause of its variations. Consequently, the isotopic ratio of $^{87}Sr/^{86}Sr$ of UOCs was tested for provenance. As the inside-mine variability of the investigated UOCs was much smaller than that found for the lead isotope ratios, this ratio tended to be a more stable measure (less influenced by the manufacturing process). The ratios also varied across a wide range (0.7034 to 0.7606) and higher of UOCs and

could therefore be used to distinguish between different samples of origin and to check their origin by comparing them with known samples (Varga & Surányi, 2009). In the forensic study of UOCs from actual events, both isotope ratios were used (Keegan *et al.*, 2014; Varga *et al.*, 2011a). It has shown that strontium isotopes vary across a wide variety of samples of different geographical origins and are affecting the deposit age and other geological factors, such as the abundance of alkali metal-rich minerals depending on the type of geological deposit (Varga & Surányi, 2009). Varga et al. (2009) utilized an isotope ratio of $^{87}Sr/^{86}Sr$, since ^{87}Sr fluctuates significantly in nature due to its parent, ^{87}Rb, having a long half-life ($4.923x10^{10}$ years). The variance in uranium deposits and modification of the isotopic signature resulting from milling is smaller than that of Pb isotopes. Related types of deposits have an isotopic composition similar to Sr, resulting in the need for a multi-variant provenance determination method.

- ***Oxygen***

The use of $^{18}O/^{16}O$ for nuclear forensic purposes in uranium oxide samples has also been exploited (Pajo, 2001). It can only be used for certain samples. Depending on geo-location, the isotopic oxygen ratio in rainwater and surface water is known to differ. As water is widely used as a solvent in the processing of uranium, variations in the UO_2 product are predicted to be the signature of the $^{18}O/^{16}O$ ratio due to geographical position (Mayer *et al.*, 2007). Isotopic oxygen can serve as a viable signature in nuclear forensic science for UOC samples. Pajo et al. (2001) worked on the applicability of nuclear forensic science of such parameters in one of his studies: selected impurities and $^{18}O/^{16}O$ ratios for geo-location. In uranium oxide samples from various mines, minor variations in $^{18}O/^{16}O$ isotope quantity ratios of less than 3 percent were observed (Mayer *et al.*, 2012).

- ***Sulfur***

Recently, the use of the sulfur isotope ratio ($^{34}S/^{32}S$) in UOCs for origin assessment has been reported. As previously, outlined, sulphuric acid is commonly used in the process of leaching. Clear variations in the isotopic sulfur composition of $\delta^{34}S$ take into account the normal $^{34}S/^{32}S$ values observed in UOCs. In some facilities such as El Mesquite, Crow Butte, USA Mobil, where *in-situ* carbonate leaching was carried out and could be used as a predictive signature, low $\delta^{34}S$ values were found. However, there were overlaps between samples with different sources in the

$\delta^{34}S$ values, and thus, the isotopic sulphur composition could instead be used as a comparative signature in such situations (Han *et al.*, 2013).

- ***Neodymium***

Measurement and use of $^{143}Nd/^{144}Nd$ as a potential signature have recently been established for uranium-bearing materials such as uranium ores and UOCs, showing differences depending on the type of geological deposit, origin, and the age of the deposit (Reading, 2016). Because it is less susceptible to weathering, this ratio offers a more durable signature (Aggarwal, 2016). However, the intra-mine differences were smaller than those found for Pb and Sr, and ratios were overlapped for some mines, so $^{143}Nd/^{144}Nd$ is not a valid signature independently (Krajkó *et al.*, 2014).

2.7.3 Age or production date

A nuclear material's age refers to the time since the last chemical separation or purification has elapsed. This parameter makes use of the fact that parent nuclides decay to daughter nuclides with principles derived from age dating in geological or archaeological processes (Wallenius *et al.*, 2000). An indication of material age is given by the ratio of parent and daughter nuclides and thus serves as a built-in chronometer. This parameter is extremely important in determining the origin of the material since it can be used to exclude certain manufacturing or reprocessing plants that, based on the stated date of manufacture, were not in service or were not processing the type of material at the given time. Various parent-daughter nuclides, such as $^{234}U/^{230}Th$, $^{235}U/^{231}$ Pa, and $^{236}U/^{232}Th$ (Wallenius *et al.*, 2002), can be based on this predictive signature. As ^{236}U does not exist in nature, the last parent-daughter pair refers only to irradiated and reprocessed uranium.

Due to the long half-lives of ^{234}U (2.46×10^5 years) and ^{235}U (7.04×10^8 years) and consequently the slow growth of the daughter nuclides, the $^{234}U/^{230}Th$ and $^{235}U/^{231}Pa$ studies need a low detection limit of ^{230}Th and ^{231}Pa (Morgenstern *et al.*, 2002). For this form of analysis, therefore, very sensitive methods such as inductively coupled plasma mass spectrometry (ICP-MS) (Varga & Surányi, 2007), thermal ionization mass spectrometry (TIMS) or alpha spectrometry must be used. Direct calculation of both parent and daughter nuclides is often constrained by the long half-lives of uranium isotopes, although indirect methods such as isotope dilution for calculating the parent/ daughter ratio have low uncertainties but include adding spikes. Due to the availability of well-certified thorium reference materials as tracers for quantification and the lack of long-lived Pa

isotopes that could serve as spike, results in the preferred application of the chronometer $^{234}U/^{230}Th$ (Varga *et al.*, 2012; Wallenius *et al.*, 2002). The alternate parent-daughter pairs are $^{234}U/^{214}Bi$ and $^{238}U/^{234}Th$, in addition to the above (Varga & Surányi, 2007). Plutonium content is also known for age determination and several pairs of parent/daughter nuclides are possible: $^{238}Pu/^{234}U$, $^{239}Pu/^{235}U$, $^{240}Pu/^{236}U$, $^{241}Pu/^{241}Am$ and $^{242}Pu/^{238}U$ (Mayer *et al.*, 2012). In addition to the era, the form of the reactor can also be defined from plutonium isotopes because it is created by uranium neutron irradiation. The fact that different types of reactors show different spectrums of neutron energy and neutron flux can explain this. Since the probabilities of reaction (known as cross sections) of the various Pu isotopes vary with the energy of the neutrons, different types of reactors produce Pu of different isotopic compositions (Mayer *et al.*, 2005b; Wallenius *et al.*, 2007).

2.7.4 Morphology

Microstructural fingerprints were developed to supplement isotopic and elemental fingerprints, particularly in circumstances where the isotopic composition was not definitive (Ray *et al.*, 2003). Furthermore, as compared to chemical analytical methods, microscopy delivers completely distinct information (i.e. morphology) about the material. The morphology of interdicted material was investigated using Scanning electron microscopy (SEM) this is described in section 2.8.3. It is also, on the other hand, a challenging technique for developing measurable parameters for powder samples like UOCs. The SEM technique is not new. It's a common instrument in the food business, for example, to test the texture of pasta (Fongaro & Kvaal, 2013). Its use in nuclear forensics, on the other hand, is novel. It has been used to make laboratory-made UOCs as well as some industrial products (Plaue, 2013). The author collected SEM images at a magnification of 50000x in that study, and the textures were analyzed utilizing techniques including pattern spectra, granulometric curve, and gray-level co-occurrence matrix. A different approach was used in this work to investigate image texture analysis. Instead, SEM images would be collected at different magnifications to access the texture of several industrial samples.

2.8 Analytical techniques used in nuclear forensics

The common analytical techniques used for measurements are illustrated in this section, in which uranium ore concentrates (UOCs) signatures for nuclear materials are discussed. Microscopic techniques that are often used in a standard nuclear forensic investigation are also illustrated in

this section. Some analytical methods provide strictly qualitative information, such as color, shape, and markings, but the majority of analytical methods are quantitative, providing means values and associated information for various material characteristics, such as mass, dimensions, and trace elemental composition.

2.8.1 Alpha spectrometry

Alpha spectrometry has been used for accurate age determination of higher enriched uranium (HEU) using the $^{234}U/^{230}Th$ chronometer and has comparable findings to inductively coupled plasma mass spectrometry (ICP-MS) methods (Wallenius *et al.*, 2002). Alpha spectrometry has also been used for the determination of ^{232}U, ^{236}U, and Pu to assess if a sample has undergone irradiation or reprocessing (Varga & Surányi, 2009).

2.8.2 Gamma spectrometry

In nuclear safeguards and in nuclear security for revealing illicit trafficking, characterization of nuclear materials is equally essential (Lakosi *et al.*, 2009). Materials analysis is a central concern in both areas. To safeguard the credibility of forensic evidence and preserve its integrity, NM nondestructive assay (NDA) procedures are recommended in charge of quick on the spot identification and evaluation of seized forensic evidence. Gamma-ray spectrometry is the non-destructive means by which illicitly recovered radioactive materials are initially identified and is one of the first analytical techniques to be used on suspected materials. Gamma spectrometry provides details on the estimated isotopic abundance of uranium. Using the $^{234}U/^{214}Bi$ chronometer, a couple of studies have also successfully determined the ages of U-bearing materials via high-resolution gamma spectrometry (Nguyen & Zsigrai, 2006). For each particular type of measurement, the detector must be selected appropriately. Some issues related to the manufacturing processes and planned end-use can be answered when characterizing nuclear material of unknown origin. The full allocation of materials to the point of loss of control may be possible if there is also a suitable knowledge foundation (Nguyen & Zsigrai, 2006).

Gamma spectrometry is commonly used to identify the isotopic makeup of radioactive materials. Each radioisotope emits γ-rays with characteristic energies upon decay, providing a fingerprint of the composition of the sample. Relative line intensities can then be used to determine isotope ratios, and to determine sample age, origin, and history of processing. High-purity germanium

(HPGe) detectors have become the industry standard for high-resolution measurements, but they need to be cooled using liquid nitrogen to reduce leakage current (Suen, 2012). HPGe detectors allow measurements of the isotope ratio with an error of ~1% or better depending on the sample, restricted either by counting statistics or by systematic detection efficiency errors or by subtraction of the history (Suen, 2012).

2.8.3 Scanning electron microscope (SEM)

A valuable instrument for nuclear forensic investigations is the scanning electron microscope (SEM). This is the most common way of examining the microstructure and morphology of samples. SEM was used to allow direct comparisons with an unknown sample between a previously characterized UOC (Keegan *et al.*, 2014). Using an electron dispersive X-ray detector, the SEM can also be used to obtain micron-scale elemental data. A centered beam of high-energy electrons is primarily rasterized over the sample and because of the interaction; various types of electrons are created and detected independently, depending on the site of the electron beam incident. Images are thus made, of the topography or the contrast captured sample depending on the Z number of the elements present. SEM is commonly used to examine particle form, appearance, and size distribution (Mayer *et al.*, 2007). On UOCs, the same notion of particle size distribution may be utilized. These quantifiable characteristics are intended to provide information on the processing history and/or origin of the material in question. So far, no research has been done utilizing SEM to characterize these industrial UOCs. In addition to the use of UOCs in forensic analysis (Mayer *et al.*, 2007; Varga *et al.*, 2011b), SEM was also used in other incidents, e.g. for the analysis of uranium pellets from Lithuania (Wallenius *et al.*, 2006), uranium pellets from Kazakhstan or Russia intended for Russian type graphite-moderated reactor (Mayer *et al.*, 2007). It was also used in highly enriched uranium powder from the Czech Republic (Wallenius *et al.*, 2006), mixed oxide (MOX) powder from Munich airport (Wallenius *et al.*, 2007) and plutonium powder (Mayer *et al.*, 2007).

2.8.4 Transitional electron microscopy (TEM)

Transmission electron microscopy (TEM) allows for the study of the internal structure or morphology of extremely small samples (microns to nanometers). The preparation of the sample and the operation is more expensive than SEM and is thus not commonly used in nuclear forensic laboratories. Unlike SEM, TEM is a method that needs a well-trained and competent operator and

sensitive preparation of the sample. Besides, any nuclear forensics needs attention to make it better. As a result, the application of TEM in nuclear forensic research has remained a mystery (Kim *et al.*, 2011).

Usually, TEM is used in nuclear forensics to analyze grain size (Mayer *et al.*, 2007). The case of seized samples of uranium-plutonium mixed oxide powder in Munich, previously reported, was a clear example of the use of TEM (and complementary to SEM). The SEM image of the PuO_2 platelets from the seized sample was compared with that of the reference material for PuO_2 (from the known manufacturing plant) and showed no difference between the two samples. TEM images of both samples, however, revealed a substantial difference between them (Mayer *et al.*, 2005a). The exclusion principle may be extended to exclude that particular fabrication plant.

2.8.5 X-ray diffraction (XRD)

X-ray diffraction (XRD) has been used in UOC samples for phase determination of uranium and trace minerals and gangue determination (Aggarwal, 2016; Reynolds *et al.*, 2010). XRD is also used to classify U-ore and UOC chemicals that may be involved with the processing of the ore. In addition to providing the material phase, the XRD pattern's line expansion can also provide the average crystallite dimension. Choi et al. (1988) compared the crystallite size of three UO^2 powders from three different AUC manufacturing plants using this approach. From the crystallite size of UO_2, (Clayton & Aronson, 1961) also determined that the preparation temperature affected the size more than the preparation method.

2.8.6 Mass spectrometry

Mass spectroscopy (MS) techniques are indispensable in modern nuclear forensics investigations. Mass spectroscopy techniques are capable of accurately providing elemental and isotopic information for a variety of materials while requiring reduced sample mass relative to counting techniques. These methods also provide quantification of nuclides of interest through the addition of a tracer; this is known as isotope dilution mass spectroscopy. The need to distinguish between highly similar analytes (e.g. ^{235}U and ^{236}U) present in drastically different proportions is one of the primary challenges with these approaches; thus, excellent resolution/mass abundance, low backgrounds, and, in general, proper instrument functioning/programming are required. Below are some other options for carrying out this sort of work.

Thermal ionization mass spectrometry* (*TIMS)

Thermal ionization mass spectrometry (TIMS), which was first used in 1918, is one of the oldest mass spectrometry technologies. It's the most well-known approach and still the gold standard for determining the isotope ratio (Becker, 2008). As a result, the regulated ionization process, TIMS can measure even fine isotopic variation in nature with a precision of 0.01 percent for single ion collectors and 0.001 percent for multi-collector systems (Becker, 2008). The samples, on the other hand, should only include the elements of interest, which frequently involves time-consuming chemical separation (De Laeter, 2001). TIMS is the standard instrument for accurate isotope ratio quantification, even though it involves significant sample preparation and extended measurement durations.

Secondary ionization mass spectrometry* (*SIMS)

Secondary ionization mass spectrometry (SIMS), analyzes the surface for several elements with minimum sample preparation (De Laeter, 2001). SIMS involves placing a sample under a high vacuum and bombarding it with a stream of primary ions such as Ar^{+}, Cs^{+}, Ga^{+}, O^{-}, and O^{2+} with energies ranging from 0.2 to 40 keV, (Becker, 2008). (Ranebo *et al.*, 2007) used SIMS to characterize individual particles with a matrix originating from a nuclear weapon. In their study, they found that the materials were a mixture of highly enriched ^{235}U (^{235}U:^{238}U ratio from 0.96 to 1.4) and weapons-grade Pu (^{240}Pu ratio from 0.028 to 0.059).

Inductively coupled plasma mass spectrometry* (*ICP-MS)

Even though inductively coupled plasma (ICP) was first designed for optical emission spectroscopy, it has become the more standard system due to its high sensitivity and relatively simple spectra (De Laeter, 2001). Induction heating of a noble gas, commonly argon, in a torch consisting of three concentric quartz tubes produces the ICP. ICP-MS may also be used to survey the elemental composition of items of interest utilizing more typical detection configurations. These approaches can be used to quantify a variety of contaminants of interest.

CHAPTER 3: RESEARCH METHODOLOGY

3.1 Introduction

For almost fifteen years the area of nuclear forensics has become a subject of concern in science, public policy, and popular press literature (L'Annunziata, 2012). The 'study' forms the cornerstone of forensic investigation and involves, but is not limited to radiometric methods of measurement. The analytical techniques used in nuclear forensics with a focus on gamma spectrometry, SEM, ICP-MS, and XRD are defined in this chapter as they are applied in the research.

3.2 Study area

The study area is a nuclear facility and the authors herein cannot give further details due to confidentiality agreements. Samples were collected from a nuclear facility in South Africa. To determine the sample origin, we were looking at trace elements, rare earth elements, isotopic ratios, and impurities. Samples used in this study consisted of a total of four UOC powders and two uranium ore collected from a nuclear facility in South Africa.

3.3 Sample analysis techniques

3.3.1. Non-destructive surface characterization techniques

Before destroying the physical appearance of a sample, scanning electron microscopy (SEM) was used to determine physical or morphologic information about the UOC and uranium samples. Energy dispersive spectroscopy (EDS) is usually coupled to an SEM and can provide qualitative or quantitative elemental composition. This is a great method to pre-screen samples for specific characteristics or elemental composition. In addition, to determine the physical phases of a sample, a gamma detector was used to characterize the samples and determine the activity level.

3.3.1.1 Gamma spectrometry

Gamma-ray spectrometry is one of the first analytical methods to be conducted on suspicious materials and is a non-destructive technique for the characterization of radioactive materials initially unlawfully recovered. Gamma-ray spectrometry provides descriptions of the measured isotopic uranium abundance, indicates in the natural sequence of decay the degree of growth of daughter radionuclides and if there are activation and fission products present. This spectrometry which is based on germanium detectors is one of the most widely used techniques for the detection

and quantification of radionuclides from various types of environmental samples (Mayer *et al.*, 2007). The technique provides an accurate characterization of radioactive samples based on measurements of uranium mass that are important for nuclear measurement and safeguarding activities. In gamma-ray spectroscopy, the energy of incident gamma rays is measured by a detector. By comparing the measured energy to the known energy of gamma rays produced by radioisotopes, the identity of the emitter can be determined. This technique has many applications, particularly in situations where rapid non-destructive analysis is required. Gamma spectrometry measures several radio-nuclei emitting gammas in a single sample measurement without damaging or handling the sample. The measurement technique used in this investigation was a Canberra well HPGe model GC2021 (Canberra Industries Inc., USA) based gamma spectrometer located at the Center for Applied Radiation Science and Technology, North-West University, Mafikeng Campus. It exhibits a 36% relative efficiency and 1.86 keV energy resolution at the 1332.5 keV line. The gamma spectrometer consists of the HPGe well detector, a pre-amplifier, a spectroscopy amplifier, and multichannel analyzer (MCA) and a high voltage supply (Figure 3.1).

Figure 3. 1: Experimental setup of an HPGe well gamma detector at NWU-CARST.

Accordingly, reliable measurements for nuclear attribution or non-proliferation applications depend on the study of extreme gamma lines with similar energies, so that statistical errors are

small and the quality of detection is similar. These lines usually fall within the ~50 to ~200 keV range and are often affected by spectral interferences. High-resolution spectrometers are important for nuclear forensics since the allocation of unknown nuclear samples or the disclosure of illicit activities always relies on the measurement of small variations in isotopic composition.

Gamma-ray spectrometry was used in this study to investigate the use of radiometric spectrometry techniques to accurately characterize UOC and U ore samples. This technique is regarded as one of the first nuclear forensic measurement techniques to identify the composition of a recovered nuclear specimen because it is non-destructive and allows one to analyze several nuclides concurrently (Yücel *et al.*, 1998).

Sample preparation and analysis

A mass of 0.5 g of each UOC and uranium ores (Figure 3.2) were sealed in vials using a black insulation tape to prevent the loss of radon and to establish equilibrium between Radium-226 (^{226}Ra), Radon-222 (^{222}Rn), and Lead-214 (^{214}Pb). The uranium ore samples were crushed using the grinding machine in Figure 3.3. The acquisition period was 12 hours; the resulting spectrum was analyzed using the Genie 2000 acquisition software to determine the approximate uranium isotope abundance. The instrument was calibrated using IAEA Certified reference material (CRM-IAEA-U/Th/K).

Uranium can be classified by calculating the ^{235}U proportion of the total uranium content. Using gamma spectrometry, this can be achieved using the ^{235}U 185.7 keV peak and the ^{234m}Pa 1001 keV peak in the gamma spectrum, assuming a nuclear equilibrium of ^{234m}Pa to ^{238}U. After separation, the gap in operation between ^{234m}Pa and ^{238}U lies within the gamma spectrometric measurement uncertainty. Hence, after this period, radioactive equilibrium can be assumed. For ^{235}U, f_{235}, is given as an abundance by:

$$f_{235} = \frac{N_{235}}{N_{235}+N_{238}} \qquad (3)$$

Where, *N* is the number of atoms of uranium isotope. Depending on the content background, the excess of ^{234}U is around 1% if the enrichment of ^{235}U exceeds 90%. (Nguyen & Zsigrai, 2006). So the sum of ^{234}U, N_{234}, is considered negligible in this case. Additionally, for processed materials, ^{226}Ra is not expected to overlap with the 185.7 keV max. This assumption is made because a

processed anthropogenic uranium material contains no significant amounts of ^{226}Ra. In addition, the spectrum can remove the ^{226}Ra originating from the background.

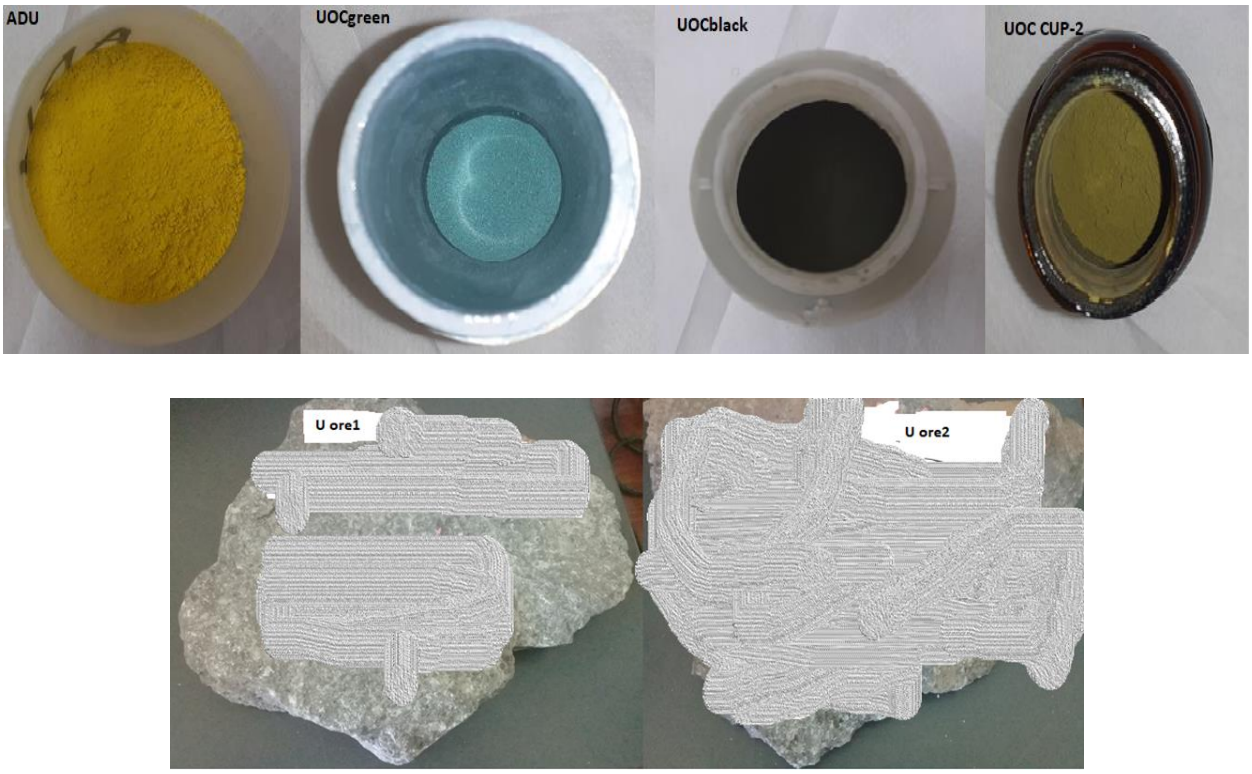

Figure 3. 2: UOCs (above) and uranium ore (bottom) samples used in this study.

Figure 3. 3: Grinding machine used for uranium ore preparations (right) and the ore product after grinding (left).

3.3.1.2 Scanning electron microscopy and energy dispersive spectroscopy (SEM/EDS)

Scanning electron microscopy (SEM) is a highly flexible method that is used in the characterization and study of the morphology of microstructure on a conducting or conducting array from the creation of a 3-D image, semiconducting materials. SEM diagram is seen in Figure 3.4 in page 41. An electron gun is used to emit an electron beam that moves through a variety of lens-focusing equipment and deflection coils to concentrate the electron beam towards the platform positioned sample. The electrons interact with the sample from the beam and send off signals such as secondary electrons, electrons backscatter, characteristic X-rays, and other photons of varying energies. These signals are collected inside the sample from various emission points that can be used to examine the surface topography, crystallography, and composition of the sample. To detect signals given off from the interaction between the electron beam and the sample, a variety of detectors is positioned in unique geometries corresponding to the position of the beam path and sample site. Backscattered electrons and secondary electrons are the two most common signals used to shape a nanometer to a micrometer scale image of a sample. Backscattered electrons (BSE) are considered incident electrons that scatter at an angle of more than 90 degrees away from the sample.

Such electrons have energies over 50 electron volts (eV). BSE is used in a sample to analyze topographical contrast and compositional characteristics. If the primary beam hits the sample surface causing the atoms of the sample to ionize, it is possible to emit loosely bound electrons producing secondary electrons (SE). Secondary electrons are considered to have energies of less than 50 eV and are used primarily for topographical contrast and visualization of a sample's surface texture (Goldstein *et al.*, 2017). The study of the characteristic X-ray signals is used primarily to determine a sample's chemical composition. The primary X-ray spectrometer used with SEM is energy dispersive spectroscopy (EDS). As a non-destructive process, this is a great technique for pre-screening samples for elemental composition. This technique can be used for quantitative chemical analysis as well as compositional sample mapping. By exposing a sample to X-rays, one may determine which elements are present and in what proportion by measuring the energy released during this relaxation process, which is specific to each element on the periodic table. The KeV and peak intensity of the EDS data are shown on an x-y axis in a graph. This is described in

section 4.1.3. A computer software converts the atoms that the energy changes represent at the highest place on the x-axis.

SEM sample preparation

SEM provides detailed high-resolution images of the sample by sweeping a focused electron beam across the sample surface and detecting secondary or backscattered electron signals. A dust of UOC and uranium ore samples were placed on a glass slide. The sample was mounted on an aluminum pin stub that was coated with double-sided carbon tape. Then, the sample was blown with the original compressed gas to remove particles. The samples were then placed on 2 mm carbon fiber and put on an EMSCOPE TB 500 carbon coater for 10 minutes for carbon coating.

Sample analysis

Physical examination of the samples was performed utilizing both optical and electron microscopy. The microstructure of UOC and U ore was characterized using scanning electron microscopy (SEM), whilst elemental composition was measured using energy-dispersive spectroscopy (EDS). The UOC powder and uranium ore samples was analyzed using SEM/EDS. The prepared samples were analyzed utilizing one of the methods: floor switch of the as-received pattern of the material.

Samples were analyzed using field emission FEI Quanta FEG 250 supplied by Thermo Fisher scanning electron microscope at NWU Potchefstroom laboratory at the accelerating voltage of 10 kV (Figure 3.4). The samples were analyzed using a secondary electron analysis at a high vacuum chamber of 6.27×10^{-5} Torr. Source of electron pressure of 8.97×10^{-10} Torr and emission current of 351.8 microamperes. An energy dispersive spectroscopy was used to provide elemental identification and quantitative compositional information using INCA software.

Figure 3. 4: Scanning electron microscope equipment at NWU Potchefstroom laboratory.

3.3.2 Destructive elemental techniques

Performing destructive analysis on nuclear forensic samples can provide a variety of information obtained with low detection limits (between ppb = µg/l and ppt = ng/l), high accuracy, and high precision techniques. Inductive coupled plasma mass spectrometry (ICP-MS) is a technique used to obtain the elemental composition of samples. ICP-MS is more sensitive to elemental isotopes as compared to Inductive coupled plasma optical emission spectrometry (ICP-OES) (Kaspar *et al.*, 2017). This type of instrumentation and methods can also provide additional information, such as isotopic ratios and concentrations.

3.3.2.1 Inductive coupled plasma mass spectrometry (ICP-MS)

One of the most extensively used analytical techniques for elemental analysis is ICP-MS. Low detection limits, exceptional precision and accuracy, and a high degree of sensitivity are all advantages of this type of study. Figure 3.5 in page 43 depicts a schematic of the ICP-MS system. ICP-MS is a destructive analytical technique used for elemental analysis. As a result of the ease of sample preparation and the short number of steps required, ICP-MS has been established for the study of radionuclides with long half-lives (>104 a) (Becker, 2005). In this study, ICP-MS has been used to determine elemental and isotopic forensic nuclear signatures.

The ICP-MS source is an ionized argon plasma with a temperature of roughly 10,000 K. Before being injected into the plasma, a sample solution is thermally nebulized into tiny aerosol droplets. ICP is generated in the center of a set of concentric quartz tubes known as plasma torches in ICP-MS (Kaspar *et al.*, 2017; Wilschefski & Baxter, 2019). An initial electric spark ionizes a small part of argon atoms, and the charged species formed fluctuate rapidly in the radiofrequency field produced by a copper induction coil wrapped around the tubes (Kaspar *et al.*, 2017). The high plasma temperature makes the sample components mainly atomized, followed by ionization into positively charged individual particles when ionized, the particles are separated from the plasma and added through a vacuum pumped interface to a quadrupole mass analyzer containing two water-cooled nickel-metal skimmer cones. By passing through four circular perpendicular pair rods, which alternate AC and DC potential in opposite pairs of the rods (De Hoffmann & Stroobant, 2007), the ions are isolated and classified based on their mass to charge ratio. The multi-element analysis capacity of ICP-MS, which allows many elements to be measured simultaneously in a single study, is likely the most important advantage from a laboratory standpoint (Wilschefski & Baxter, 2019).

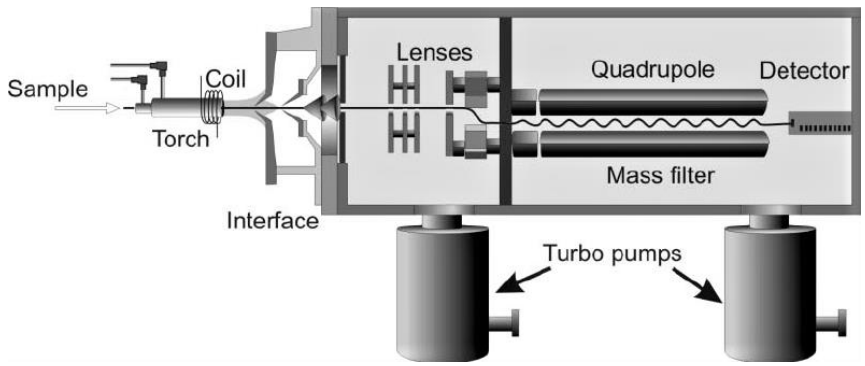

Figure 3. 5: Schematic of an ICP-MS instrument (Wilschefski & Baxter, 2019).

3.3.2.2 Experimental procedure

Uranium samples were digested using a Perkin Elmer Titan microwave digester (Figure 3.6). About 0.5 g of each sample was weighed into a Microwave digester 75ml standard vessel. Three (3) ml of 70% HNO_3 and 9 ml of 32% HCl were added to the samples and the mixture was digested

for 30 minutes at a temperature of 160 ℃ and pressure of 50 kPa. After digestion, the sample was then transferred into 50 ml vials and diluted with distilled water. The solution was then left overnight to allow the sediments to settle. One (1) ml of each solution was transferred into 10 ml vails and diluted with distilled water and the solution was then analyzed using ICP-MS.

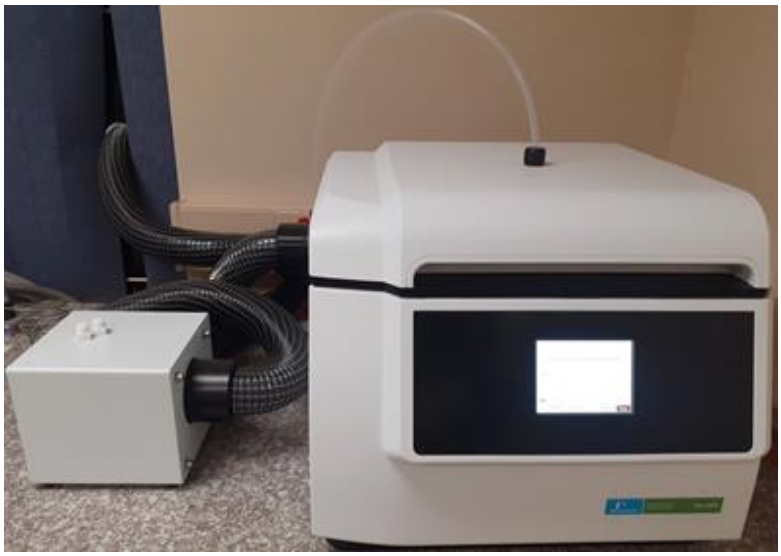

Figure 3. 6: Perkin Elmer Titan microwave digester.

3.3.2.3 Sample analysis using ICP-MS

All samples analyzed in this study were done with a Perkin Elmer NeXION 2000 ICP-MS system (Figure 3.7). The ion beam was focused on the Dual-mode detector by a Quadrupole ion deflector. The samples were loaded onto the autosampler and initialized using the ICP-MS Instrument Syngistix software. The instrument was configured to the TotalQuant method in standard mode for mass-energy discrimination and interference filtration. The samples were analyzed alongside with blanks, duplicates, and reference standards as part of the quality management of the process. (Keegan *et al.*, 2008b). A multi-elements standard 3 calibration solution for trace element analysis with 10 mg / L of Ag, Al, As, Ba, Be, Bi, Cd, Co, Cr, Cs, Cu, Fe, Ga, In, K, Li, Mg, Mn, Na, Ni, Pb, Rb, Se, Sr, Ti, U, V, and Zn were used for quality control. The instrument was set to run a blank and a standard check at every 10 samples for each measurement. The optimized operating parameters are summarized in Table 3.1.

Figure 3. 7: Instrument set up for Perkin Elmer NexION 2000 ICP-MS at NWU- CARST laboratories.

Table 3. 1: Perkin Elmer NexION 2000C ICP-MS instrumental working parameters.

Parameters	**Type/ Values**
Nebulizer	Meinhard® glass microconcentric
Cones	Nickel
Spray chamber	Glass cyclonic
Plasma gas flow	15.0 L/min
Nebulizer gas flow	1.00 – 1.05 L/min
RF power	1600 W
Mode of Operation	Standard mode (using argon gas)
Sweeps/readings	9
Replicates	3
Time per sample	4.5 minutes

CHAPTER 4: RESULTS AND DISCUSSIONS

4.1 Introduction

Uranium ore and uranium ore concentrate (UOCs) also known as yellow cakes are intermediate products that result from mining and milling of uranium ore in the early stages of the nuclear fuel cycle. Due to the ease of access compared to enriched samples, these nuclear fuel precursors are often exchanged in large amounts, and diversions or thefts are common. Chemical and elemental signatures, as well as physical features, are the focus of this study. Despite being relatively new, nuclear forensics is a growing field that is essential for handling nuclear security cases. This project aimed to apply nuclear forensic signatures in responding to nuclear security events from a nuclear facility in South Africa. Different techniques were used to acquire all the data presented in this chapter.

The data analysis of this work is divided into two sections:

1. Non-destructive analysis results:

- Characterization of uranium samples using HPGe
- Morphology and particle size of UOC and uranium ore using SEM

2. Destructive analysis results:

- Chemical impurities concentrations
- C1 Chondrite normalized REE patterns
- Isotopic ratio analysis

4.2 Non-destructive analysis results

Visual observations and other basic measurement methods, in particular for UOC samples, can already provide a lot of useful information on the degree of similarity between samples. The predominant ore minerals, as well as the major and minor elemental composition of uranium phases, were determined using a variety of non-destructive sample analytical methods discussed in Chapter 3.

4.1.1 Analysis of UOC and U ore samples using HPGe

Gamma spectrometry was used to characterize the UOC and U ore samples before they were analyzed in ICP-MS. The element of interest in this research was uranium. Direct determination of the ^{238}U activity is impossible because it emits two gamma rays with very low intensities, at energies of 49.55keV and 113.5keV, which are scattered widely in the gamma spectrum by Compton scattering (Huy *et al.*, 2013). The detection of gamma rays released by daughter nuclides in the uranium decay chain can be used to do an indirect analysis of ^{238}U. Hence, ^{238}U's activity was determined using its daughter nuclide ^{234m}Pa at the energy 1001.1 keV. The daughter nuclide ^{234m}Pa was chosen to investigate the activity of ^{238}U in this work because it is the closest daughter nuclide, has a shorter half-life than ^{238}U, and establishes radioactive secular equilibrium between the parent and the daughter nuclides (Huy *et al.*, 2013). At the energy line 185.7 keV, the activity of ^{235}U concentration was measured directly. This was mostly because the other energy transitions would be below the HPGe detector's detection limits (Ebaid, 2010).

Figures 4.1 and 4.2 show the activity ratio ($^{235}U/^{238}U$) in Bq/kg, for UOC and uranium ore samples. ADU, UOC_{black} and UOC CUP-2 shows the average activity ratio of 0.0393 ± 0.0082, 0.0344 ± 0.0072 and 0.0365 ± 0.0075 respectively, while UOC_{green} activity ratio is 0.0271 ± 0.0016. The activity ratio for uranium ore samples U ore1 and U ore2 was 0.0326 ± 0.0021 and 0.0391 ± 0.0037 respectively. The activity ratio of $^{235}U/^{238}U$ for UOC samples ranged between 0.0271 ± 0.0016 and 0.0393 ± 0.0082 respectively, while the activity ratio of $^{235}U/^{238}U$ for uranium ore samples ranged from 0.0326 ± 0.0021 and 0.0391 ± 0.00037. The activity ratio of ADU was similar to the activity ratio of U ore2.

The activity ratio of the UOC samples was higher in ADU, UOC CUP-2 samples as compared to the UOC_{green} and UOC_{black} samples. The activity ratio of the uranium ore samples was higher in U ore2 than in U ore1. The activity ratio of the uranium ore samples was comparable. Furthermore, we can see from Figure 4.1 that sample ADU, $UOC_{black,}$ and UOC CUP-2 are enriched with ^{335}U. The differences in the activity ratio of UOC and uranium ore samples could be used as a possible signature. Detailed results are presented in Appendix B. Due to its non-destructive capabilities; gamma spectrometry is suitable for initial sample characterization.

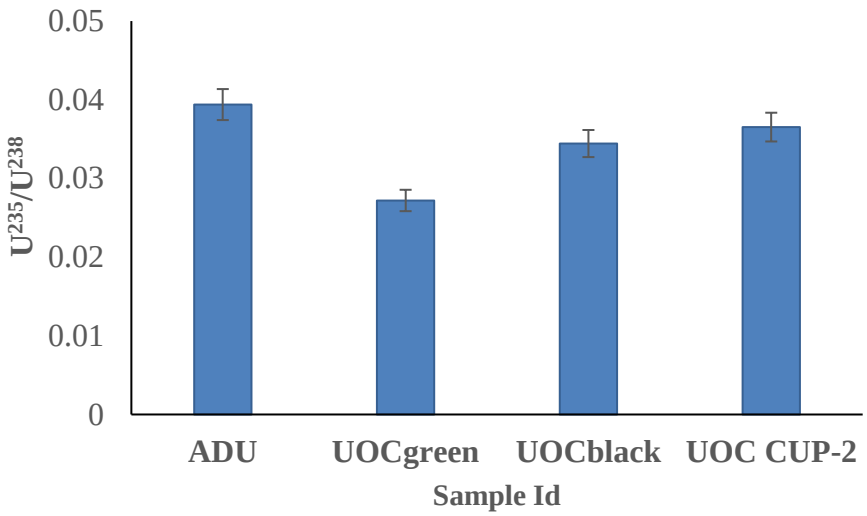

Figure 4. 1: $^{235}U/^{238}U$ activity ratio for UOC sample ADU, UOC_{green}, UOC_{black}, and UOC CUP-2.

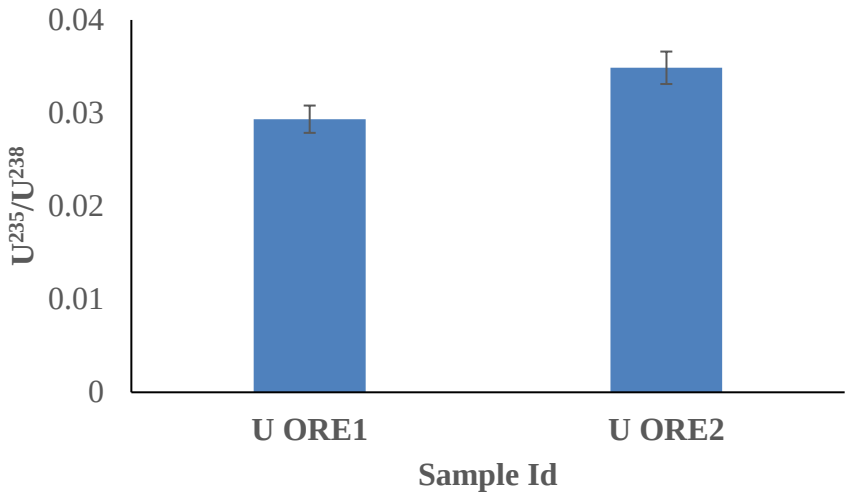

Figure 4. 2: Activity ratio of $^{235}U/^{238}U$ for U ore1 and ore2.

4.1.2 Morphology of UOC and uranium ore samples

As a result, the difficulties experienced by researchers in this subject, the morphology of UOCs is a considerably less established study topic, as evidenced by the literature. To completely understand the significance of this component of the signature, one must first comprehend the

crystallization process of the various precipitation processes to build a relationship between sample morphology and processing history.

The morphology of final products like U_3O_8 or UO_2 is considered to be affected by the morphology of initial products like uncalcined UOC (Choi *et al.*, 1988). If this observation is right, morphological parameters could be used as a signature for attribution of origin. At the very least, in the case of an unknown UOC, such as U_3O_8, its composition can be quickly determined using rapid techniques such as IR and/or Raman spectroscopy, and its morphological parameters can then be evaluated for origin determination. The X-rays generated during SEM analysis carry elemental information and are a convenient way of measuring the elemental composition on a fine spatial scale. The X-rays are analyzed in an energy dispersive spectrometer (EDS) which uses a state detector to measure simultaneously the energy and rate of incident X-rays. To obtain higher magnification images of the sample morphology, electron microscope imaging combined with energy-dispersive X-ray analyses (SEM-EDX) was used. The results contain the SEM images of different UOC samples that were scanned at different magnifications. The images of UOC and uranium ores are presented in Figures 4.3 to 4.8. The elemental composition of these samples are discussed in the following section.

***Results on images of* $\mathbf{UOC_{black}}$**

Imaging of UOC_{black} material was from the uniformity of the particle morphology, the powder was mostly homogeneous. The shaped particles were analyzed in various magnifications, 2 000x, 15 000x, and 25 000x. The higher magnification of images revealed the difference in the microstructure of smaller grains. The particles size was observed in 5, 10, and 50 µm diameter. The particles presented in Figure 4.3 are spherical and are comprised of agglomerated grains and rod-shaped. Figure 4.3 displays a well-preserved uranium oxide sphere obtained from a UOC sample, and the surface shows large pores. We view the cavities in the surface of spheres as potential stress corrosion cracking proof based on their geometry. Energy-dispersive X-ray spectroscopy analysis found the material to consist predominantly of uranium and oxygen. The elemental composition was found to be a UO_4 (uranium tetraoxide) compound.

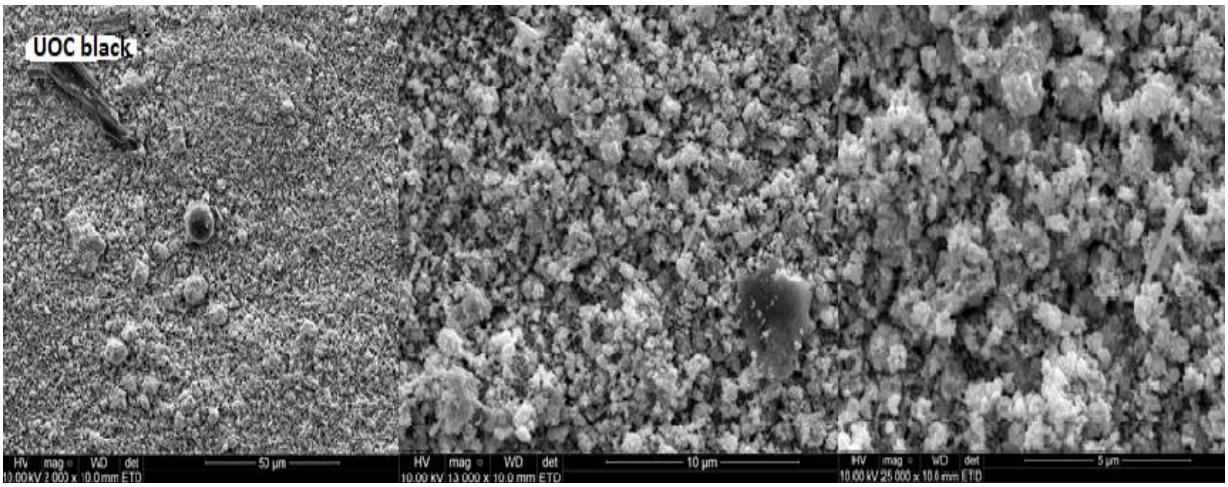

Figure 4. 3: SEM image analysis for $UOC_{black.}$

Results on images of ADU

Figure 4.4 in page 51 presents SEM micrographs of particles identified for the ADU sample. The particle sizes and shapes were also taken into account when examining these samples. The particles size was observed in 3, 5, and 10 µm diameter. In this work, it was found that durable agglomerates and conglomerates characterize ADU. The ADU powders represent a middle ground in terms of both aggregate forms, which are more egg-shaped, and the surface morphology, which is, on average, hedgehog-like. ADU powder conglomerates are made up of spherical agglomerates with gaps that are not filled with a loose mass of crystals and crystallites in most circumstances. These findings were similar to the results found by Andreev and his colleagues (Andreev *et al.*, 2009). ADU structure may have been formed during the operation of drying ammonium polyuranates and reduction of uranium trioxide to its oxide. The agglomerates and conglomerates generated by electrostatic forces may be subjected to sintering as a result of diffusion processes under the influence of temperature, resulting in enhanced strength (Andreev *et al.*, 2009). It should be observed that their forms become spherical in rotating furnaces, but they are uneven during powder reduction at rest, similar to hard rocks.

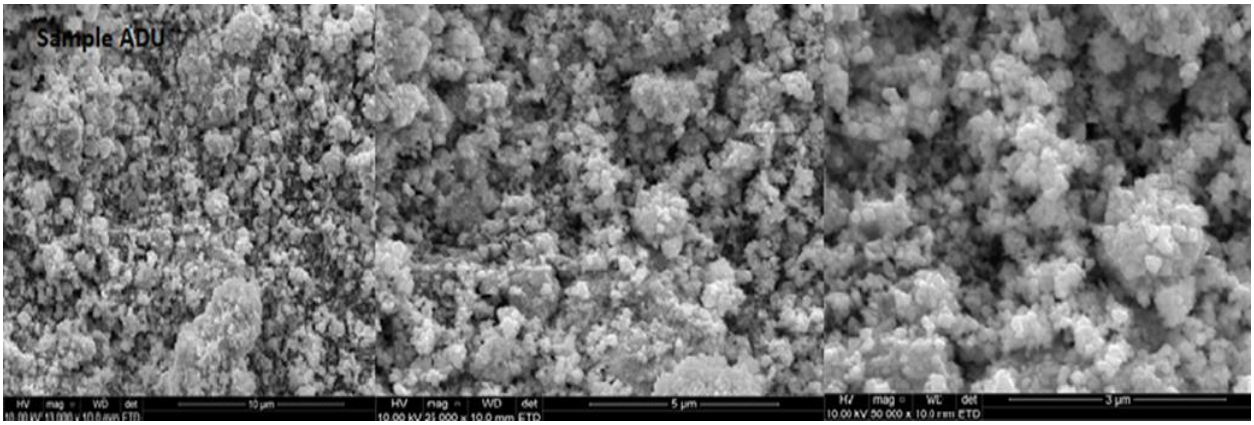

Figure 4. 4: SEM image analysis of ADU.

Results on images of UOC_{green}

Morphology analysis of UOC_{green} using SEM/EDS was observed. Figure 4.5 in page 52 shows huge, clumped agglomerates particles. These particles were analyzed at magnifications of 5 000x, 10 000x, and 20 000x and respectively. The higher magnification of images revealed a difference in the microstructure of smaller grains. These particles differ because they consist of small sub-rounded platelets. The particles presented in Figure 4.5 are non-spherical and are comprised of agglomerated grains. The pictured sub-particles with magnifications of 25 000x and 50 000x are described as having a rounded/sub-rounded habit arranged in irregular clumps of semi-rounded grains (i.e. they are not completely spherical) (Tamasi *et al.*, 2017).

The shape of the particle produced at 20 000x magnification, is more rounded than the particles produced in 5 000x and 10 000x magnification. These particles are recognized as stacked clusters, irregularly shaped, and have large pores. This makes it more distinct from the UOC magnification images of 5 000x and 10 000x. There are overlapping particles found in the UOC picture with a magnification of 100 000x and a diameter of 10 μm. The EDS analysis for this material consists of uranium, oxygen, and fluorine. The inclusion of fluorine in the sample indicates that the sample might have undergone fluorination in the nuclear fuel cycle. The elemental composition is found to be UO_2F_2 (uranium oxyfluoride) compound.

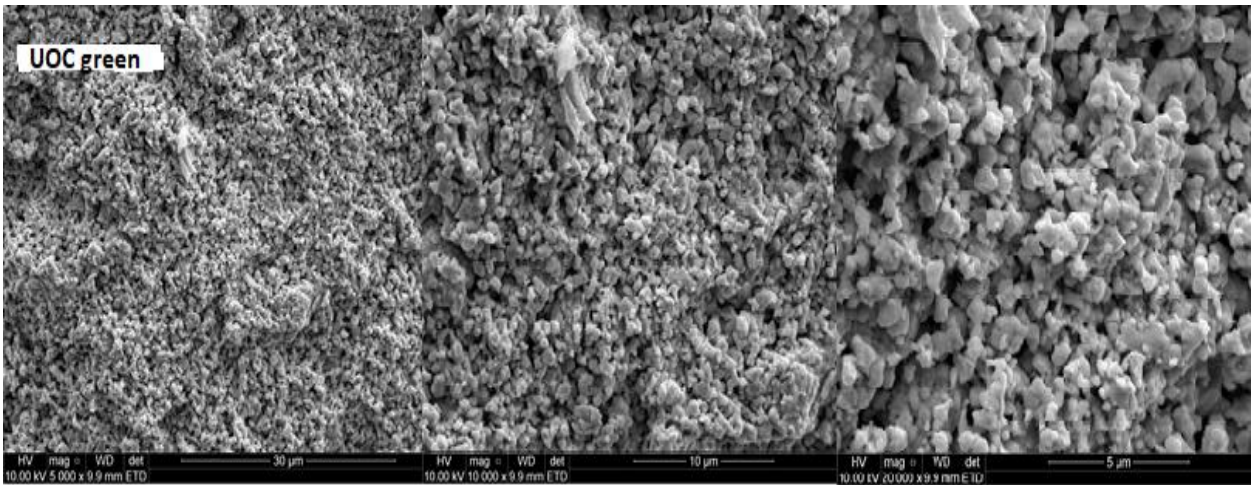

Figure 4. 5: SEM image analysis for $UOC_{green.}$

Results on images of UOC CUP-2

The particle shape of UOC CUP-2 was examined using SEM/EDS at 13 000x, 25 000x, and 50 000x respectively. Individual micro-particles are rod-shaped and smooth. The higher magnification of images revealed the difference in the microstructure of smaller grains. Figure 4.6 in page 53 presents SEM micrographs of particles identified for this sample. These particles can best be defined as non-spherical sub-angular clusters of elongated complex particles, and are comprised of agglomerated grains. This texture could have been created by compression of aggregates in the furnace grate, under the weight of other material. Alternately, powder metallurgy-type processes at the mine may have formed the texture, but it is distinct from sintered UO_2 fuel. The EDS analysis for this material consists of uranium and oxygen. The elemental composition is found to be a UO_2 (uranium dioxide) compound.

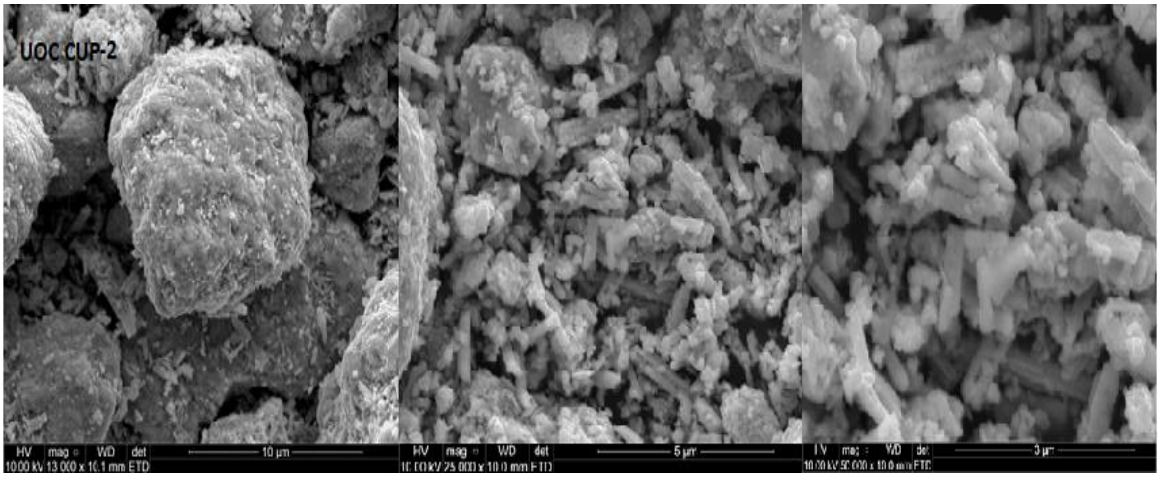

Figure 4. 6: SEM image analysis for UOC CUP-2.

The sample images of uranium ore concentrates have similar characteristics, as both have pores (spaces) between their grains. They both have a grape-like shape stacked together. The fluffy aggregates of fine particles are reasonably common in all the UOCs samples and may have been produced by vapor condensation, nucleation, and coagulation of particulates in the mines' furnace. The UOC samples studied displayed a high degree of agglomeration, with particle sizes varying from submicron to many hundreds of micrometers for the largest agglomerates, according to SEM-EDX research.

Image acquisition for U ore1 and U ore2

The morphology of uranium ore samples was analyzed using SEM/EDS in various magnifications between 500x, 8 000x, and 15 000x for U ore1, and 4 000x, 8 000x, and 15 000x U ore2 respectively. The particle sizes and shapes were also taken into account when examining these samples. The particles size was observed in 200 µm, 20 µm, 10 µm diameter for U ore1, 40 µm, 200 µm, and 10 µm for U ore2. The particles of U ore1 and U ore2 are shown in Figures 4.7 and 4.8 in page 54 and are best described as an agglomeration of complex particles. Individual micro-particles are smooth inside the agglomeration. These particles show foliated texture. The two U ore samples show similarity in images with magnifications of 8 000x and 15 000x. There are no large voids between the grains of this image and this distinguishes it from the UOC samples.

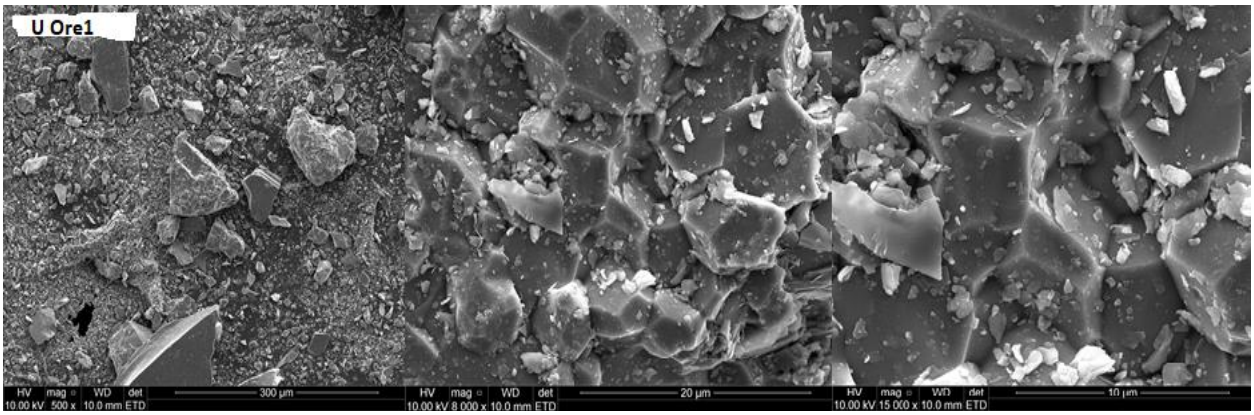

Figure 4. 7: SEM image analysis for uranium ore1.

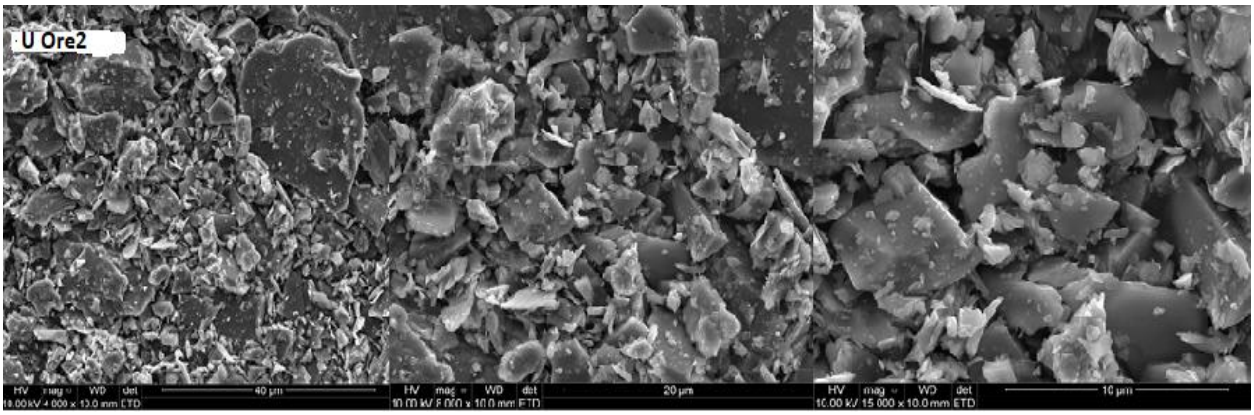

Figure 4. 8: SEM image analysis for uranium ore2.

4.1.3 Analysis of the elemental composition of UOCs by SEM/EDS

The elemental composition of UOC samples was done with the SEM/EDS, the results are presented in Tables 4.1, and the spectrum is shown in Figures 4.9 and Figure 4.10 for UOC_{green} and UOC_{black}. The weight % of ADU values was 62.67 % for uranium and 37.33 % for oxygen. The weight % of UOC_{green} was 65.96 % for uranium (U), 5.1 9% for oxygen (O) and 28.85 % for Florine (F). The EDS spectrum (Figure 4.9) showed element Florine. It was assumed that this UOC sample might have gone through a fluorination process, which is one-step before enrichment during the apartheid era in South Africa. The weight % of UOC_{black} was 75.45 % for uranium (U) and 24.55 % for oxygen (O). The weight % of UOC CUP-2 was 65.9 % for uranium (U) and 34.1 % for oxygen (O). These results confirmed that these samples are uranium oxides. The atomic ratio values were based on UO_2 for ADU and UOC CUP-2 respectively and the atomic ratio values was UO_4 for UOC_{black}. The atomic ratio values were of UO_2F_2 for UOC_{green}. These findings suggest

that analyzing the residual quantity of fluorine in UOC_{green} can supplement uranium isotopic ratio measurements for environmental sampling by giving information on the history and source of the particles that are relevant to IAEA Safeguards.

Table 4. 1: SEM/EDS elemental composition in weight (wt%) and atomic (at%) of UOCs.

	U		O		F		Formulae
Sample ID	**wt%**	**at%**	**wt%**	**at%**	**wt%**	**at%**	**Based on at% ratio**
ADU	62.67	28.84	37.33	78.16	-	-	UO_2
UOC_{green}	65.96	13.07	5.19	15.29	28.85	71.64	UO_2F_2
UOC_{black}	75.45	17.22	24.55	82.78	-	-	UO_4
UOC CUP-2	65.9	38.57	34.1	61.43	-	-	UO_2

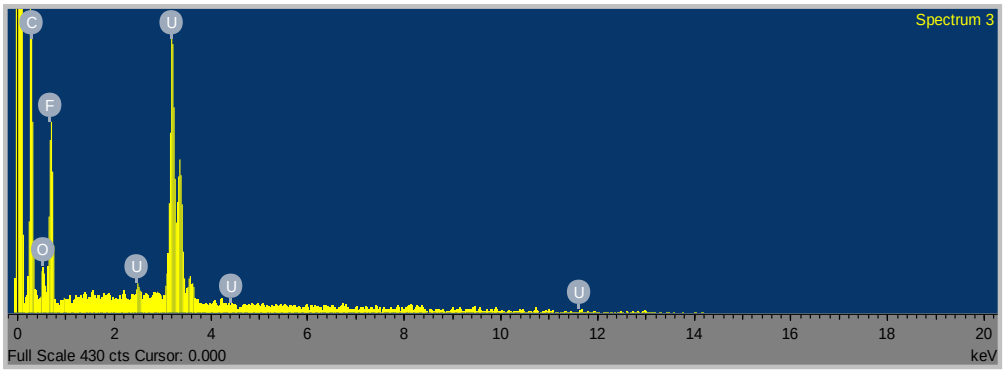

Figure 4. 9: EDS spectrum of UOC_{green}.

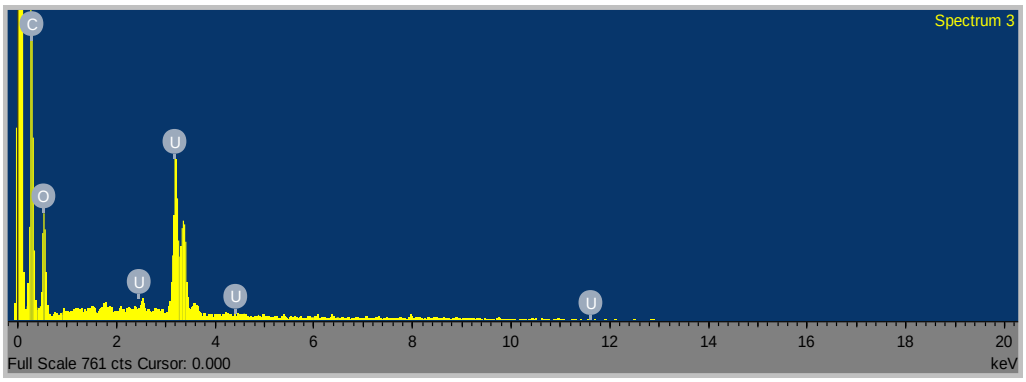

Figure 4. 10: EDS spectrum of mine UOC_{black}.

Analysis of impurities of uranium ore samples by SEM/EDS

The analysis of impurities of uranium ore samples were done with the SEM/EDS and the results are presented in Tables 4.2. Na, O, K, C, Al, and Si were detected as surface contaminants. The weight % of impurities found in U ore1 were C (4.55 %), O (52.95 %), Na (0.29 %), Al (4.13 %), Si (36.39 %) and K (1.69 %) for uranium. The weight % impurities found in U ore2 were C (3.75 %), O (53.53 %), Al (0.22 %), and Si (42.5 %). Uranium was not detected in both ores; this might be due to its concentration being lower than the limit of detection (0.1 wt%) of SEM/EDS. These impurities were also detected during ICP-MS analysis.

Table 4. 2: Impurities in weight (wt%) and atomic (at%) of U ores.

	C		**O**		**Na**		**Al**		**Si**		**K**	
Sample ID	wt%	at%	wt%	at%	wt%	at%	wt%	at%	wt%	at%	wt%	at%
U ore1	4.55	7.3	52.95	63.72	0.29	0.25	4.13	2.95	36.39	24.95	1.69	0.83
U ore2	3.75	6.03	53.53	64.59	-	-	0.22	0.16	42.5	29.22	-	-

4.3. Destructive analysis results:

Destructive analysis on nuclear forensic evidence can yield a wealth of information using procedures that have low detection limits, high accuracy, and high precision. The REE patterns, chemical impurities, and isotopic ratios in different UOC samples were measured by inductively

coupled plasma mass spectrometry (ICP-MS). Some of the impurities levels were close to the detection limit of the mass spectrometers applied in this study.

4.3.1 Trace elemental impurity concentrations

Elemental impurity concentrations for UOC samples

Analytical scientists frequently measure trace elemental impurities levels in various products and this expertise can be directly applied to nuclear forensics where the product is nuclear material. As noted above, elemental impurities in uranium materials can be from source already present in the original ore material or added during processing, either intentionally e.g. gadolinium addition to nuclear fuel to achieve higher burn-up or unintentionally e.g. such as reaction vessel corrosion products (Keegan *et al.*, 2016). As uranium is progressively processed to produce nuclear fuel, it is purified, thereby removing most endogenous elemental impurities. Analytical results for elements Al, Ba, Bi, Ca, Ce, Cr, K, Fe, La, Mg, Mn, Mo, Na, P, Pr, Ni, Nb, Nd, S, Sr, W, Yb, Th, Zn, and Zr mean concentrations are reported in this section for both UOC and U ore samples.

Figure 4.11 in page 59 shows the mean concentrations of the individual elements, and the difference of impurity spectrum according to the ADU, UOC_{green}, $UOC_{black,}$ and UOC CUP-2 respectively. Anion (e.g. sulfate) and their relative amounts might be linked to recognized processes; hence, this anion appears to represent process signature. Al and Fe for UOC and U ore were removed from the figures because they overshadow other elemental impurities. The mean concentration was reported in parts per billion (ppb). The overall shapes of the spectrum for each sample were different. ADU had its major peaks at Bi, Ca, Mg, Na, Sr, and Zr, minor elements were Ba, Ce, Cr, K, Mn, Nb, Nd, Ni, P, Pr, Th, Ti, W, Yb, and Zn. The most dominant element is Ca with a mean concentration of 2582.71 ppb. UOC_{green} had major peaks at Mg, Na, Ni, Zn, and Zr, while, UOC_{black} had major peaks at Ba, Bi, Cr, Mn, Mo, Sr, Th, Ti, W, and Zr. The most dominant element is Zr in UOC_{green}, and UOC_{black} with a mean concentration of 15381.72 ppb and 1380.99 ppb respectively. UOC CUP-2 had its major peaks at Ba, Ca, Mg, Mn, Mo, Yb, Zr, and Th. Th proved to be a major impurity in UOC CUP-2. The results showed that the elemental concentrations of the UOC samples might be used to differentiate them from one another. Therefore, the differences displayed by impurity elements were in the concentrations of these elements but the shapes of the spectrum formed were also significantly different.

There was a significant amount of Mo in UOC samples as compared to the U ore samples with an average of 402.24 ppb, 374.79 ppb, 671.85 ppb, and 6224.74 ppb for ADU, UOC_{green}, $UOC_{black,}$ and UOC CUP-2 respectively. The Mo values in UOCs show a wide range of ore processing techniques, such as leaching, solvent extraction, resin extraction, and UOC precipitation, in addition to differences in ore compositions (Migeon *et al.*, 2020). Megion *et al* stated that the laboratory tests based on existing uranium ore separation techniques show that these procedures are linked with significant Mo isotope fractionation. With this study, a similar observation was made. Nb, Th, and Zr are extremely refractory elements that are unlikely to fractionate due to evaporation or condensation. The relatively high Zr concentrations in ADU, UOC_{green}, and UOC_{black} remained a probable process signature, as Zr is most likely inherited from the original ore minerals (Jones *et al.*, 2018). The associated enrichments in Zr, Hf, U, Y, and the heavy rare earth elements (HREE) indicate the existence of zirconium. Higher levels of Th, Y, and LREE indicate the presence of monazite and/or apatite. Detailed data on elemental concentration is shown in Appendix C.

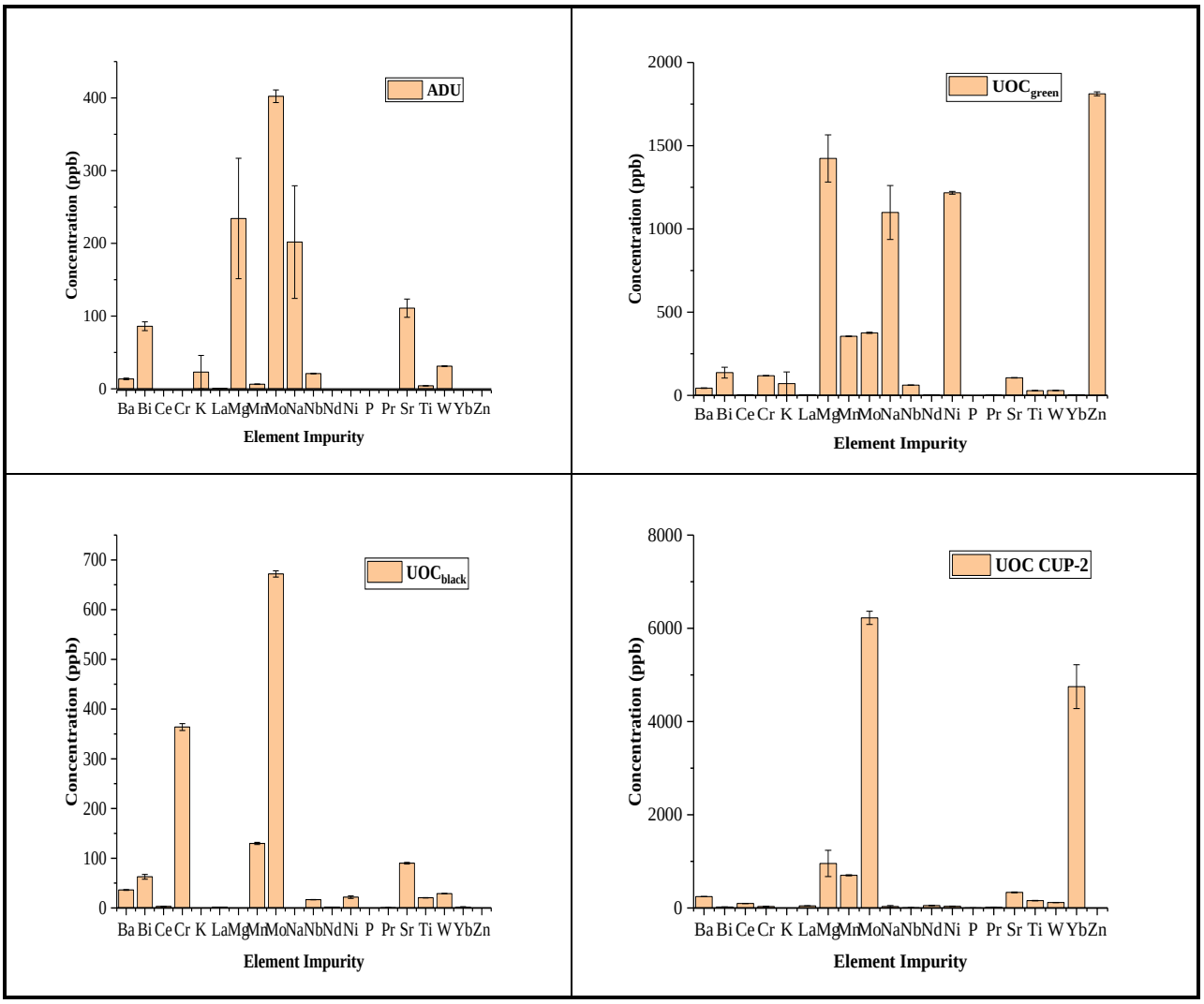

Figure 4. 11: Bar graphs of chemical impurities for UOCs; ADU, UOC_{green}, $UOC_{black,}$ and UOC CUP-2 respectively.

Elemental impurity concentrations for uranium ore samples

Uranium ores are an essential raw element for the production of nuclear fuel and are now being intensively prospected. Unlike the majority of metals, uranium's metallogeny is distinguished by an exceptional diversity of deposits that are directly tied to the varied geological circumstances under which U deposits developed. Uranium ore samples contain a significant number of first series transition metal impurities at varying concentrations, in particular, distinct differences exist between localities and deposit types. The ICP-MS technique was used to analyze uranium ore samples, U ore1 and U ore2. The mean concentration of the elemental impurity determined in the uranium ore samples is shown in Figures 4.12 and Figure 4.13 respectively. U ore1 were mostly dominated with Ca, K, Mg, and Na elements (24409.94, 299511.1, 40727.14, and 29516.69 ppb) respectively. U ore2 were mostly dominated with Ca, Ce, Cr, K, La, Mn, Na, Ni, Th, Ti, Zn, and Zr elements, the minor elements were Bi, Mo, Nb, Nd, P, Pr, Sr, W, and Yb. Impurity elements, Ca, K, Mg and Na, were the most dominant elements in both uranium ore samples. The mean concentrations of Ca, K, Mg, and Na in U ore1 were in the order K > Mg > Na > Ca (2999511.1 ppb, 40727.14 ppb, 29516.69 ppb, and 24409.94 ppb) respectively, while the mean concentrations in U ore2 were in the order K > Mg > Ca > Na (165881.8 ppb, 69446.03 ppb, 40934.09ppb and 33366.86 ppb) respectively.

The U ore samples revealed K as its major impurity element. The results (Figure 4.13) showed that the elemental concentrations of the U ore samples might be used to differentiate them from one another. High concentrations of Ni is linked with unconformity-type ore deposits, which are characterized by pitchblende and carnotite uranium minerals. High concentration of Th represent a Quartz-pebble conglomerate deposit (Keegan *et al.*, 2012). As a result, the high concentration of Ca and K in these uranium ores, they constitute a distinguishing feature of these mines. The differences between the U ore samples were shown by the mean concentrations of these elemental impurities and by the shapes of the spectrum formed. The detailed results of these impurities are presented in Appendix C. The difference in elemental impurity seen here is substantial; however, caution should be exercised when comparing ores and ore concentrates. This comparison might simply mean that low impurity concentrations are carried through from ore to ore concentrate during processing. More studies need to be done to confirm whether this is true.

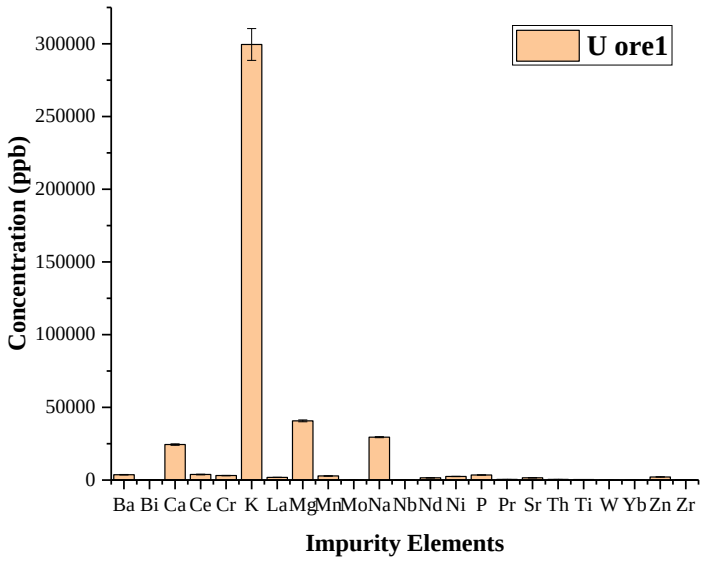

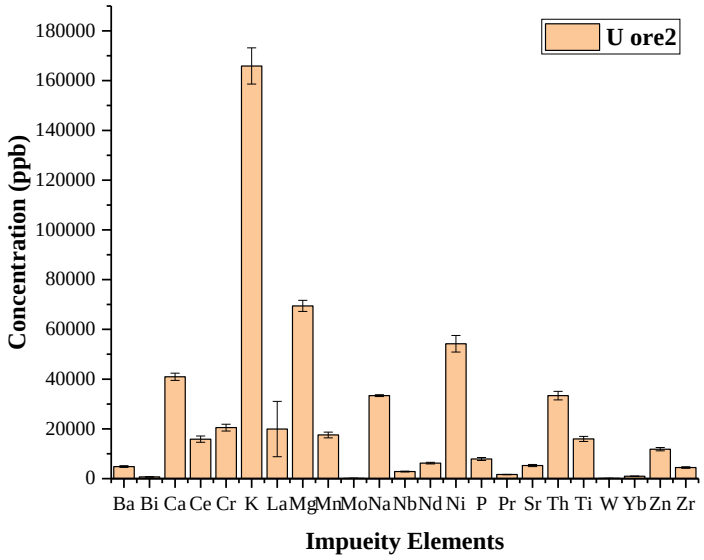

Figure 4. 12: Bar graph of chemical impurities of sample U ore1 and U ore2 respectively.

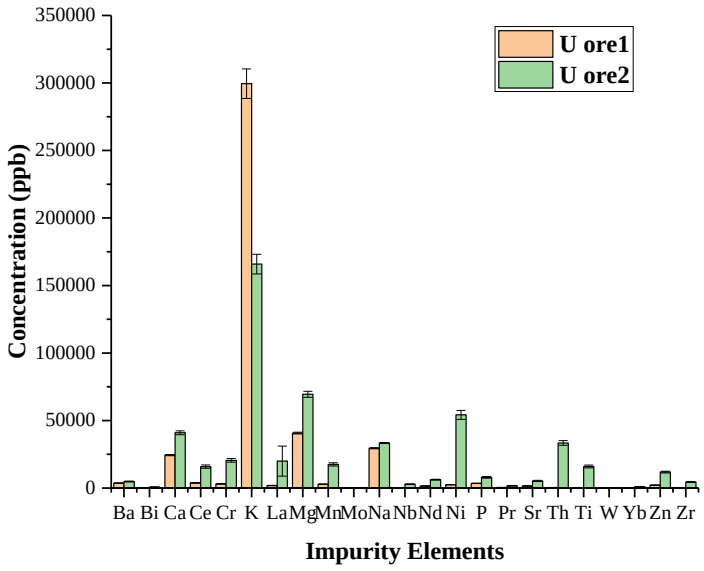

Figure 4. 13: The mean concentrations of chemical impurities of U ore samples (U ore1 and U ore2).

4.3.2 C1 chondrite normalized REE patterns

Uranium ore concentrates results

The rare-earth elemental (REE) pattern is invariable in most hydrometallurgical processes, hence it was discovered to be a key signature for determining the ore-type employed as a source for the manufacture of uranium ore concentrate. The concentrations of the REE, that show persistent patterns under different geochemical settings in UOC and U ore samples, have been examined. REE concentrations vary with provenance, according to literature (Spano *et al.*, 2017). To accomplish this, samples from several mines must be compared. One technique to do this is to use C1 chondrite values to normalize the REE data. To analyze statistical variations, the REE data in this study was standardized. These differences in UOC_{green}, UOC_{black}, ADU, and UOC CUP-2 are depicted in Figures 4.14 to 4.17. The goal was to use ICP-MS to evaluate the nuclear forensic parameters present in various UOC and uranium ore samples obtained from a South African nuclear facility.

Some nuclear forensic fingerprints may be lost during the uranium ore processing. REE, on the other hand, maintains their chemical characteristics after processing (Hall, 2005), and are thus

utilized to establish the original deposit type after processing. Differences in REE concentrations generate a uranium deposition fingerprint and a uranium mining variety (Keatley *et al.*, 2015). The REE series comprises fifteen elements of which, due to its instability, promethium (Pm) is not analytically captured. The concentration range of the REE is 0.025 ± 0.0037 ppb (Tm) to 1.702 ± 0.0348 ppb (La) with a mean of 0.025 ppb for UOC_{green}. The concentration of REE is 0.345 ± 0.0079 ppb (Lu) to 2.846 ± 0.0852 ppb (La) with a mean of 0.174 ppb for UOC_{black}, and 2.554 ± 0.4934 ppb (Eu) to 101.708 ± 2.2887 ppb (Dy) with a mean of 2.604 ppb for UOC CUP-2. The concentration of REE ranges from 0.893 ± 0.212 ppb (Eu) to 31.768 ± 0.326 ppb (La) with a mean of 0.893 ppb for ADU. The sum of rare earth elements (ΣREE) concentration for the investigated samples varies from 8.197 ± 0.278 ppb to 540.274 ± 10.656 ppb.

The concentration of REE decreases when the atomic numbers increases according Oddo-Harkins rule: Ce > La > Pr > Sm > Gd > Dy > Er > Yb > Eu > Tb > Ho > Tm > Lu. A similar order was presented by the UOC samples UOC_{green} and UOC CUP-2 in this study, with few exceptions in Dy enrichment and Eu depletion and enrichment of La for UOC_{black}. The sum of light rare earth elements (ΣLREE) concentrations ranged from 7.610 ppb to 292.784 ppb higher than that of sum of heavy rare earth elements (ΣHREE) concentrations, which varied from 0.865 ppb to 258.145 ppb. The ΣLREE/ΣHREE ratio presented varied values for the samples, indicative of LREE enrichment and depletion of HREE for sample UOC_{green}, while the ratio showed slight depletion of LREE and enrichment of HREE showed for UOC_{black} and UOC CUP-2. Different patterns with differing concentrations are seen in REE bar graphs in Figures 4.14 through 4.17 for each UOC sample. UOC_{green}, $UOC_{black,}$ and UOC CUP-2, although in varying concentrations, showed peaks at Cerium (Ce), Lanthanum (La), and Neodymium (Nd). Detailed data on rare earth elements concentration is shown in Appendix D. SPSS has been run on the data set to evaluate the importance of these changes. Section 4.4.1 will describe the findings of the analysis later.

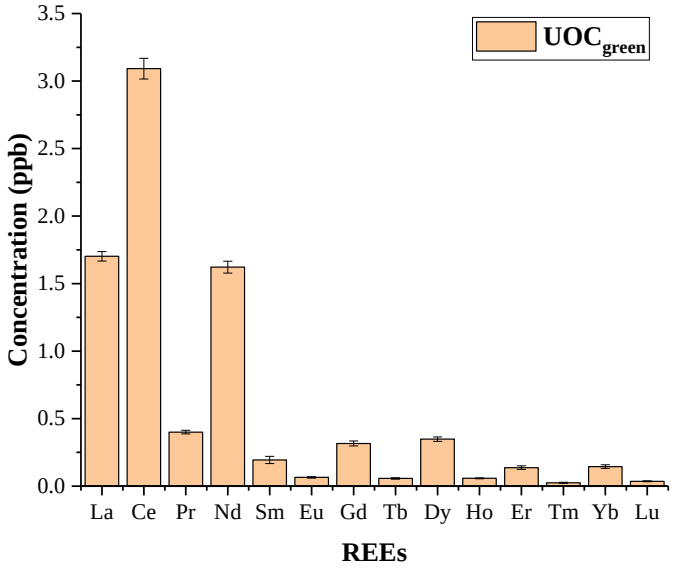

Figure 4. 14: Bar graph of REE concentrations for UOC_{green} as observed from ICP-MS analysis.

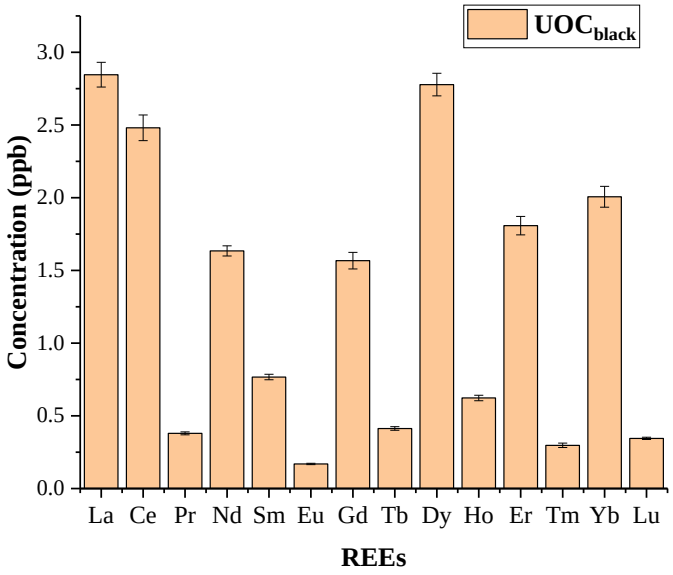

Figure 4. 15: Bar graph of REE concentrations for UOC_{black} as observed from ICP-MS analysis.

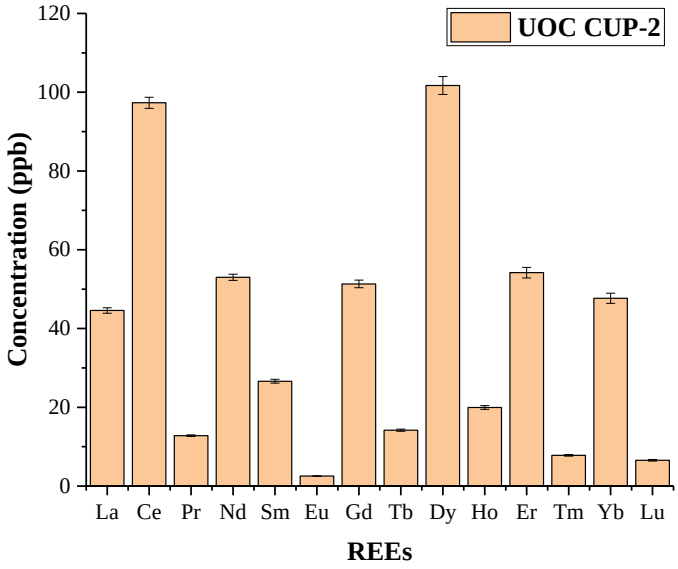

Figure 4. 16: Bar graph of REE concentrations for UOC CUOP-2 as observed from ICP-MS analysis.

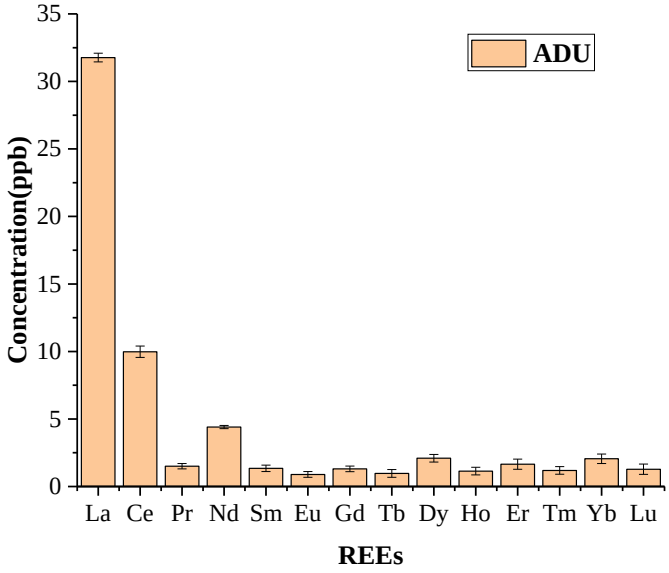

Figure 4. 17: Bar graph of REE concentrations for ADU as observed from ICP-MS analysis.

Chondrite normalize REE patterns

Concentrations of REE were divided by chondrite abundances to get (Chondrite normalized) CN values. The REEs of UOCs and U ores were analyzed against REE standard CRM004. The normalized patterns for REEs/ C1-chondrite are shown in Figure 4.18 in page 67 for all UOCs. The standardized REE/C1-chondrite pattern displays LREE enrichment, heavy REE breaking with a negative Eu anomaly for UOC_{black}. According to Figure 4.18, UOC CUP-2 had the highest quantities of all elements, whereas UOC_{green} and UOC_{black} had the lowest concentrations. UOC CUP-2 shows a slope of depleted Light REEs (La – Nd), a positive Sm anomaly, a negative Eu anomaly, and relative flat heavy REEs. The REE pattern is notable by a significant negative Eu anomaly for UOC_{black} and UOC CUP-2, which indicates that Eu has a lower abundance than its surrounding REEs. UOC_{green}, UOC_{black}, and UOC CUP-2 all have line spectra that follow similar patterns. For UOC_{black} and UOC CUP-2, the chondrite standard REE patterns exhibit a relatively flat HREE with significant Eu negative, characteristic for the uranium originating from a quartz conglomerate, and therefore consistent with the geological source proposed for the U-ore. The REE pattern in the UOC_{black} sample shows fractionation on light REEs, flat heavy REEs, and a negative Eu anomaly. UOC_{green}, on the other hand, is an unconformity-related uranium ore concentrate with a bell-shaped REE pattern. ADU shows similar elements flat LREE (Ce, Pr, Nd) which are similar to UOC_{green} and UOC_{black} samples. ADU (Figure 4.18) shows fractionation of HREE and looks similar to the REE standard used in this study. All the UOCs were analyzed against an REE standard solution. It can be concluded that from these results the UOCs were from different uranium ore deposits.

The chondrite normalizes REE patterns of UOC CUP-2 (Figure 4.18) show a strong negative Eu anomaly, and positive Sm fractionation and flat HREEs. The high uranium concentration of the CUP-2 (75.42 +/- 0.17 wt % Canada, 2016-05) most certainly enhances the matrix effect and suppresses the ionization efficiency of the remaining elements inside the plasma/introduction zone of the ICP-MS instrument, which is not surprising (Balboni *et al.*, 2017). The REEs pattern of UOC CUP-2 is similar to the results found by (Balboni *et al.*, 2017; Varga *et al.*, 2010a) even though this REE did not undergo chemical separation. The UOCs analyzed for chemical elements show large variability in terms of both REE concentrations and fractionation patterns as well as Eu anomalies, with the highest concentrations in potassium. Although there are differences in total

concentrations, the CN-REE patterns differ (Figure 4.18) when REE concentrations are normalized, demonstrating that REE signatures remain effective forensic indications despite *in-situ* leaching processes. The corroborating REE signatures for UOC samples can be used to positively identify the origin.

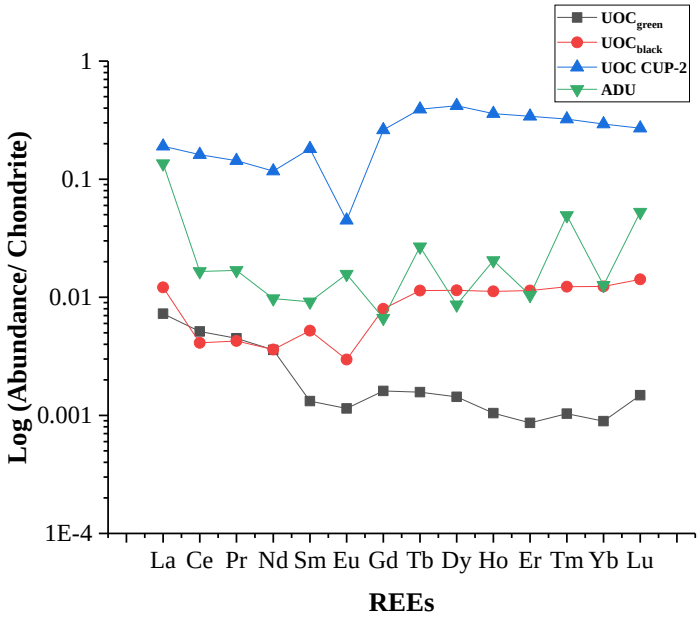

Figure 4. 18: C1 Chondrite normalized REE patterns for UOC$_{green}$, UOC$_{black}$, UOC CUP-2, and ADU.

Uranium ore results

Figure 4.19 shows the bar graph of REEs concentrations of uranium ore1 and ore2. Both ores have high peaks at La, Ce, Pr, Nd, Eu, and Gd at different concentrations. As shown in Figure 4.19, uranium ore2 had the highest concentrations of all the elements, whereas uranium ore1 had the lowest concentrations. In Figure 4.19, the ΣREE concentrations in the studied uranium ores are 29.047 ppb for ore1 and 188.153 ppb for ore2. ΣLREE concentrations were 27.329 ppb to 131.830 ppb greater than ΣHREE concentrations, which were 1.688 ppb to 55.717 ppb higher. Figure 4.18 show the enrichment of LREE and depletion of HREE. For the samples, the ΣLREE/ΣHREE ratio showed a wide range of values, indicating LREE enrichment. The normalized REE pattern reveals a close link between the ores. The REEs concentration is notable by a significantly low concentration of Eu anomaly for uranium ore1 and ore2, which indicates that Eu was more depleted than its surrounding REEs. Both uranium ore's REEs pattern showed enriched LREE and depleted

HREEs. The dominant outcome of uranium ores is LREE, which serves as a characteristic for these mines. Ore1 and ore2 are shown moving quite close together in the figures below. However, there is a significant difference between the two ores. This implies that ore1 and ore2 came from different mines. As a result, the REE spectrum can be used as a source attribution signature.

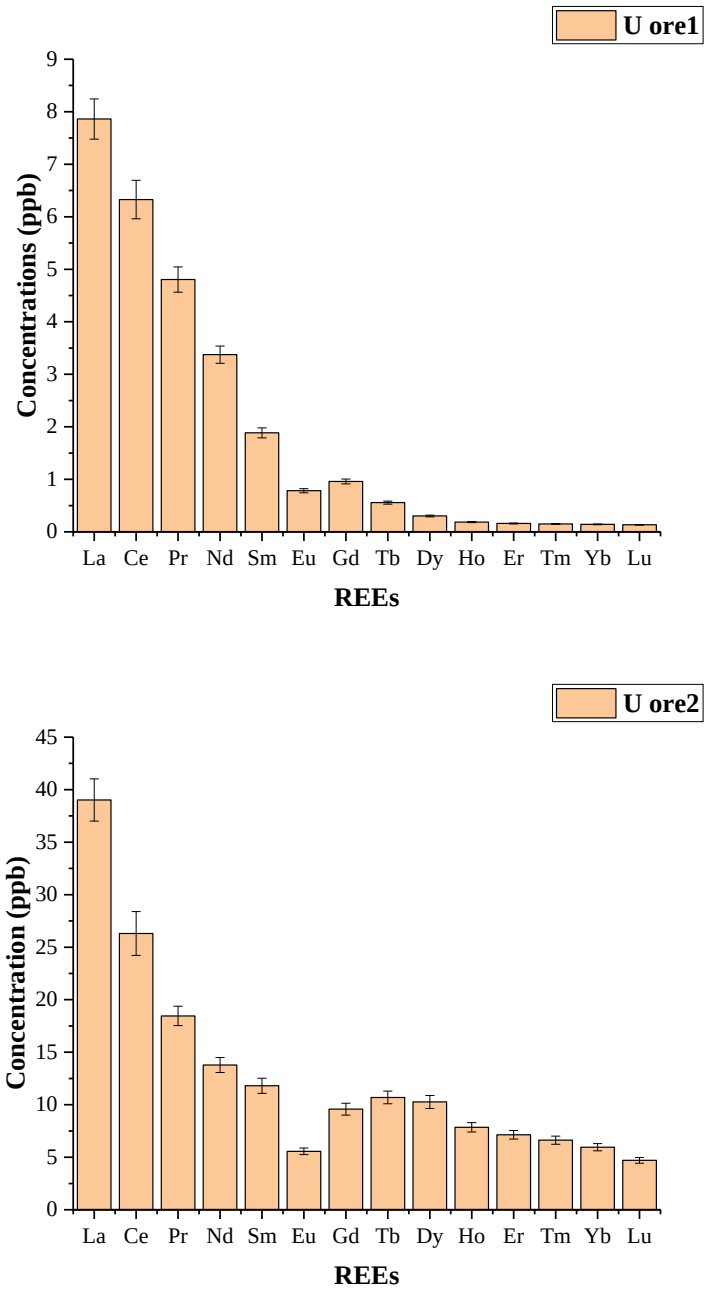

Figure 4. 19: Bar graph of REE concentrations for uranium ore1and uranium ore2 respectively.

According to Figure 4.20, uranium ore2 had the highest quantities of all elements, whereas uranium ore1 had the lowest concentrations. Figure 4.20 shows the chondrite normalized REE patterns for uranium ore1 with a negative Eu anomaly and a positive Gd fractionation, which is typical of uranium supplied from quartz pebble conglomerate and hence consistent with the suggested geologic origin of the U ore. Although there are differences in absolute concentrations, the CN-REE patterns are different when REE concentrations are normalized to total REE content, demonstrating that REE signatures remain effective forensic indications during *in-situ* leaching processes. In the instance of U, verified REE spectrum from these ores can be used to positively identify the origin. The REEs decrease might be due to the adsorption and co-precipitation of Al and Fe hydroxides.

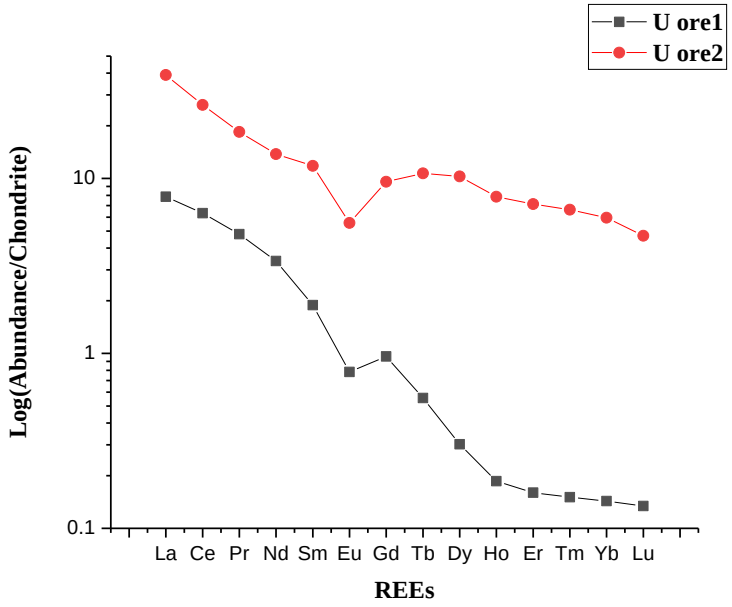

Figure 4. 20: C1 Chondrite normalized REE patterns for uranium samples ore1 and ore2.

4.3.3 Isotopic ratio analysis of uranium

Uranium isotope analysis

The uranium isotope ratios (^{234}U)/(^{238}U), and (^{235}U)/ (^{238}U) for UOC and uranium ore samples, were determined using inductively coupled plasma mass spectroscopy (ICP-MS). These differences may be due to mass-dependent isotope fractionation. The (^{234}U)/ (^{238}U) isotope ratios UOC samples are between 0.169 ± 0.00936 and 4.810 ± 4.540, whereas the (^{235}U)/ (^{238}U) is

between 0.00615 ± 0.00005309 and 0.348 ± 0.326. The (^{234}U)/ (^{238}U) isotope ratios of U ore1 and U ore2 samples are between (21.90 ± 4.08) x $10^{-5}$and (5.65 ± 1.17) x 10^{-5}, where the (^{235}U)/ (^{238}U) is between 0.0289 ± 0.00496 and 0.00760 ± 0.00167 respectively.

Measurement using ICP-MS found that the results for the (^{235}U)/ (^{238}U) ratios showed large differences between the UOC and uranium ore samples. Similar to the (^{235}U)/ (^{238}U) ratios, there is a significant difference for the (^{234}U)/ (^{238}U) ratios of the UOC and uranium ore samples. U ore2 (^{234}U)/ (^{238}U) and (^{235}U)/ (^{238}U) ratio is (5.65 ± 1.17) x 10^{-5} and 0.00760 ± 0.00167 respectively similar to that of natural uranium. This observation can be seen in Tables 4.3 and 4.4 in page 71. The isotopic ratios presented in Table 4.3 show ADU is depleted uranium, UOC_{green}, UOC_{black} are low enriched uranium, and UOC CUP-2 is highly enriched. U ore2 isotopic results in Table 4.4 show that the ore contains natural uranium, while isotopic ratios of U ore1 are low enriched. Natural isotope fractionation can be ascribed to extremely minor fluctuations in the (^{235}U)/ (^{238}U) ratio, according to more current high precision, and high accuracy measuring techniques (Mayer *et al.*, 2013). The (^{234}U)/ (^{238}U) ratio, on the other hand, displays substantially bigger relative changes due to the preferential leaching of ^{234}U from uranium ore deposits. The recoil experienced by the daughter nucleus following alpha decay of the parent nuclide ^{238}U explains this. The daughter atom is less tightly bonded in its chemical environment than the parent atom as a result of this recoil (Mayer *et al.*, 2013). These little changes, on the other hand, can be used in nuclear forensic investigations. The uranium isotopic abundances determined using ICP-MS for both UOC and uranium ore samples were not consistent with each other and with that of natural uranium, and these differences can be confirmed in the initial gamma spectrometry results.

Table 4. 3: Uranium isotope ratios of UOC samples determined by ICP-MS analysis.

Sample ID	$^{234}U/^{238}U$	$^{235}U/^{238}U$
ADU	0.169 ± 0.00936	0.00615 ± 5.309 x 10^{-05}
UOC_{green}	0.184 ± 0.0241	0.0226 ± 0.00125
UOC_{black}	0.188 ± 0.00214	0.0213 ± 7.747 x 10^{-05}
UOC CUP-2	4.810 ± 0.4540	0.348 ± 0.0326

Table 4. 4: Uranium isotope ratios of uranium ore samples determined by ICP-MS analysis.

Sample ID	$^{234}U/^{238}U$	$^{235}U/^{238}U$
U ore1	(21.90 ± 4.08) x 10^{-5}	0.0289 ± 0.00496
U ore2	(5.65 ± 1.17) x 10^{-5}	0.00760 ± 0.00167

Determination of the activity ratio of uranium isotopes

The geological and geographical features of an environment determine its natural radioactivity. These circumstances are linked to the Th, U, and K activity concentrations in each rock type (Bajoga *et al.*, 2019). For this study, the focus is primarily on uranium. The determination of the elemental and isotopic concentrations of the samples under investigation was obtained using ICP-MS. The evaluation of activity concentration of this radionuclide (^{234}U, ^{235}U, and ^{238}U) was carried out using the conversion factors shown in equation 4 below (Bajoga *et al.*, 2019):

$$Ae = \frac{\lambda e Ne Fe}{Me} \qquad (4)$$

where, *Ae* is the activity concentration in Bq/kg, λe is decay constant, *Ne* is Avogadro's number, *Me* is atomic mass and *Fe* is measured elemental concentration (ppm). The activity ratio of $^{234}U/^{238}U$ and $^{235}U/^{238}U$ shown in Table 4.5 in page 72 of UOC and uranium ore samples was 10.144 and 0.047 respectively. Detailed data activity concentration ratio is shown in Appendix D.

Because the natural abundance of ^{235}U was utilized to derive its isotopic concentration from the observed isotopic concentration of ^{238}U, the activity ratio for $^{235}U/^{238}U$ was equal to the continental average of 0.047 for all samples. There were no significant differences in the values obtained for all the samples. In the study conducted by Ntsohi et al (2020), it was found that the isotopic ratios revealed that $^{235}U/^{238}U$ was equal to the continental average of 0.047 for all samples (Ntsohi *et al.*, 2021). A similar finding was obtained in this study. ICP-MS was used to compute the concentration of ^{235}U, which was not directly measured. As a result, concentrations were not exact, and no variations could be seen. Because the activity ratio was the same for all samples, it could not be used to create a unique fingerprint.

Table 4. 5: Activity concentration ratios $^{234}U/^{238}U$ and $^{235}U/^{238}U$ of UOC and uranium ore samples.

Sample ID	**$^{234}U/^{238}U$**	**$^{235}U/^{238}U$**
UOC_{green}	10.144	0.047
UOC_{black}	10.144	0.047
UOC CUP-2	10.144	0.047
ADU	10.144	0.047
U ore1	10.144	0.047
U ore2	10.144	0.047

4.4 Statistical Analysis of result

The difference in the means of two mutually independent groups can be determined by comparing them using the Kruskal Wallis test. However, when determining the differences in means of three or more groups, the most popular method is the one-way SPSS. SPSS was applied to the REE data and impurity data to determine if there was any statistical significance in the differences displayed in the results of the samples under investigation. The F-value, significance P-value and F-critical for the samples are shown in Table 4.6 in page 73.

4.4.1 SPSS analysis of REE

The p-values for all REEs found are listed in Table 4.6. There is a similarity between UOC_{green} and UOC_{black} for elements Ce, Pr, and Nd because the P-values were above 0.05. This can also be seen in Figure 4.18 as the three elements overlap with one another. The differences between the three mines (UOC_{black} - UOC_{green} and UOC CUP-2) are represented by the nuclides La, Sm, Gd, Tb, Dy, Ho, Er, Yb, and Lu. This suggests that the discrepancies in the measured values between different REEs were not random. The P-values found were less than 0.05 (<0.05) for other REEs (La, Sm, Gd, Tb, Dy, Ho, Er, Yb, and Lu), indicating that there was a very small chance that the differences were due to coincidence. As a result, the REE elements, in this case, were statistically significant, which is a good signature for nuclear forensic studies.

Table 4. 6: REE P-statistics for UOCs samples.

	SAMPLES		
REEs	**UOC_{black} - UOC_{green}**	**UOC_{black} - UOC CUP-2**	**UOC_{green} - UOC CUP-2**
La	0.033	0	0.033
Ce	0.067	0	0.023
Pr	1	0	0.002
Nd	1	0	0.001
Sm	0.033	0	0.033
Eu	0.033	0	0.033
Gd	0.033	0	0.033
Tb	0.033	0	0.033
Dy	0.033	0	0.033
Ho	0.033	0	0.033
Er	0.033	0	0.033
Tm	0.033	0	0.033
Yb	0.033	0	0.033
Lu	0.033	0	0.033

CHAPTER 5: CONCLUSION AND RECOMMENDATIONS

5.1 Conclusions

This project aimed to apply nuclear forensic signatures in responding to nuclear security and safeguards events from a nuclear facility in South Africa. In a multi-faceted analytical discipline, the aim was built around investigating signatures in responding to nuclear security and safeguards events. This study was mainly focusing on the samples found in the front end of the nuclear fuel cycle. Gamma spectrometry, SEM/EDS, and ICP-MS systems were used to determine the uranium activity, morphology, elemental concentrations, REEs of UOC and uranium ore samples.

In the investigation using gamma spectrometry, it was discovered that the $^{235}U/^{238}U$ activity ratio varied greatly for both UOC and uranium ore samples and this constituted a distinct fingerprint. The differences in the isotopic ratio of UOC and uranium ore samples found in this study could be used as a possible signature to determine the origin of UOC samples in South Africa. The results obtained from the gamma spectrometry technique showed that the ^{235}U /^{238}U activity ratios were precisely determined and found to be less than the natural ratio (0.0462). It can be concluded that the nondestructive technique is a recommended tool to analyze uranium activity ratios in environmental samples.

The morphology study provided results that could distinguish differences in UOC and uranium ore samples in terms of particle shape, and texture. UOC and uranium ore samples were analyzed using SEM/EDS at different magnification. The form of the particles from the UOCs and uranium ore samples used in this study differed significantly. The results were extremely promising and strongly suggested that different UOC and uranium ore samples could be differentiated by their structural appearance. Particle shape is therefore potentially a useful fingerprint. The EDS revealed uranium and oxygen compositions of UOCs and fluorine in the UOC_{green} sample, this might be due to the fluorination process of the material. In the uranium ore1 sample, EDS revealed C, O, Na, Al, Si, and K impurities, and in U ore2 samples C, O, Al, and Si impurities were detected. Therefore, SEM/EDS can be used to distinguish the morphology and impurities of nuclear material for nuclear forensics.

The results showed that the elemental concentrations of the UOC and uranium ore samples might be used to distinguish them from one another. Therefore, the differences displayed by impurity elements were not only different in the concentrations of these elements but the shapes of the

spectrum formed were also significantly different. Impurity elements, Ca, K, Mg and Na were the most dominant elements in both uranium ore samples. The mean concentrations of Ca, K, Mg, and Na in U ore1 were in the order K > Mg > Na > Ca (2999511.1 ppb, 40727.14 ppb, 29516.69 ppb, and 24409.94 ppb) respectively, while the mean concentrations in U ore2 were in the order K > Mg > Ca > Na (165881.8 ppb, 69446.03 ppb, 40934.09 ppb and 33366.86 ppb) respectively. UOC and uranium ore samples contained Zr. In UOCs samples Zr was high and might be due to extremely refractory elements that are unlikely to fractionate due to evaporation or condensation.

The UOCs analyzed showed large variability in terms of both REE concentrations and fractionation patterns as well as Eu anomalies. Uranium ore2 had the highest quantities of all elements, whereas uranium ore1 had the lowest concentrations. Both uranium ore's REEs pattern showed enriched LREE and depleted HREEs. The CN-REE pattern differences demonstrate that REE signatures remain effective forensic indications during in-situ leaching processes.

The uranium isotope ratios (^{234}U)/(^{238}U), and (^{235}U)/ (^{238}U) for UOC and uranium ore samples were different, and these differences may be due to mass-dependent isotope fractionation. The results of the uranium isotopic abundances determined using ICP-MS for both UOC and uranium ore samples were not consistent with each other and with that of natural uranium. Based on the results obtained by the ICP-MS technique, the ^{235}U /^{238}U activity concentration ratios were found to be very close to the natural ratio (0.047).

Based on the findings of this study, the UOC and uranium ore samples show that they can be differentiated from one another. Several measurements of distinct signatures are necessary to establish high confidence in the sample investigations. The results reported here demonstrate that they can be applied during nuclear forensic events.

The identification of the origin of radioactive material is a key priority for the forensic community to control the spread of uranium trafficking. One of the most important aspects to fight the battle against illegal nuclear trafficking is the availability of signatures that can identify the source of uranium samples. The REE composition, morphology, and isotopic ratios, as proven in our work, are some of the most potent techniques for determining the kind of uranium deposit from which uranium oxide originates.

5.2 Recommendations

- Few nuclear materials collected from a facility in South Africa were investigated; it is therefore recommended that samples from other facilities be examined. For the precise assessment of sample isotope composition using gamma spectrometry, the Multigroup gamma-ray analysis method for uranium (MGAU) code and Monte Carlo are recommended.
- Following a mine's UOC production process from uranium ore, samples should be collected from all the stages of the product during the mining and milling in the nuclear fuel cycle and could help in revealing when the signatures began. It is recommended that analysis of REEs should undergo chemical separation prior analyzed by ICP-MS.
- Testing the REE signature of uranium concentrates after uranium mining and milling processes, and comparing it to the initial deposit signature, would be a future study in this subject.
- Other analytical techniques such as alpha spectrometry, SIMS, TIMS, or XRD are recommended to get comprehensive signatures and to answer other possibly un-answered questions during nuclear forensic investigations.

REFERENCES

Aggarwal, S.K. 2016. Nuclear forensics: what, why and how. *Journal of Curr Science*, 110(5):782-791.

Andreev, E., Glavin, K., Ivanov, A., Malovik, V., Martynov, V. & Panov, V. 2009. Some results uranium dioxide powder structure investigation. *Russian Journal of Non-Ferrous Metals*, 50(3):281-285.

Badaut, V., Wallenius, M. & Mayer, K. 2009. Anion analysis in uranium ore concentrates by ion chromatography. *Journal of radioanalytical and nuclear chemistry*, 280(1):57-61.

Bajoga, A., Al-Dabbous, A., Abdullahi, A., Alazemi, N., Bachama, Y. & Alaswad, S. 2019. Evaluation of elemental concentrations of uranium, thorium and potassium in top soils from Kuwait. *Nuclear Engineering and Technology*, 51(6):1638-1649.

Balboni, E., Simonetti, A., Spano, T., Cook, N.D. & Burns, P.C. 2017. Rare-earth element fractionation in uranium ore and its U (VI) alteration minerals. *Applied Geochemistry*, 87:84-92.

Becker, J.S. 2005. Inductively coupled plasma mass spectrometry (ICP-MS) and laser ablation ICP-MS for isotope analysis of long-lived radionuclides. *International Journal of Mass Spectrometry*, 242(2-3):183-195.

Becker, S. 2008. Inorganic mass spectrometry: principles and applications: John Wiley & Sons.

Brennecka, G.A., Borg, L.E., Hutcheon, I.D., Sharp, M.A. & Anbar, A.D. 2010. Natural variations in uranium isotope ratios of uranium ore concentrates: Understanding the 238U/235U fractionation mechanism. *Journal of Earth Planetary Science Letters*, 291(1-4):228-233.

Budinger, P., Drenski, T., Varnes, A. & Mooney, J. 1980. The case of the great yellow cake caper. *Analytical Chemistry*, 52(8):942A-948A.

Bull, T. & Smith, D. 2015. IAEA Coordinated Research Project: Application of Nuclear Forensics in Combating Illicit Trafficking of Nuclear and Other Radioactive Material. (*In*. Advances in Nuclear Forensics: Countering the Evolving Threat of Nuclear and Other Radioactive Material out of Regulatory Control. Proceedings of an International Conference. Companion CD-ROM organised by.

Chen, J., Edwards, R.L. & Wasserburg, G.J. 1986. 238U, 234U and232Th in seawater. *Earth and Planetary Science Letters*, 80(3-4):241-251.

Choi, C., Park, J., Kim, E., Shin, H. & Chang, I. 1988. The influence of AUC powder characteristics on UO2 pellets. *Journal of nuclear materials*, 153:148-155.

Clayton, J. & Aronson, S. 1961. Some Preparative Methods and Physical Characteristics of Uranium Dioxide Powders. *Journal of Chemical and Engineering Data*, 6(1):43-51.

De Hoffmann, E. & Stroobant, V. 2007. Mass spectrometry: principles and applications: John Wiley & Sons.

De Laeter, J.R. 2001. Applications of inorganic mass spectrometry. Vol. 3: John Wiley & Sons.

de Souza, A.L., Cotrim, M.E.B. & Pires, M.A.F. 2013. An overview of spectrometric techniques and sample preparation for the determination of impurities in uranium nuclear fuel grade. *Journal of Microchemical* 106:194-201.

Dill, H.G. 2011. A comparative study of uranium–thorium accumulation at the western edge of the Arabian Peninsula and mineral deposits worldwide. *Arabian Journal of Geosciences*, 4(1):123-146.

Ebaid, Y. 2010. Use of gamma-ray spectrometry for uranium isotopic analysis in environmental samples. *Rom J Phys*, 55(1-2):69-74.

Evans, W.J. & Hanusa, T.P. 2019. The Heaviest Metals: Science and Technology of the Actinides and Beyond: John Wiley & Sons.

Fahey, A., Ritchie, N., Newbury, D. & Small, J. 2010. The use of lead isotopic abundances in trace uranium samples for nuclear forensics analysis. *Journal of radioanalytical and nuclear chemistry*, 284(3):575-581.

Fedchenko, V. 2014. The role of nuclear forensics in nuclear security. *Strategic Analysis*, 38(2):230-247.

Fongaro, L. & Kvaal, K. 2013. Surface texture characterization of an Italian pasta by means of univariate and multivariate feature extraction from their texture images. *Food research international*, 51(2):693-705.

Frimmel, H.E., Schedel, S. & Brätz, H. 2014. Uraninite chemistry as forensic tool for provenance analysis. *Applied Geochemistry*, 48:104-121.

Goldstein, J.I., Newbury, D.E., Michael, J.R., Ritchie, N.W., Scott, J.H.J. & Joy, D.C. 2017. Scanning electron microscopy and X-ray microanalysis: Springer.

Guenther, R., Lowenthal, M., Nagappa, R. & Mancheri, N. 2013. India-United States cooperation on global security: Summary of a workshop on technical aspects of civilian nuclear materials security: National Academies Press.

Hall, G. 2005. Uranium age determination by measuring the 230Th/234U ratio. *Journal of radioanalytical and nuclear chemistry*, 264(2):423-427.

Han, S.-H., Varga, Z., Krajkó, J., Wallenius, M., Song, K. & Mayer, K. 2013. Measurement of the sulphur isotope ratio (34 S/32 S) in uranium ore concentrates (yellow cakes) for origin assessment. *Journal of Analytical Atomic Spectrometry*, 28(12):1919-1925.

Hiess, J., Condon, D.J., McLean, N. & Noble, S.R. 2012. 238U/235U systematics in terrestrial uranium-bearing minerals. *Science*, 335(6076):1610-1614.

Huy, N.Q., An, V.X., Loan, T.T.H. & Can, N.T. 2013. Self-absorption correction in determining the 238U activity of soil samples via 63.3 keV gamma ray using MCNP5 code. *Applied Radiation and Isotopes*, 71(1):11-20.

IAEA. 2001. Manual of acid in situ leach uranium mining technology.

IAEA. 2006. Nuclear Forensics Support. *IAEA nuclear Security series No. 2: Vienna, Austria*.

IAEA. 2013. Objective and Essential Elements of a State's Nuclear Security Regime. *IAEA Nuclear Security Series No. 20*.

IAEA. 2015. Implementing guide: Nuclear Forensics in Support of Investigations. *IAEA Nuclear Security Series No. 2-G*(2-G).

IAEA. 2019. Incident and Trafficking Database (ITDB).

IAEA. 2020. IAEA incident and trafficking database (ITDB).

Jones, A., Keatley, A.C., Goulermas, J.Y., Scott, T.B., Turner, P., Awbery, R. & Stapleton, M. 2018. Machine learning techniques to repurpose Uranium Ore Concentrate (UOC) industrial records and their application to nuclear forensic investigation. *Applied Geochemistry*, 91:221-227.

Jones, A.E., Turner, P., Zimmerman, C. & Goulermas, J.Y. 2014. Classification of spent reactor fuel for nuclear forensics. *Journal of Analytical chemistry*, 86(11):5399-5405.

Kaspar, T.C., Lavender, C.A. & Dibert, M.W. 2017. Evaluation of Uranium-235 Measurement Techniques.

Keatley, A., Scott, T., Davis, S., Jones, C. & Turner, P. 2015. An investigation into heterogeneity in a single vein-type uranium ore deposit: Implications for nuclear forensics. *Journal of environmental radioactivity*, 150:75-85.

and nuclear security investigations: ACS Publications.

Keegan, E., Richter, S., Kelly, I., Wong, H., Gadd, P., Kuehn, H. & Alonso-Munoz, A. 2008a. The provenance of Australian uranium ore concentrates by elemental and isotopic analysis.

Applied Geochemistry, 23(4):765-777. Keegan, E., Kristo, M.J., Colella, M., Robel, M., Williams, R., Lindvall, R., Eppich, G., Roberts, S., Borg, L. & Gaffney, A. 2014. Nuclear forensic analysis of an unknown uranium ore concentrate sample seized in a criminal investigation in Australia. *Journal of Forensic science international*, 240:111-121.

Keegan, E., Kristo, M.J., Toole, K., Kips, R. & Young, E. 2016. Nuclear forensics: scientific analysis supporting law enforcement

Keegan, E., Richter, S., Kelly, I., Wong, H., Gadd, P., Kuehn, H. & Alonso-Munoz, A. 2008b. The provenance of Australian uranium ore concentrates by elemental and isotopic analysis. *Journal of Applied Geochemistry*, 23(4):765-777.

Keegan, E., Wallenius, M., Mayer, K., Varga, Z. & Rasmussen, G. 2012. Attribution of uranium ore concentrates using elemental and anionic data. *Journal of Applied geochemistry*, 27(8):1600-1609.

Kennedy, A., Bostick, D., Hexel, C., Smith, R. & Giaquinto, J. 2013. Non-volatile organic analysis of uranium ore concentrates. *Journal of Radioanalytical and Nuclear Chemistry*, 296(2):817-821.

Kim, K.-W., Hyun, J.-T., Lee, K.-Y., Lee, E.-H., Lee, K.-W., Song, K.-C. & Moon, J.-K. 2011. Effects of the different conditions of uranyl and hydrogen peroxide solutions on the behavior of the uranium peroxide precipitation. *Journal of hazardous materials*, 193:52-58.

Koch, L. 2003. Traces of evidence. Nuclear forensics and illicit trafficking. *IAEA Bulletin*, 45(1):21-23.

Krajko, J. 2016. Isotopic signatures for origin assessment of natural uranium samples.

Krajkó, J., Varga, Z., Yalcintas, E., Wallenius, M. & Mayer, K. 2014. Application of neodymium isotope ratio measurements for the origin assessment of uranium ore concentrates. *Journal of Talanta*, 129:499-504.

Kristo, M. 2011. Nuclear Forensics in Radiometric Methods of Detection.

Kristo, M.J. 2020. Nuclear forensics. Handbook of Radioactivity Analysis: Volume 2. Elsevier. p. 921-951).

Kristo, M.J., Gaffney, A.M., Marks, N., Knight, K., Cassata, W.S. & Hutcheon, I.D. 2016. Nuclear forensic science: analysis of nuclear material out of regulatory control. *Journal of Annual Review of EarthmPlanetary Sciences*, 44:555-579.

Kristo, M.J. & Tumey, S.J. 2013a. The state of nuclear forensics. *Nuclear Instruments and Methods in Physics Research Section B: Beam Interactions with Materials and Atoms*, 294:656-661.

Kristo, M.J. & Tumey, S.J. 2013b. The state of nuclear forensics. *Journal of Nuclear Instruments Methods in Physics Research Section B: Beam Interactions with Materials Atoms*, 294:656-661.

Kweto, B., Groot, D., Stassen, E., Suthiram, J. & Zeevaart, J.R. 2014. Kinetic study of uranium residue dissolution in ammonium carbonate media. *Journal of radioanalytical and nuclear chemistry*, 302(1):131-137.

L'Annunziata, M.F. 2012. Handbook of radioactivity analysis: Academic press.

Lakosi, L., Zsigrai, J. & Nguyen, C. 2009. Characterization of Uranium-Bearing Material by Passive Non-Destructive Gamma Spectrometry.

Lilley, J. 2013. Nuclear physics: principles and applications: John Wiley & Sons.

Lina, M., Zhaoa, Y., Wanga, T., Zhua, L. & Zhaoa, X. 2014. Attribution of uranium ore concentrates (UOCs) by rare-earth element (REE) signatures.

Lunt, D., Boshoff, P., Boylett, M. & El-Ansary, Z. 2007. Uranium extraction: the key process drivers. *Journal of the Southern African Institute of Mining and Metallurgy*, 107(7):419-426.

Martin, A. 2012. An Introduction to Radiation Protection 6E: CRC Press.

Mayer, K., Wallenius, M. & Fanghänel, T. 2007. Nuclear forensic science—from cradle to maturity. *Journal of Alloys and Compounds*, 444:50-56.

Mayer, K., Wallenius, M., Lützenkirchen, K., Galy, J., Varga, Z., Erdmann, N., Buda, R., Kratz, J., Trautmann, N. & Fifield, K. 2011. Nuclear forensics: a methodology applicable to nuclear security and to non-proliferation. (*In*. Journal of Physics: Conference Series organised by: IOP Publishing. p. 062003).

Mayer, K., Wallenius, M. & Ray, I. 2005a. Nuclear forensics—a methodology providing clues on the origin of illicitly trafficked nuclear materials. *Analyst*, 130(4):433-441.

Mayer, K., Wallenius, M. & Ray, I. 2005b. Nuclear forensics—a methodology providing clues on the origin of illicitly trafficked nuclear materials. *Journal of Analyst*, 130(4):433-441.

Mayer, K., Wallenius, M. & Varga, Z. 2012. Nuclear forensic science: correlating measurable material parameters to the history of nuclear material. *Journal of Chemical reviews*, 113(2):884-900.

Mayer, K., Wallenius, M. & Varga, Z. 2013. Nuclear forensic science: correlating measurable material parameters to the history of nuclear material. *Chemical reviews*, 113(2):884-900.

Mayer, K., Wallenius, M. & Varga, Z. 2015. Interviewing a silent (radioactive) witness through nuclear forensic analysis: ACS Publications.

Mercadier, J., Cuney, M., Lach, P., Boiron, M.C., Bonhoure, J., Richard, A., Leisen, M. & Kister, P. 2011. Origin of uranium deposits revealed by their rare earth element signature. *Journal of Terra Nova*, 23(4):264-269.

Migeon, V., Fitoussi, C., Pili, E. & Bourdon, B. 2020. Molybdenum isotope fractionation in uranium oxides and during key processes of the nuclear fuel cycle: Towards a new nuclear forensic tool. *Geochimica et Cosmochimica Acta*, 279:238-257.

Mogafe, P., Kokwane, B., Tshidada, P. & Matshiga, A. 2015. South Africa's Nuclear Forensics Response Plan Step 1-In Support of Nuclear Security Investigations. (*In*. Advances in Nuclear Forensics: Countering the Evolving Threat of Nuclear and Other Radioactive Material out of Regulatory Control. Proceedings of an International Conference. Companion CD-ROM organised by.

Moody, K.J., Grant, P.M., Hutcheon, I.D. & Varoufakis, Y. 2014. Nuclear forensic analysis: CRC Press.

Morgenstern, A., Apostolidis, C. & Mayer, K. 2002. Age determination of highly enriched uranium: separation and analysis of 231Pa. *Analytical Chemistry*, 74(21):5513-5516.

Nguyen, C.T. & Zsigrai, J. 2006. Basic characterization of highly enriched uranium by gamma spectrometry. *Journal of Nuclear Instruments Methods in Physics Research Section B: Beam Interactions with Materials Atoms*, 246(2):417-424.

Nicolaou, G. 2006. Determination of the origin of unknown irradiated nuclear fuel. *Journal of environmental radioactivity*, 86(3):313-318.

Nikitin, M.B.D., Andrews, A. & Holt, M. 2010. Managing the nuclear fuel cycle: Policy implications of expanding global access to nuclear power: DIANE Publishing.

Ntsohi, L., Usman, I., Mavunda, R. & Kureba, O. 2021. Characterization of uranium in soil samples from a prospective uranium mining in Serule, Botswana for nuclear forensic application. *Journal of Radiation Research and Applied Sciences*, 14(1):23-33.

Pabian, F.V. 2015. The South African denuclearization exemplar: Insights for nonproliferation monitoring and verification. *The Nonproliferation Review*, 22(1):27-52.

Pajo, L. 2001. UO2 Fuel pellet impurities, pellet surface roughness and n (18O)/n (16O) ratios, applied to nuclear forensic science.

Plaue, J. 2013. Forensic signatures of chemical process history in uranium oxides.

Quinn, J.E., Wilkins, D. & Soldenhoff, K.H. 2013. Solvent extraction of uranium from saline leach liquors using DEHPA/Alamine 336 mixed reagent. *Hydrometallurgy*, 134:74-79.

Ranebo, Y., Eriksson, M., Tamborini, G., Niagolova, N., Bildstein, O. & Betti, M. 2007. The use of SIMS and SEM for the characterization of individual particles with a matrix originating from a nuclear weapon. *microscopy and microanalysis*, 13(3):179-190.

Ray, I., Schubert, A. & Wallenius, M. 2003. The concept of a'microstructural fingerprint'for the characterization of samples in nuclear forensic science. (*In*. Advances in destructive and non-destructive analysis for environmental monitoring and nuclear forensics. Proceedings of an international conference organised by.

Reading, D.G. 2016. Nuclear forensics: determining the origin of uranium ores and uranium ore concentrates via radiological, elemental and isotopic signatures. University of Southampton.

Reynolds, H.S., Ram, R., Charalambous, F.A., Antolasic, F., Tardio, J. & Bhargava, S. 2010. Characterisation of a uranium ore using multiple X-ray diffraction based methods. *Journal of Minerals Engineering*, 23(9):739-745.

Rosman, K. & Taylor, P. 1998. Isotopic compositions of the elements 1997 (Technical Report). *Pure and Applied Chemistry*, 70(1):217-235.

Saleh, I. & Abdel-Halim, A. 2016. Determination of depleted uranium using a high-resolution gamma-ray spectrometer and its applications in soil and sediments. *Journal of Taibah University for Science*, 10(2):205-211.

Scheele, F. 2011. Uranium from Africa: Mitigation of Uranium Mining Impacts on Society and Environment by Industry and Governments. *Available at SSRN 1892775*.

Schenkel, R., Cromboom, O., Daures, P., Janssens, W., Koch, L., Mayer, K., Ray, I.J.A.i.D., Monitoring, N.-D.A.f.E. & Forensics, N. 2003. FROM ILLICIT TRAFFICKING TO NUCLEAR TERRORISM—THE ROLE OF NUCLEAR FORENSIC SCIENCE.9.

Schwerdt, I.J., Brenkmann, A., Martinson, S., Albrecht, B.D., Heffernan, S., Klosterman, M.R., Kirkham, T., Tasdizen, T. & McDonald IV, L.W. 2018. Nuclear proliferomics: a new field of study to identify signatures of nuclear materials as demonstrated on alpha-UO3. *Talanta*, 186:433-444.

Simonetti, A., Bellucci, J.J., Wallace, C., Koeman, E. & Burns, P.C. 2013. Nonproliferation and nuclear forensics: detailed, multi-analytical investigation of trinitite post-detonation materials.

Sirven, J.-B., Pailloux, A., M'Baye, Y., Coulon, N., Alpettaz, T. & Gosse, S.J.J.o.A.A.S. 2009. Towards the determination of the geographical origin of yellow cake samples by laser-induced breakdown spectroscopy and chemometrics. 24(4):451-459.

Smith, D. & Niemeyer, S. 2004. International technical working group cooperation to counter illicit nuclear trafficking.

Spano, T.L., Simonetti, A., Wheeler, T., Carpenter, G., Freet, D., Balboni, E., Dorais, C. & Burns, P.C. 2017. A novel nuclear forensic tool involving deposit type normalized rare earth element signatures. *Terra Nova*, 29(5):294-305.

Srncik, M. 2011. Investigation of the 236 U occurrence in the environment.

Stanley, F. 2012. A beginner's guide to uranium chronometry in nuclear forensics and safeguards. *Journal of Analytical Atomic Spectrometry*, 27(11):1821-1830.

Suen, T.W. 2012. A mass spectrometry study of isotope separation in the laser plume: University of California, Berkeley.

Švedkauskaitė-LeGore, J., Rasmussen, G., Abousahl, S. & Van Belle, P. 2008. Investigation of the sample characteristics needed for the determination of the origin of uranium-bearing materials. *Journal of Radioanalytical and Nuclear Chemistry*, 278(1):201-209.

Tamasi, A.L., Cash, L.J., Mullen, W.T., Pugmire, A.L., Ross, A.R., Ruggiero, C.E., Scott, B.L., Wagner, G.L., Walensky, J.R. & Wilkerson, M.P. 2017. Morphology of U3O8 materials following storage under controlled conditions of temperature and relative humidity. *Journal of Radioanalytical and Nuclear Chemistry*, 311(1):35-42.

Varga, Z., Katona, R., Stefánka, Z., Wallenius, M., Mayer, K. & Nicholl, A. 2010a. Determination of rare-earth elements in uranium-bearing materials by inductively coupled plasma mass spectrometry. *Journal of Talanta*, 80(5):1744-1749.

Varga, Z., Krajkó, J., Peńkin, M., Novák, M., Eke, Z., Wallenius, M. & Mayer, K. 2017. Identification of uranium signatures relevant for nuclear safeguards and forensics. *Journal of radioanalytical and nuclear chemistry*, 312(3):639-654.

Varga, Z., Nicholl, A., Wallenius, M. & Mayer, K. 2012. Development and validation of a methodology for uranium radiochronometry reference material preparation. *Journal of Analytica chimica acta*, 718:25-31.

Varga, Z., Öztürk, B., Meppen, M., Mayer, K., Wallenius, M. & Apostolidis, C. 2011a. Characterization and classification of uranium ore concentrates (yellow cakes) using infrared spectrometry. *Journal of Radiochimica Acta* 99(12):807-813.

Varga, Z. & Surányi, G. 2007. Production date determination of uranium-oxide materials by inductively coupled plasma mass spectrometry. *Analytica chimica acta*, 599(1):16-23.

Varga, Z. & Surányi, G. 2009. Detection of previous neutron irradiation and reprocessing of uranium materials for nuclear forensic purposes. *Journal of Applied Radiation and Isotopes*, 67(4):516-522.

Varga, Z., Wallenius, M. & Mayer, K. 2010b. Origin assessment of uranium ore concentrates based on their rare-earth elemental impurity pattern. *Radiochimica Acta*, 98(12):771-778.

Varga, Z., Wallenius, M., Mayer, K., Keegan, E. & Millet, S. 2009. Application of lead and strontium isotope ratio measurements for the origin assessment of uranium ore concentrates. *Journal of Analytical chemistry*, 81(20):8327-8334.

Varga, Z., Wallenius, M., Mayer, K. & Meppen, M. 2011b. Analysis of uranium ore concentrates for origin assessment. *Journal of Proceedings in Radiochemistry A Supplement to Radiochimica Acta*, 1(1):27-30.

Wallenius, M., Lützenkirchen, K., Mayer, K., Ray, I., de las Heras, L.A., Betti, M., Cromboom, O., Hild, M., Lynch, B. & Nicholl, A. 2007. Nuclear forensic investigations with a focus on plutonium. *Journal of Alloys and Compounds*, 444:57-62.

Wallenius, M., Mayer, K. & Ray, I. 2006. Nuclear forensic investigations: two case studies. *Journal of Forensic science international*, 156(1):55-62.

Wallenius, M., Mayer, K. & Varga, Z. 2014. Procedures and Techniques for Nuclear Forensics Investigations.

Wallenius, M., Morgenstern, A., Apostolidis, C. & Mayer, K. 2002. Determination of the age of highly enriched uranium. *Analytical and bioanalytical chemistry*, 374(3):379-384.

Wallenius, M., Peerani, P. & Koch, L. 2000. Origin determination of plutonium material in nuclear forensics. *Journal of Radioanalytical and Nuclear Chemistry*, 246(2):317-321.

Weyer, S., Anbar, A., Gerdes, A., Gordon, G., Algeo, T. & Boyle, E. 2008. Natural fractionation of 238U/235U. *Geochimica et Cosmochimica Acta*, 72(2):345-359.

Wilschefski, S.C. & Baxter, M.R. 2019. Inductively Coupled Plasma Mass Spectrometry: Introduction to Analytical Aspects. *The Clinical biochemist. Reviews*, 40(3):115-133.

Winde, F., Brugge, D., Nidecker, A. & Ruegg, U. 2017. Uranium from Africa–An overview on past and current mining activities: Re-appraising associated risks and chances in a global context. *Journal of African Earth Sciences*, 129:759-778.

WNA. 2020a. In Situ Leach Mining of Uranium. https://world-nuclear.org/information-library/nuclear-fuel-cycle/mining-of-uranium/in-situ-leach-mining-of-uranium.aspx Date of access: 24 January 2022.

WNA. 2020b. Naturally Occurring Radioactive Materials (NORM). https://world-nuclear.org/information-library/safety-and-security/radiation-and-health/naturally-occurring-radioactive-materials-norm.aspx Date of access: 03 March 2022.

WNA. 2021. Nuclear Fuel Cycle Overview. http://www.world-nuclear.org/information-library/nuclear-fuel-cycle/introduction/nuclear-fuel-cycle-overview.aspx Date of access.

Wong, F.M., Hinton, T. & Smith, D.K. 2015. Overview of Nuclear Forensics in Support of Investigations. (*In*. Advances in Nuclear Forensics: Countering the Evolving Threat of Nuclear and Other Radioactive Material out of Regulatory Control. Proceedings of an International Conference. Companion CD-ROM organised by.

Yücel, H., Cetiner, M. & Demirel, H. 1998. Use of the 1001 keV peak of 234mPa daughter of 238U in measurement of uranium concentration by HPGe gamma-ray spectrometry. *Nuclear Instruments and Methods in Physics Research Section A: Accelerators, Spectrometers, Detectors and Associated Equipment*, 413(1):74-82.

Závodská, L., Kosorinova, E., Scerbakova, L. & Lesny, J. 2008. Environmental chemistry of uranium. *HV ISSN*:1418-7108.

APPENDICES

Appendix A: List of publications.

V Uushona, N D Mokhine, M Mathuthu, I Shuro, T G Kupi, Analysis of UOC for nuclear forensics using Scanning Electron Microscope, SAIP conference proceedings (2021).

Mathuthu, J.; Mokhine, N.D.; Mkiva, N.; Nde, S.C.; Dennis, I.; Hendriks, J.; Palamuleni, L.; Kupi, T.G.; Mathuthu, M. Determining Water Isotope Compositions for the IAEA WICO and North West Villages, South Africa. *Water* **2021**, *13*, 2801. https://doi.org/10.3390/w13202801

Appendix B: Data for uranium isotopic ratio for UOCs and uranium ores.

Table 1: Uranium isotopic for UOCs

	U238 (Bq/kg)	**U235 (Bq/kg)**
Sample ID	**1001 keV**	**185.71 keV**
ADU-1	938.1 ± 15.02	36.89 ± 1.23336
ADU-2	949.8 ± 1.17	37.52 ± 1.256
ADU-3	893.3 ± 14.4	35.49 ± 1.194
ADU-4	964.7 ± 15.27	37.96 ± 1.275
ADU-5	954.1 ± 15.38	37.1 ± 1.236
UOCgreen-1	1058 ± 16.52	28.6 ± 0.9202
UOCgreen-2	1490 ± 24.54	38.97 ± 1.31
UOCgreen-3	1347 ± 22.27	35.03 ± 1.174
UOCgreen-4	1037 ± 16.73	29.54 ± 1.001
UOCgreen-5	1010 ± 16.9	28.29 ± 2.794
UOCblack-1	1053 ± 16.72	34.97 ± 1.219
UOCblack-2	1085 ± 17.73	36.98 ± 1.246
UOCblack-3	1086 ± 17.43	38.37 ± 1.295
UOCblack-4	1089 ± 17.4	37.24 ± 1.25
UOCblack-5	1083 ± 17.56	38.21 ± 1.2578
UOC CUP-2 1	965.9 ± 15.64	36.51 ± 1.197
UOC CUP-2 2	892.1 ± 14.47	34 ± 1.141
UOC CUP-2 3	969.8 ± 15.72	34.34 ± 1.154
UOC CUP-2 4	971.3 ± 15.86	34.96 ± 1.154
UOC CUP-2 5	1157 ± 18.68	40.6 ± 1.37

Table 2: Uranium isotopic for uranium ores

	^{238}U (Bq/kg)	^{235}U (Bq/kg)
Sample ID	**1001 keV**	**185.71 keV**
U ore1 - 1	0.19454 ± 0.0579	0.008918 ± 0.000841
U ore1 - 2	0.3416 ± 0.0631	0.007783 ± 0.000822
U ore1 - 3	0.2601 ± 0.0620	0.0072294 ± 0.00155
U ore1 - 4	223.61 ± 0.0562	9.1761 ± 0.0562
U ore1 - 5	0.1686 ± 0.05515	0.004293 ± 0.0007769
U ore2 - 1	4.318 ± 0.0749	0.03299 ± 0.00364
U ore2 - 2	0.5414 ± 0.0762	0.01175 ± 0.00304
U ore2 - 3	0.472 ± 0.0753	0.04205 ± 0.00188
U ore2 - 4	4.654 ± 0.0688	0.01149 v 0.00332
U ore2 - 5	0.5072 ± 0.0760	0.03795 ± 0.00179

Appendix C: Chemical impurities of UOC and U ore materials statistics.
Table 1: ADU average, maximum and minimum concentrations (ppb).

Elements	Avg	Stdev	Std Error	Max	Min
Al	122.398	62.29102	19.69815	242.91	0
Ba	13.668	3.486561	1.102547	20.01	7.51
Bi	86.093	19.24755	6.086611	140.58	76.97
Ca	2582.713	405.7975	128.3244	3216.87	1634.39
Ce	0	0	0	0	0
Cr	0	0	0	0	0
Fe	0	0	0	0	0
K	22.992	72.70709	22.992	229.92	0
La	0.336	0.110272	0.034871	0.55	0.16
Mg	234.22	261.8433	82.80212	713.47	0
Mn	6.308	1.206029	0.38138	8.48	4.52
Mo	402.238	27.38569	8.660116	428.7	338.29
Na	201.796	244.8496	77.42824	600.83	0
Nb	21.055	1.432412	0.452969	23.16	18.03
Nd	0	0	0	0	0
Ni	0	0	0	0	0
P	0	0	0	0	0
Pr	0	0	0	0	0
Sr	110.953	39.65382	12.53964	129.93	0
Th	2.33	0.341109	0.107868	3.21	2.01
Ti	4.169	0.583047	0.184376	5	3.07
W	31.212	1.359271	0.429839	32.52	27.9
Yb	0	0	0	0	0
Zn	0	0	0	0	0
Zr	1050.101	62.53508	19.77533	1119.29	904.38

Table 2: UOC_{green} average, maximum and minimum concentrations (ppb).

Elements	Avg	Stdev	Std Error	Max	Min
Al	828.226	61.73609	19.52267	914.21	698.68
Ba	43.348	5.602501	1.771666	56.92	38.24
Bi	136.629	102.2911	32.34728	427.17	94.56
Ca	0	0	0	0	0
Ce	2.481	0.278865	0.088185	2.95	2.14
Cr	118.198	3.575537	1.130684	122.12	109.54
Fe	6572.664	172.9174	54.68127	6749.57	6257.01
K	70.468	222.8394	70.468	704.68	0
La	2.846	0.269287	0.085156	3.29	2.51
Mg	1423.375	448.0326	141.6804	2487.11	982.1
Mn	354.921	4.757615	1.50449	361.18	347.08
Mo	375.789	10.94143	3.459985	391.01	353.41
Na	1098.825	512.0778	161.9332	2329.68	583.93
Nb	61.398	3.586957	1.134295	71.39	59.03
Nd	1.634	0.109869	0.034744	1.87	1.46
Ni	1217.239	26.22781	8.293962	1249.9	1157.71
P	0	0	0	0	0
Pr	0.381	0.03178	0.01005	0.43	0.33
Sr	105.487	3.636897	1.150088	109.2	96.82
Th	65.583	16.37883	5.179441	110.47	54.51
Ti	28.449	0.759773	0.240261	29.39	26.64
W	29.491	3.131654	0.990316	35.93	25.72
Yb	2.005	0.227657	0.071992	2.4	1.69
Zn	1811.562	37.4068	11.82907	1859.37	1729.42
Zr	15381.72	245.3202	77.57704	15804.41	14868.83

Table 3: UOC_{black} average, maximum and minimum concentrations (ppb).

Elements	Avg	Stdev	Std Error	Max	Min
Al	2556.689	221.2614	69.96899	2810.44	2264.23
Ba	36.172	2.353049	0.744099	40.26	33.2
Bi	62.71	14.9394	4.724254	104.93	55.47
Ca	0	0	0	0	0
Ce	3.092	0.24257	0.076707	3.49	2.65
Cr	363.877	22.00362	6.958156	389.57	326.54
Fe	16283.22	5165.609	1633.509	18728.24	1757.34
K	0	0	0	0	0
La	1.702	0.110131	0.034827	1.88	1.53
Mg	0	0	0	0	0
Mn	129.748	6.733777	2.129407	140.53	120.22
Mo	671.847	19.89073	6.29	694.84	640.6
Na	0	0	0	0	0
Nb	16.702	0.704333	0.22273	17.69	15.59
Nd	1.622	0.139507	0.044116	1.79	1.38
Ni	21.757	7.812507	2.470532	32.01	9.06
P	0	0	0	0	0
Pr	0.4	0.041899	0.01325	0.45	0.34
Sr	90.069	5.219435	1.65053	97	82.16
Th	44.768	1.892739	0.598537	47.2	42.15
Ti	20.476	0.921993	0.29156	21.52	18.89
W	28.747	0.920097	0.29096	30.27	27.46
Yb	1.333	3.748223	1.185292	12	0.09
Zn	0	0	0	0	0
Zr	1380.987	48.33111	15.28364	1428.26	1263.43

Table 4: UOC CUP-2 average, maximum and minimum concentrations (ppb).

Elements	Avg	Stdev	Std Error	Max	Min
Al	13811.8	3546.106	1121.377	19603.2	10219.22
Ba	243.864	7.177818	2.269825	251.97	227.55
Bi	19.59	17.23097	5.448912	19.59	12.57
Ca	4831.017	1056.624	334.134	6259.21	3291.96
Ce	97.318	4.436219	1.402856	101.45	88.04
Cr	32.554	1051.932	4.404759	52.73	13.47
Fe	21390.26	1051.932	332.65	22649.53	19793.49
K	0	0	0	0	0
La	44.586	2.199875	0.695661	46.51	40.04
Mg	955.181	890.3579	281.5559	2530.2	0
Mn	701.573	38.46281	12.16301	751.4	644.66
Mo	6224.744	447.8966	141.6373	6950.8	5670.27
Na	30.737	67.96012	21.49088	197.14	0
Nb	3.715	0.327253	0.103486	4.24	3.35
Nd	53.007	2.475004	0.782665	55.51	48.18
Ni	36.926	9.28666	2.9367	48.02	21.14
P	1.861	3.927528	1.241993	9.69	0
Pr	12.79	0.647731	0.204831	13.29	11.49
Sr	335.321	27.69072	8.756576	379.06	301.81
Th	47529.55	72134.78	22811.02	252553.3	18260.18
Ti	158.05	15.36023	4.857331	180.97	139.43
W	117.269	7.961964	2.517794	127.08	102.27
Yb	4748.02	14863.75	4700.331	47051	39.72
Zn	0	0	0	0	0
Zr	3748.084	820.8667	259.5808	4329.8	1491.72

Table 5: U ore1 average, maximum and minimum concentrations (ppb).

Elements	Avg	Stdev	Std Error	Max	Min
Al	1371715	222554.2	70377.82	1733391	1110843
Ba	3658.767	500.3406	158.2216	4389.03	3145.4
Bi	91.873	45.06358	14.25035	217.93	66.77
Ca	24409.94	1514.244	478.846	26562.28	22341.39
Ce	3816.302	698.9634	221.0316	4964.02	3118.56
Cr	3095.834	464.6542	146.9366	3826.58	2469.89
Fe	761321.9	143271.6	45306.46	1001539	609520.7
K	299511.1	34595.08	10939.93	353104	258143.6
La	1844.977	283.6931	89.71164	2271.77	1550.91
Mg	40727.14	2130.176	673.6209	43969.99	38279.21
Mn	2826.184	433.2888	137.018	3518.6	2314.6
Mo	23.342	2.870241	0.90765	28	19.82
Na	29516.69	1200.926	379.7662	31393.91	27734.43
Nb	10.642	1.523321	0.481716	13.65	8.53
Nd	1526.411	235.8382	74.57859	1872.78	1271.45
Ni	2510.792	267.6086	84.62528	2995.65	2130.47
P	3454.843	305.8335	96.71305	3941.28	3070.96
Pr	428.058	67.79728	21.43938	529.08	357.51
Sr	1557.579	202.6804	64.09317	1887.93	1326.53
Th	420.686	66.6819	21.08667	517.39	350.26
Ti	323.597	52.08224	16.46985	406.58	260.67
W	9.87	27.10272	8.570632	87	0.92
Yb	23.265	3.884114	1.228265	29.31	19.06
Zn	2159.512	187.1391	59.17856	2450.14	1905.77
Zr	251.592	38.10449	12.0497	315.76	205.66

Table 6: U ore2 average, maximum and minimum concentrations (ppb).

Elements	Avg	Stdev	Std Error	Max	Min
Al	1349091	272889.3	86295.18	1915204	1012905
Ba	4846.953	1082.134	342.2008	7457.87	3765.59
Bi	699.367	170.0524	53.7753	1092.91	531.11
Ca	40934.09	4607.623	1457.058	47159.61	35060.2
Ce	15867.33	3975.668	1257.217	24340.46	11686.06
Cr	20500.68	4258.144	1346.543	29678.83	15286.53
Fe	10521432	2267409	717017.8	15336119	7845987
K	165881.8	23025.96	7281.449	212273.3	137515.7
La	19957	35168.13	11121.14	119997.5	7001.38
Mg	69446.03	7052.788	2230.287	84011.33	61031.22
Mn	17547.54	3701.898	1170.643	25573.88	13145.6
Mo	128.728	27.48972	8.693013	180.03	95.51
Na	33366.82	1210.259	382.7174	35401.14	31448.61
Nb	2854.503	567.7628	179.5424	3980.72	2159.71
Nd	6235.806	1014.194	320.7162	8366.82	4880.31
Ni	54222.23	10495.73	3319.041	78288.98	43255.89
P	7893.591	1897.965	600.1892	11431.36	5519.57
Pr	1644.362	259.3431	82.0115	2197.63	1298.76
Sr	5269.641	1379.691	436.2964	8441.52	3898.93
Th	33380.71	5474.803	1731.285	44494.44	27097.82
Ti	15962.32	3228.772	1021.027	22948.67	12019.54
W	123.429	22.2016	7.020761	169.44	97.62
Yb	968.074	178.6256	56.48638	1342.9	734.63
Zn	11839.53	2090.196	660.9781	16112.56	9203.59
Zr	4461.248	955.383	302.1186	6481.33	3297.63

Appendix D: REE Concentrations statistics of UOC and U ore samples.

Table1: Rare Earth Elements (REE) concentration (ppb) from uranium ore concentrate samples.

	UOC samples Id			
REE	**UOC_{green}**	**UOC_{black}**	**UCO CUP-2**	**ADU**
La	1.702 ± 0.0348	2.846 ± 0.0852	44.586 ± 0.6957	31.768 ± 0.326
Ce	3.092 ± 0.0767	2.481 ± 0.0882	97.32 ± 1.4014	9.921 ± 0.422
Pr	0.4 ± 0.00132	0.38 ± 0.0101	12.79 ± 0.2048	1.505 ± 0.198
Nd	1.622 ± 0.0441	1.634 ± 0.0347	53.007 ± 0.7827	4.404 ± 0.119
Sm	0.194 ± 0.0266	0.767 ± 0.0189	26.612 ± 0.4934	1.345 ± 0.237
Eu	0.065± 0.0052	0.169 ± 0.0046	2.554 ± 0.0495	0.893 ± 0.212
Gd	0.316 ± 0.0183	1.567 ± 0.0569	51.323 ± 0.9649	1.309 ± 0.210
Tb	0.057 ± 0.0056	0.413 ± 0.0122	14.187 ± 0.2759	0.971 ± 0.285
Dy	0.348 ± 0.0167	2.778 ± 0.0777	101.708 ± 2.2887	2.096 ± 0.284
Ho	0.058 ± 0.0033	0.623 ± 0.0187	19.963 ± 0.4758	1.139 ± 0.282
Er	0.137 ± 0.0132	1.808 ± 0.0632	54.183 ± 1.3464	1.653 ± 0.379
Tm	0.025 ± 0.0037	0.297 ± 0.0151	7.808 ± 0.1897	1.192 ± 0.283
Yb	0.145 ± 0.0132	2.006 ± 0.0717	47.671 ± 1.2861	2.055 ± 0.355
Lu	0.036 ± 0.0037	0.345 ± 0.0079	6.562 ± 0.2005	1.279 ± 0.379
ΣLREE	7.610	10.143	292.784	52.930
ΣHREE	0.865	8.536	258.145	12.633
ΣREE	8.475	18.679	550.930	65.563
ΣLREE/HREE	8.794	1.188	1.134	4.190

Table 2: Rare Earth Elements (REE) contents (ppb) from uranium ore samples.

REE	U ore1	U ore2
La	1844.977 ± 89.712	9156.998 ± 471.602
Ce	3816.302 ± 221.032	15867.326 ± 1257.217
Pr	428.064 ± 21.437	1644.462 ± 81.992
Nd	1526.411 ± 74.579	6235.806 ± 320.716
Sm	1551.606 ± 13.979	1736.38 ± 105.771
Eu	44.562 ± 2.221	316.672 ± 17.756
Gd	188.846 ± 9.016	1882.945 ± 111.745
Tb	20.188 ± 1.063	388.155 ± 21.976
Dy	73.353 ± 3.901	2491.008 ± 149.322
Ho	10.351 ± 0.537	436.63 ± 24.512
Er	25.406 ± 1.383	1134.199 ± 64.877
Tm	3.647 ± 0.168	160.315 ± 9.525
Yb	23.265 ± 1.228	968.074 ± 56.486
Lu	3.26 ± 0.169	114.307 ± 6.747
ΣLREE	9832.743	39207.388
ΣHREE	167.920	6026.134
ΣREE	10000.663	45233.522
ΣLREE/HREE	58.556	6.506

Appendix E: Activity concentration data for UOC and uranium ore samples.

Table 7: Activity concentration (measured in ppb) data for UOC and uranium ore samples

Sample ID	^{234}U	^{235}U	^{238}U
ADU	777368	3618.94126	76636.108
UOCgreen	777368	3618.94126	76636.108
UOCblack	777368	3618.94126	76636.108
UOC CUP-2	777368	3618.94126	76636.108

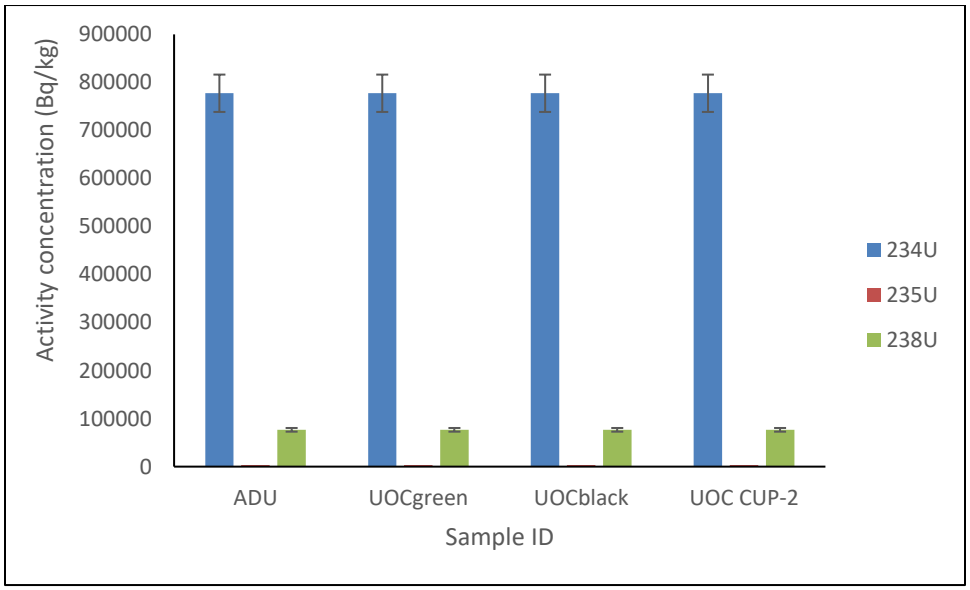

Figure 1: Graph showing the activity concentration of UOC samples.

Table 8: Activity concentration (measured in ppb) data for uranium ore samples in Bq/kg.

Sample ID	^{234}U	^{235}U	^{238}U
U ore1	20.960 ± 6.786	0.0976 ± 0.03159	2.0663 ± 0.669
U ore2	29631.991 ± 2609.991	137.948 ± 12.149	2921.241 ± 257.262

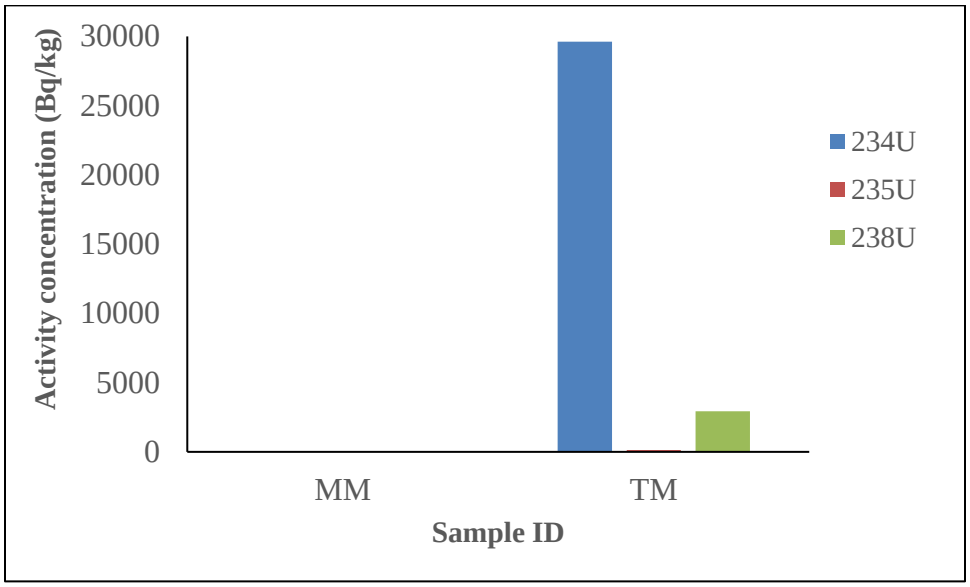

Figure 2: Graph showing the activity concentration of U ore1 and U ore2.